THE CRYSTAL STRUCTURES OF SEVERAL ORGANIC COMPOUNDS

I. α-KETO-1, 1'-TRIMETHYLENEFERROCENE

II. THE CHLORANIL-HEXAMETHYLBENZENE COMPLEX, A REFINEMENT

III. TWO PHENAZINE DERIVATIVES FROM PSEUDOMONAS AUREOFACIENS

Thesis by

Noel Duane Jones

In Partial Fulfillment of the Requirements

For the Degree of

Doctor of Philosophy

California Institute of Technology

Pasadena, California

1964

To my parents

Walter and Iva Maude Jones

who have made this thesis possible

and to my wife

Katharine Jean Jones

who has made it worth doing

ACKNOWLEDGEMENTS

Whatever the reader may find of merit in this thesis is derived in large part from the patient guidance of Dr. Richard Marsh. He has contributed unselfishly of his time and talents to the work reported herein. I thank him most gratefully.

My thanks also go to Professor John Richards who has on many occasions provided me with encouragement and wise counsel.

I feel honored to have had the privilege of associating with the postdoctoral fellows and graduate students, past and present, at Caltech. Most especially I would like to express my appreciation to Ned Webb, Al Hybl, Dave Duchamp and B. D. Sharma for helping to create an atmosphere of stimulation and good fellowship.

I wish to acknowledge with thanks the financial support I have received from the National Science Foundation, the National Institutes of Health and the California Institute of Technology.

And, to my wife, Katharine, I owe a deep debt of gratitude for her patient understanding and hard work during the preparation of this manuscript. The completion of my thesis marks the beginning of hers.

ABSTRACT

I. The three-dimensional crystal structure of α-keto-1,1'-trimethyleneferrocene has been determined by X-ray diffraction analysis. This compound crystallizes in the centrosymmetric monoclinic space group $C_{2h}^{5} - P2_1/a$. The unit cell contains four molecules and has the dimensions $a = 22.981 \pm 0.002$ Å, $b = 7.381 \pm 0.001$ Å, $c = 5.833 \pm 0.001$ Å and $\beta = 93.38 \pm 0.02°$. The structure was solved from the locations of the iron-iron vectors in the (001) Patterson projection and was refined in both two and three-dimensions by the method of least-squares. The final reliability factor, R, was 0.067. The dihedral angle between the best planes through the two nearly planar cyclopentadienyl rings is about 9.8°. The average ring carbon-carbon bond is 1.428 ± 0.010 Å and the average iron-ring bond is 2.040 ± 0.006 Å. The principal thermal motion is a vibration of the entire molecule in a direction roughly parallel to the c^* axis.

II. The crystal structure of the chloranil-hexamethylbenzene complex, as first reported by Harding and Wallwork [*Acta Cryst.*, *8*, 787 (1955)], has been refined in order to show that their data are consistent with a more reasonable structure than that proposed by them. The molecular dimensions of the refined structure show no

significant deviations from the expected values. In addition, the molecules are nearly planar.

III. The crystal structures of two phenazine derivatives from extracts of <u>Pseudomonas aureofaciens</u> have been determined. The first of these, 1-phenazinecarboxylic acid, has been solved and refined in two dimensions. The molecular structure of the other derivative, 2-hydroxy-1-phenazinecarboxylic acid, was unknown at the time this work was begun. It has been solved in three dimensions and partially refined by the method of least-squares.

1-Phenazinecarboxylic acid crystallizes in the space group C_{2h}^{5} - $P2_1/a$ with four molecules in the monoclinic unit cell. The lattice constants are a = 18.5 ± 0.1 Å, b = 14.3 ± 0.1 Å, c = 3.87 ± 0.02 Å, and β = 99.5 ± 0.5°. The structure was solved from the weighted hk0 reciprocal lattice net and from the (001) Patterson map. The molecule is tilted 20-25° with respect to the (001) plane and is internally hydrogen bonded. The principal thermal vibration is a torsion motion about an axis which passes through the center ring of the phenazine nucleus.

2-Hydroxy-1-phenazinecarboxylic acid also crystallizes in the space group C_{2h}^{5} - $P2_1/a$ with four molecules in a unit cell which has the dimensions a = 21.777 ± 0.002 Å, b = 5.896 ± 0.001 Å, c = 8.416 ± 0.001 Å and β = 107.02 ± 0.02°. This structure was solved from the weighted $h0\ell$ reciprocal lattice net and from the (010) Patterson vector map. The average ring carbon-carbon bond length, calculated from the partially refined positional parameters, is 1.41 ± 0.03 Å and the average carbon-nitrogen bond length is 1.36 ± 0.03 Å. The molecules lie parallel and coplanar in "ribbons" which are stacked normal to the a^* axis and very nearly parallel to the (012) plane. The hydroxyl hydrogen atom is internally bonded to the carboxyl group and the carboxyl hydrogen atom possibly forms a "bifurcated" bond, being bonded both intra- and intermolecularly.

TABLE OF CONTENTS

Table of Contents (continued)

THE CRYSTAL STRUCTURES OF SEVERAL ORGANIC COMPOUNDS

I. α-Keto-1, 1'-trimethyleneferrocene

1. Introduction

In slightly more than a decade since ferrocene was first synthesized by Kealy and Pauson (1) and independently by Miller, Tebboth and Tremain (2), the literature of the chemistry of cyclopentadienyl derivatives of the transition metals has become voluminous. This interest has been aroused by the unusual structures and properties of these so-called "sandwich" compounds. Of particular interest have been metallocene derivatives in which one or more carbon bridges join the two rings. Ferrocene bridged by a single carbon chain was first prepared by Woodward and Csendes (3) and by Rinehart and Curby (4). Doubly and triply bridged ferrocene derivatives have been prepared by Schlögl, Peterlik and Seiler (5) and by Rinehart, Bublitz and Gustafson (6). Finally, a derivative of ferrocene with four bridges of three carbon units each has been recently announced by Schlögl and Peterlik (7). The fully spanned ferrocene molecule has not yet been synthesized; the prospects, however, are intriguing since reduction of such a compound should lead to a "caged" iron atom. The synthesis of a variety of substituted bridged metallocenes has been vigorously pursued because these systems provide a scaffold for the study of reactive sites in the vicinity of transition metals. Some of this work is discussed below.

The first bridged ferrocene to be synthesized (3, 4) was α-keto-1,1′-trimethyleneferrocene, the subject of this investigation. The sample used in this study was prepared by Hill (8) by the method outlined below.

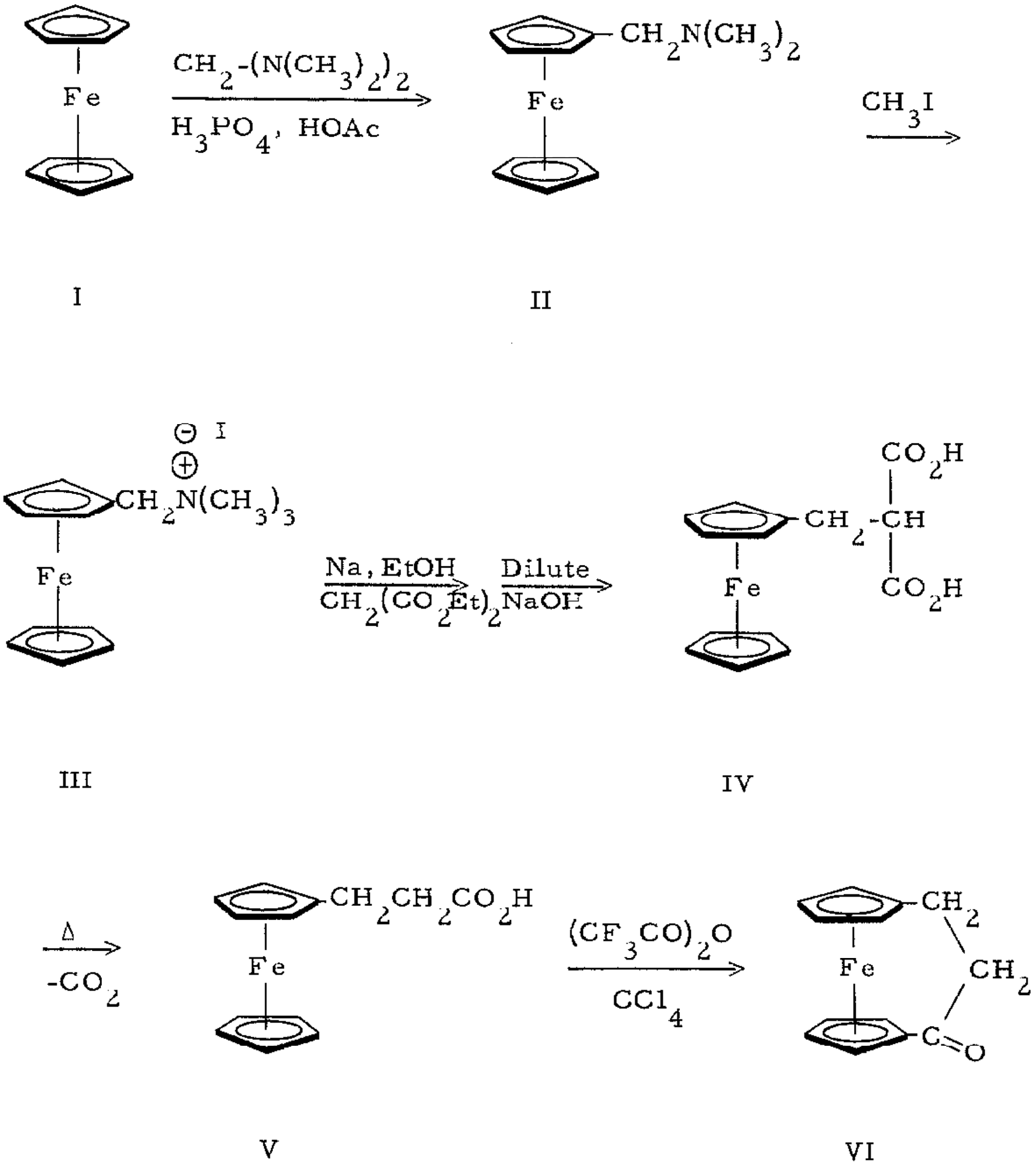

Ferrocene, I, was aminomethylated with methylenebisdimethylamine to give ferrocenylmethyldimethylamine, II, which was quaternized with methyl iodide to give ferrocenylmethyltrimethylammonium iodide, III. Treatment of III by the malonic ester synthesis gave ferrocenylmethylmalonic acid, IV, which was decarboxylated to 3-ferrocenylpropionic acid, V. In the presence of trifluoroacetic anhydride, V underwent cyclization to give the desired product, α-keto-1, 1'-trimethyleneferrocene, VI.

The infrared spectrum of α-keto-1, 1'-trimethyleneferrocene shows a carbonyl stretching band at 1682 $cm.^{-1}$ compared to 1661 $cm.^{-1}$ for the same band in the spectrum of acetylferrocene (6). This shift to higher frequency in the bridged metallocene may be interpreted on the basis of a carbonyl group which is twisted out of the plane of the cyclopentadienyl ring. The decreased conjugation which results from this non-coplanarity increases the double bond character of the carbonyl group. The effect of this twisted carbonyl group is even more pronounced in the ultraviolet spectrum of VI. Acetylferrocene exhibits a $\pi \rightarrow \pi$ electronic transition bond at 226 mμ (ϵ_{max} = 16, 500) while the corresponding band in α-keto-1, 1'-trimethyleneferrocene is at 227 mμ (ϵ_{max} = 8, 030). The large difference in intensity for these two peaks is due to the reduced transition probability for the non-coplanar (bridged) ketone. Still further evidence for the configuration of the bridged ketone is provided by its nuclear magnetic resonance spectrum (6). The positions of the ring proton peaks in the spectra of acetylferrocene and VI are essentially the same except for the two protons at the 2' and 5' positions of VI (adjacent to the bridge, on the ring to which the carbonyl group is not attached). These proton peaks occur at significantly lower field in the spectrum of the bridged ketone due to less diamagnetic shielding by the carbonyl group. This is true because the axis of the cone of shielding due to the diamagnetic anisotropy of the carbonyl group (9) is tilted with respect to the ring-iron-ring axis of the molecule.

Recent studies in these laboratories by Hill and Richards (10) have led them to propose that direct interaction with the electrons of the transition metal of a metallocene group may serve to stabilize a neighboring carbonium ion. The reactions studied were the solvolyses of a number of α-acetoxy derivatives of several metallocenes. The reaction of greatest interest in the present context is the solvolysis of α-acetoxy-1, 1'-trimethyleneferrocene, VII,

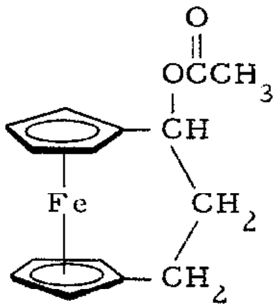

VII

which may be prepared from the bridged ketone, VI, by reduction to the alcohol with sodium borohydride, followed by esterification with acetyl chloride. The rate of solvolysis of VII at 30° in 80% acetone/water is about 0.23 times that of trityl acetate under the same conditions. Hill and Richards have shown that the solvolysis is first order and proceeds by alkyl-oxygen fission of the neutral ester. This evidence indicates a relatively stable carbonium ion intermediate, VIII, which they postulate is stabilized by a direct participation of the iron electrons. The validity of this hypothesis depends upon a favorable stereochemical relationship of the carbonium ion site and the iron atom. The crystal structure of α-keto-1, 1'-trimethyleneferrocene was undertaken because this molecule was the best model available for the study of a bridged ferrocene with a trigonal α-carbon atom. Whether indeed the bridged ketone is a good model for the carbonium ion will be discussed in more detail later.

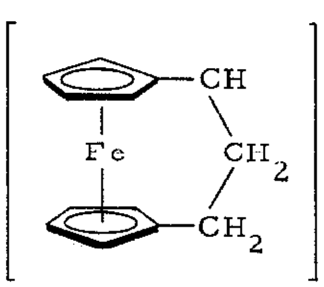

VIII

2. Determination and refinement of the structure.

i. Preliminary crystallographic measurements.

A crystalline sample of α-keto-1, 1'-trimethyleneferrocene, m. p. 144.5-145.5°,(lit. (4) m. p. 144-144.5°) was obtained from E. A. Hill. Microscopic examination of the sample showed that the dark red-orange compound crystallizes in an acicular (needle-like) habit. Several crystals, about 0.3 mm. in diameter and 2 mm. long with well-developed faces and no apparent twinning, were selected. One of these crystals was mounted with its prismatic zone axis approximately parallel to the rotation axis of an optical goniometer. The two unique sets (forms) of faces of the crystal, figure 1, were indexed using the observed goniometric measurements listed in table 1.

The first X-ray diffraction pattern observed was a 20° oscillation photograph (*) taken with the needle axis, c, as the rotation axis. Measurements from this photograph gave a value for c of approximately 5.86 Å. A set of layer-line photographs (hk0 to hk3 incl.) was taken using the equi-inclination Weissenberg technique (11). Measurements from the hk0 photograph gave values of 7.38 Å for b and 22.9 Å for 1/a*. In addition, an h0ℓ photograph was taken using the precession technique (12) with unfiltered molybdenum radiation; measurements from this photograph gave a β-angle of 93.5°. The a axial length then

---

* Unless otherwise noted, copper K_α (nickel filtered) radiation excited at 45 kv. and 15 ma. was used for all photographs.

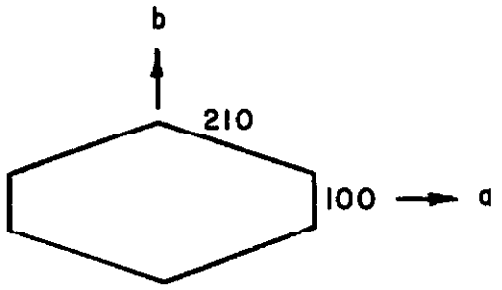

Figure 1. Cross section of a crystal of α-keto-1, 1'-trimethyleneferrocene with its faces indexed and the positions of the crystallographic axes indicated.

Table 1. Goniometric measurements taken on a crystal of α-keto-1, 1'-trimethyleneferrocene.

Longitude	Latitude	Index
133° 00'	359° 20'	100
189° 52'	359° 25'	$2\bar{1}0$
255° 58'	0° 00'	$\bar{2}\bar{1}0$
313° 00'	0° 37'	$\bar{1}00$
9° 23'	359° 40'	$\bar{2}10$
76° 22'	359° 50'	210

is 22.9 Å.

More precise lattice constants were obtained later from Straumanis-type, zero-layer Weissenberg photographs taken at room temperature using crystals mounted about the b and c axes. The relative positions of a total of 189 reflections on the h0ℓ and hk0 photographs were measured with an optical comparator and the Bragg angle was calculated for each reflection. From these data, the lattice parameters were calculated using a computer program written for the Burroughs 220 digital computer by the author (see Appendix, part I); the values are

$a = 22.981 \pm 0.002$ Å , $\beta = 93.38 \pm 0.02°$,

$b = 7.381 \pm 0.001$ Å ,

$c = 5.833 \pm 0.001$ Å ,

where the uncertainties listed are about ten times the calculated standard deviations. The corrections for absorption and eccentricity were found to be negligible.

The density of a crystal of α-keto-1, 1'-trimethyleneferrocene was determined to be 1.60 g. cm.$^{-3}$ by flotation in a mixture of carbon tetrachloride and ethylene bromide. Assuming four molecules in the unit cell, the calculated density for $C_{13}H_{12}OFe$ (m. w., 240.08) is 1.61 g. cm.$^{-3}$

The systematic extinctions gave the following conditions limiting possible reflections: hkℓ, no conditions; h0ℓ, h = 2n; 0k0, k = 2n.

These conditions are indicative of the centrosymmetric, monoclinic space group C_{2h}^{5} - $P\,2_1/a$. Since the molecules possess no symmetry, they must lie in general symmetry positions in the unit cell.

ii. Intensity data.

In order to minimize absorption errors, a small acicular crystal with roughly hexagonal cross section was chosen for the c axis intensity photographs. Two packs of three films each were exposed for each layer, the first for 16 to 20 hours and the second for about two hours. Intensity data for reflections hk0 to hk5, inclusive, were collected in this manner. The same crystal was used to make a graduated intensity strip and was also used for the hk0 precision Weissenberg photograph discussed earlier. Contrary to the experiences of Burke (13), who has determined the crystal structure of 1,1'-tetramethylethyleneferrocene, the bridged ketone is quite stable to X-rays. There was no noticeable change in the crystal after exposure to radiation for over 250 hours. However, all photographs taken with copper radiation from crystals of both of these bridged ferrocenes exhibit a high background due to fluorescent scattering by the iron atoms. Fluorescence occurs when an incident quantum of X-rays has just sufficient energy to excite secondary X-rays in the absorber atom. This is true if the wavelength of the characteristic line of the incident radiation (1.542 Å for copper K_α) is slightly shorter than the wavelength of the absorption edge of the excited atom (1.743 Å for the iron K edge).

Some difficulty was experienced in cutting a crystal of α-keto-1,1'-trimethyleneferrocene in order to obtain satisfactory diffraction photographs about the b axis. The long, slender needles fractured unevenly; after several dozen unsuccessful attempts, a rather unsatisfactory fragment was mounted. The multiple film Weissenberg technique was again used to collect intensity data, reflections $h0\ell$ to $h2\ell$, inclusive, being recorded. No attempt was made to prepare an intensity scale from this crystal.

The intensities were estimated visually by comparison with the intensity scale prepared from the crystal mounted about the c axis. The comparisons were made with the aid of a binocular microscope. This investigator has concluded, in retrospect, that a simple magnifying glass is more useful in the estimation of intensities; it is less tiring on the eyes, permits a larger field of vision to prevent indexing errors, and its lower magnification probably makes possible a more accurate estimation of the integrated intensities. The measured intensities were scaled within each layer using an average film factor calculated for each set of photographs.

Lorentz and polarization corrections were applied to the intensity data using a Burroughs 220 computer program written by Hybl (14). No correction was made for absorption at this point; it was decided to wait to see if the structure could be refined without this correction.

Layer scale factors, K_i, for the corrected intensities, I_{ij}, were calculated using the 220 computer least-squares scaling program written by Deverill. This program minimizes the function

$$R = \sum_i \sum_j w_{ij} (K_i I_j - I_{ij})^2 \tag{1}$$

where $w_{ij} = \frac{1}{I_{ij}}$ if $I_{ij} \geq I_M$

or $w_{ij} = \frac{1}{\sqrt{I_M I_{ij}}}$ if $I_{ij} < I_M$

and $K_1 = 1$. Any arbitrary value of I_{ij} may be taken for I_M.

The program prints lists of the scaled $|F|^2$'s, and a list of the weighted average $|F|^2$'s and the $|F|$'s. Although the $h0\ell$ data were initially included in the average $|F|^2$'s, it was decided to use them only to scale the hk0 data because of the large number of discrepancies between the high angle reflections of the two sets. These discrepancies may be due to a possible misalignment of the crystal while the b axis photographs were being taken.

iii. The two-dimensional structure.

Measurements from a scale model of α-keto-1,1'-trimethyleneferrocene indicated that the volume occupied by the molecule (assuming normal van der Waals radii (16)) is roughly that of a 5.5 x 6.5 x 7.5 Å rectangular prism, as shown in figure 2. The volume of this prism is about 268 Å^3. This agrees reasonably well with the value of 246.9 Å^3, which is the volume occupied by a single molecule as calculated from the unit cell parameters. Since the c axis is only 5.8 Å long, the molecule must lie in the unit cell with the plane formed by the iron atom and the carbon bridge approximately normal to the c axis. Fortunately, the atoms of the molecule are best resolved when viewed down this short axis. It appeared, therefore, that it might be possible to determine the structure in the (001) projection.

The most obvious way to solve this structure was to look for the large peaks representing vectors between the iron atoms in the (001) Patterson projection. In this projection of the unit cell the iron atoms lie at x, y; $\bar{x}, \bar{y}$; $\frac{1}{2}+x$, $\frac{1}{2}-y$ and $\frac{1}{2}-x, \frac{1}{2}+y$. The asymmetric unit of the Patterson projection will, therefore, contain iron-iron vector peaks at $(2x, 2y)$, $(\frac{1}{2} - 2x, \frac{1}{2})$ and $(\frac{1}{2}, \frac{1}{2} - 2y)$. Since the Laue symmetry for the monoclinic crystal system is 2/m, the hk0 vector map will have pmm symmetry. The Patterson expression for this projection is

$$P(UVO) = \frac{4}{A} \sum_{o}^{\infty} h \sum_{o}^{\infty} k \, |F(hk0)|^2 \cos 2\pi hU \cos 2\pi kV. \qquad (2)$$

An hk0 vector map was calculated from equation 2 using a Burroughs 220 computer program written by Hoogsteen (17). The summation was carried out in intervals of 0.01 a and 0.02 b. No attempt was made to

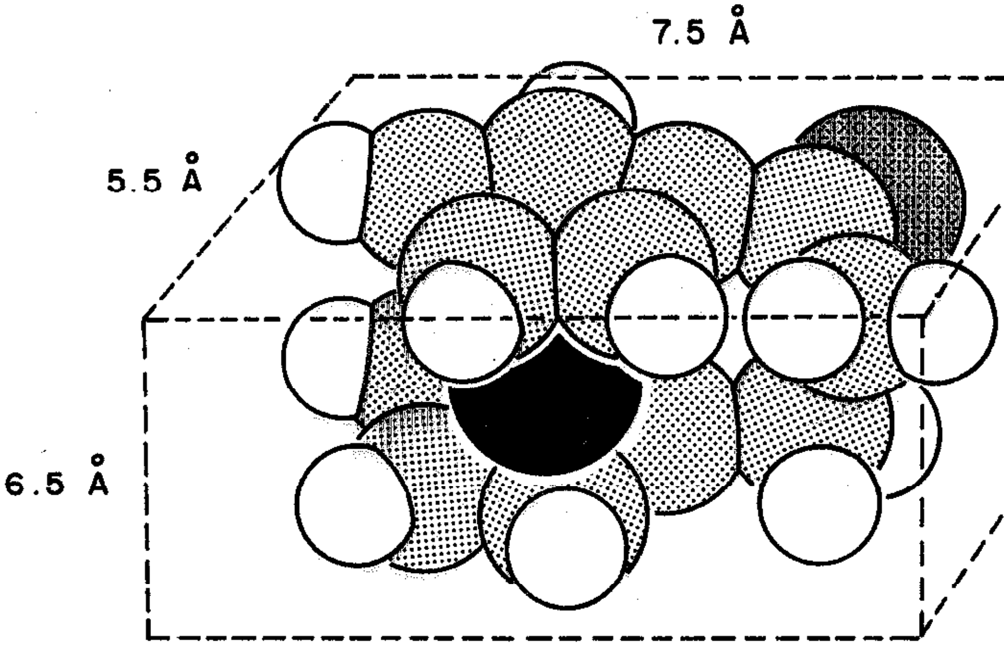

Figure 2. A model of α-keto-1, 1'-trimethyleneferrocene showing the approximate overall dimensions of the molecule.

remove the original peak or sharpen the Patterson map, which is shown in figure 3. The iron-iron vector peaks may be clearly seen in this drawing. From these peaks the coordinates x = 0.150 and y = 0.125 were derived for the iron atom.

In the (001) projection, the space group $P2_1/a$ degenerates to the plane group pgg. The structure factor expression for this projection is

$$F(hk0) = 4\sum_i f_i \cos 2\pi hx_i \cos 2\pi ky_i \qquad \text{for } h + k = 2n$$
$$F(hk0) = -4\sum_i f_i \sin 2\pi hx_i \sin 2\pi ky_i \qquad \text{for } h + k = 2n + 1 \qquad (3)$$

The electron density expression is

$$\rho(XYO) = \frac{4}{A}\Big[\overset{h+k=2n}{\sum_{o}^{\infty} h \sum_{o}^{\infty} k}\, F(hk0) \cos 2\pi hx \cos 2\pi ky \; - \overset{h+k=2n+1}{\sum_{o}^{\infty} h \sum_{o}^{\infty} k}\, F(hk0) \sin 2\pi hx \sin 2\pi ky\Big]. \qquad (4)$$

Using the coordinates determined from the vector map, the contribution of the iron atom to about 100 of the largest hk0 structure factors was calculated from equation 3. For about 25 of these reflections the iron atom contribution was sufficiently large to determine with certainty the sign of the structure factor. An hk0 electron density map was calculated from these phased structure factors using the trigonometric terms of equation 4 in the Hoogsteen program. This map clearly showed the

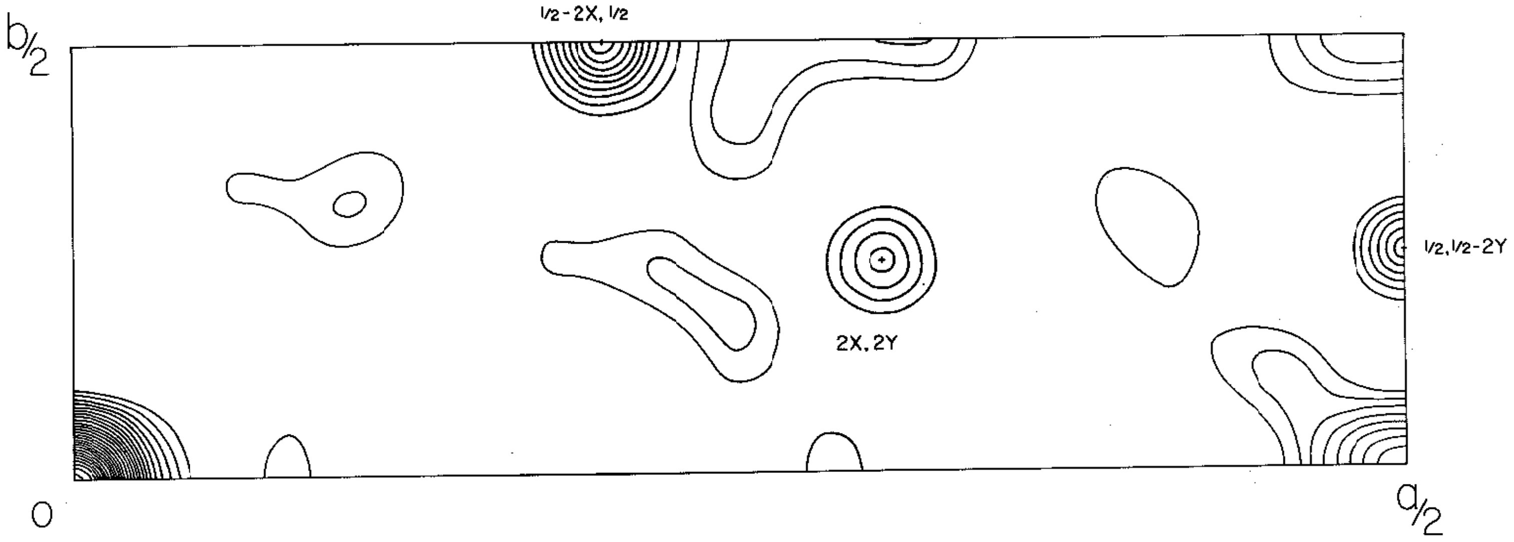

Figure 3. The (001) Patterson projection of α-keto-1, 1'-trimethyleneferrocene, with the iron-iron vector peaks indicated. The contours are drawn at arbitrary but equal levels.

positions of the iron atom, the α' and β carbon atoms of the bridge and one carbon atom in each ring. The atoms of the carbonyl group and the rest of the ring atoms were poorly resolved due to overlaps in this projection. However, from a consideration of the geometry of the molecule it was possible to assign trial coordinates to all of the atoms.

At this point the first structure factor calculation and least-squares refinement was performed using the Burroughs 220 program written by Marsh (18) for the monoclinic space groups. This program minimizes the function

$$\Sigma w[|F_{obs}|^2 - |F_{calc}|^2]^2 . \tag{5}$$

A block diagonal approximation is used in setting up the least-squares matrices. The x and z parameters for each atom are handled as a 2 x 2 matrix and the y parameter as a 1 x 1 matrix. The anisotropic temperature factors and the population parameter are included in a 7 x 7 matrix (2 x 2 for isotropic atoms) for each atom. The atomic scattering factors for carbon and oxygen which were used in all of the structure factor calculations on this compound were an average of the values given by Berghuis et al. (19) and Hoerni and Ibers (20). The atomic form factor curve for iron was taken from Thomas and Umeda (21). The isotropic temperature factor, B, was given the value 3.0 Å^2 for all the atoms. Each observation in the least-squares calculation was weighted according to the function

$$\sqrt{w} = \frac{1}{f_c} \quad , \tag{6}$$

where f_c is the value of the atomic form factor of carbon at the calculated value of sin Θ /λ. Unobserved reflections were given zero weight unless they calculated larger than the threshold value, in which case they were included in the least-squares and were weighted according to equation 6.

The first two-dimensional structure factor calculation showed good agreement between the observed and calculated F's. The R factor, defined as

$$R = \frac{\Sigma \left| \, |k F_{obs}| - |F_{calc}| \, \right|}{\Sigma |k F_{obs}|} \tag{7}$$

was 0.16. Several cycles of least-squares refinement, without letting the isotropic temperature parameters change, brought R down to 0.085. At this point all of the positional parameter shifts were less than one-tenth of their standard deviations. No attempt was made to refine the structure further in projection. In the final two-dimensional calculation 146 reflections were included in the least-squares, 21 of which were "less than" reflections which calculated too large.

All the phased structure factors were used in the calculation of a final (001) electron density map, shown in figure 4. Although this

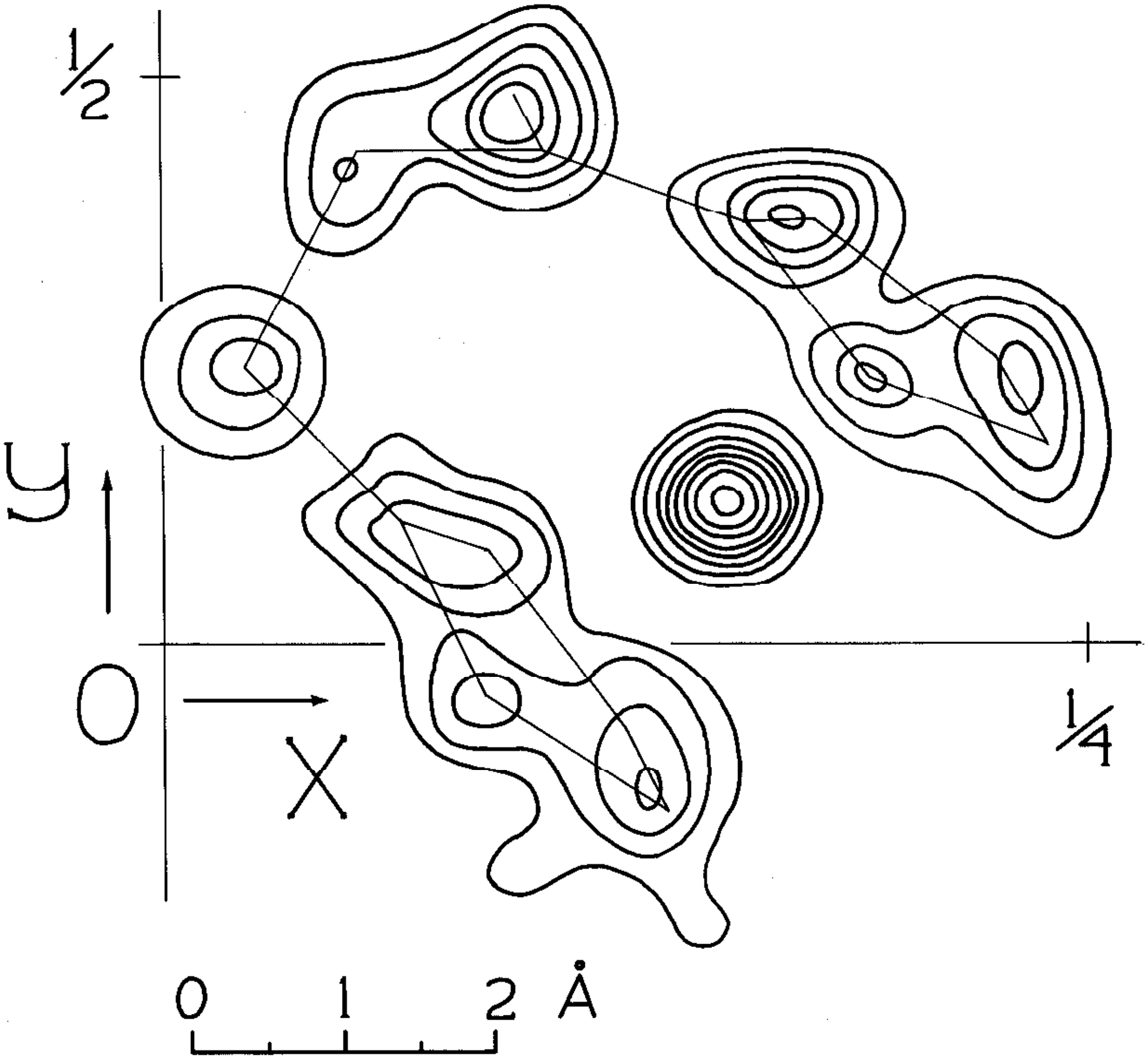

Figure 4. Final (001) electron density map of α-keto-1, 1'-trimethyleneferrocene. The contours are drawn at 4, 6, 8 .... e. $Å^{-2}$, except for the iron atom, where the contours are at 5, 10, 15 .... e. $Å^{-2}$.

map showed somewhat more detail than the first one which was calculated, many of the atoms were still poorly resolved.

iv. The three-dimensional structure

From packing considerations, particularly the proximity of two molecules related by a center of symmetry, an estimate of 0.250 was made for the z coordinate of the iron atom. Using the refined x and y atomic coordinates from above and a table of expected interatomic distances and angles (22), the approximate z coordinate was calculated for each of the other atoms.

The first cycle of three-dimensional structure factor calculations and least-squares refinement was run using isotropic temperature factors with $B = 3.0 \text{ Å}^2$ for all atoms. The observations were weighted according to equation 6. It was immediately apparent from the poor agreement ($R \cong 0.50$) between the observed and calculated structure factors and from the large negative z shifts for many of the atoms that the molecule should be moved in the negative z direction. A shift of -0.05 in z was applied to all of the coordinates and another structure factor and least-squares calculation was performed. R for this calculation dropped to 0.37 and the shifts, though still mostly negative, were considerably smaller. Several more least-squares cycles, permitting the isotropic temperature factors to change, saw the R factor decrease rapidly to 0.12. At this point, anisotropic temperature factors were introduced for the iron atom and the weighting scheme was changed to

$$\sqrt{w} = \frac{1}{F_{obs}} \qquad \text{if} \qquad F_{obs} \geq 4F_{min} \tag{8}$$

or

$$\sqrt{w} = \frac{1}{\sqrt{(F_{obs})(4F_{min})}} \qquad \text{if} \qquad F_{obs} < 4F_{min}$$

where F_{min} is the smallest observable F. This weighting function is essentially that of Hughes (23). Two more least-squares cycles were run and R dropped to 0.092. The approximate positions of the hydrogen atoms were calculated assuming C - H bond distances of 1.0 Å. The hydrogen atoms were arbitrarily assigned isotropic temperature factors equal to those of the heavy atoms to which they are attached. These parameters, along with anisotropic temperature factors for the oxygen atom and the carbon atoms, caused R to decrease to 0.080 after four more least-squares cycles. The weighting scheme was then changed to

$$\sqrt{w} = \frac{1}{F_{obs}^{2}} \qquad \text{if} \qquad F_{obs} \geq 4F_{min}$$

or (9)

$$\sqrt{w} = \frac{1}{(F_{obs})(4F_{min})} \qquad \text{if} \qquad F_{obs} < 4F_{min}$$

This weighting scheme was used because the Marsh least-squares program minimizes the sum of the squares of the residuals in F^2; therefore, the weights for the final best fit probably should be taken inversely proportional to the squares of the uncertainties in F^2_{obs}. Five more cycles of least-squares, during which the hydrogen atom coordinates were readjusted, brought the R factor down to 0.067. At this point none of the parameter shifts was larger than one-third of its standard deviation , and the refinement was considered complete. A total of 1466 reflections were included in the final structure factor calculation, of which 1196 contributed to the least-squares sums. Only 16 of the "less than" reflections calculated larger than the threshold value. Table 2 lists the final heavy atom parameters and their standard deviations and table 3 gives the assumed hydrogen atom parameters. The standard deviations in the heavy atom parameters were calculated from the diagonal terms of the inverse matrix. The final observed and calculated structure factors are given in table 4.

The observed structure factors and their calculated signs were used in the calculation of a three-dimensional electron density map using the Hoogsteen program and a first dimension program written by the author. The first summation was carried out in intervals of 0.01 in x up to 0.25 along a ; the second and third summations were performed in intervals of 0.02 y and 0.02 z along the full range of the b and c axes. Figure 5 shows the plotted map, the section through each atom being

Table 2. Final heavy atom parameters and their standard deviations for α-keto-1,1'-trimethyleneferrocene. The temperature factors are expressed in the form $T = \exp(-B_{11}h^2 - B_{22}k^2 - B_{33}\ell^2 - B_{12}hk - B_{13}h\ell - B_{23}k\ell)$. The atoms are numbered as in figure 5. All values have been multiplied by 10^4.

	x	y	z	B_{11}	B_{22}	B_{33}	B_{12}	B_{13}	B_{23}
Fe	1515(.4)	1259(1)	1913(1)	12(.2)	75(2)	211(4)	- 4(1)	- 3(1)	4(3)
O	955(3)	4880(7)	6090(9)	26(2)	188(13)	274(21)	34(7)	26(9)	-83(22)
C_1	1584(3)	3702(8)	3418(12)	12(1)	88(11)	264(25)	-13(6)	-12(9)	-52(21)
C_2	1925(3)	2429(9)	4727(11)	14(2)	115(12)	262(26)	- 9(6)	-32(10)	-13(24)
C_3	2350(3)	1701(10)	3344(12)	12(2)	157(15)	293(28)	8(6)	-40(10)	- 8(26)
C_4	2278(3)	2544(9)	1141(14)	12(2)	115(13)	404(33)	-15(7)	10(11)	9(29)
C_5	1794(3)	3767(8)	1161(12)	15(2)	85(11)	264(25)	-23(6)	-11(10)	55(22)
C_6	634(3)	985(8)	1599(13)	12(2)	101(13)	344(29)	-22(6)	- 4(11)	-37(24)
C_7	892(3)	- 438(9)	3029(12)	17(2)	120(13)	243(25)	-28(7)	10(10)	15(24)
C_8	1285(3)	-1426(8)	1736(14)	14(2)	56(11)	446(33)	- 9(6)	23(12)	3(24)
C_9	1275(4)	- 637(9)	- 508(13)	22(2)	116(13)	297(29)	-15(8)	-26(12)	-125(27)
C_{10}	873(3)	815(8)	- 580(12)	14(2)	102(12)	244(26)	- 6(6)	-28(10)	- 52(22)
C_{11}	1014(3)	4421(8)	4123(12)	15(2)	78(11)	256(25)	- 3(6)	18(10)	- 49(22)
C_{12}	501(3)	4343(9)	2391(12)	14(2)	108(12)	275(26)	22(6)	1(10)	- 47(24)
C_{13}	224(3)	2460(9)	2396(13)	11(2)	148(14)	351(31)	- 6(7)	8(11)	- 68(29)

Table 3. Assumed hydrogen atom parameters. The temperature factors are expressed in the form $T = \exp(-B \sin^2 \Theta/\lambda^2)$. The atoms are numbered as in figure 6.

	x	y	z	B
$H_{14}(C_2)$	0.187	0.211	0.641	3.5
$H_{15}(C_3)$	0.267	0.075	0.374	4.4
$H_{16}(C_4)$	0.252	0.228	-0.020	4.1
$H_{17}(C_5)$	0.164	0.453	-0.019	3.2
$H_{18}(C_7)$	0.080	-0.063	0.465	3.9
$H_{19}(C_8)$	0.153	-0.246	0.228	3.7
$H_{20}(C_9)$	0.153	-0.109	-0.183	3.7
$H_{21}(C_{10})$	0.073	0.162	-0.192	2.7
$H_{22}(C_{12})$	0.066	0.455	0.076	3.8
$H_{23}(C_{12})$	0.023	0.531	0.264	3.8
$H_{24}(C_{13})$	-0.015	0.245	0.140	4.4
$H_{25}(C_{13})$	0.013	0.219	0.403	4.4

Table 4. Observed and calculated structure factors for α-keto-1, 1'-trimethyleneferrocene. The three columns in each group contain the values of h, $10|F_{obs}|$ and $10F_{calc}$. Reflections indicated by an asterisk were omitted from the least-squares calculations due to extinction effects or especially poor intensity estimation. "Less than" reflections were included in the least-squares only if they calculated larger than the threshold value.

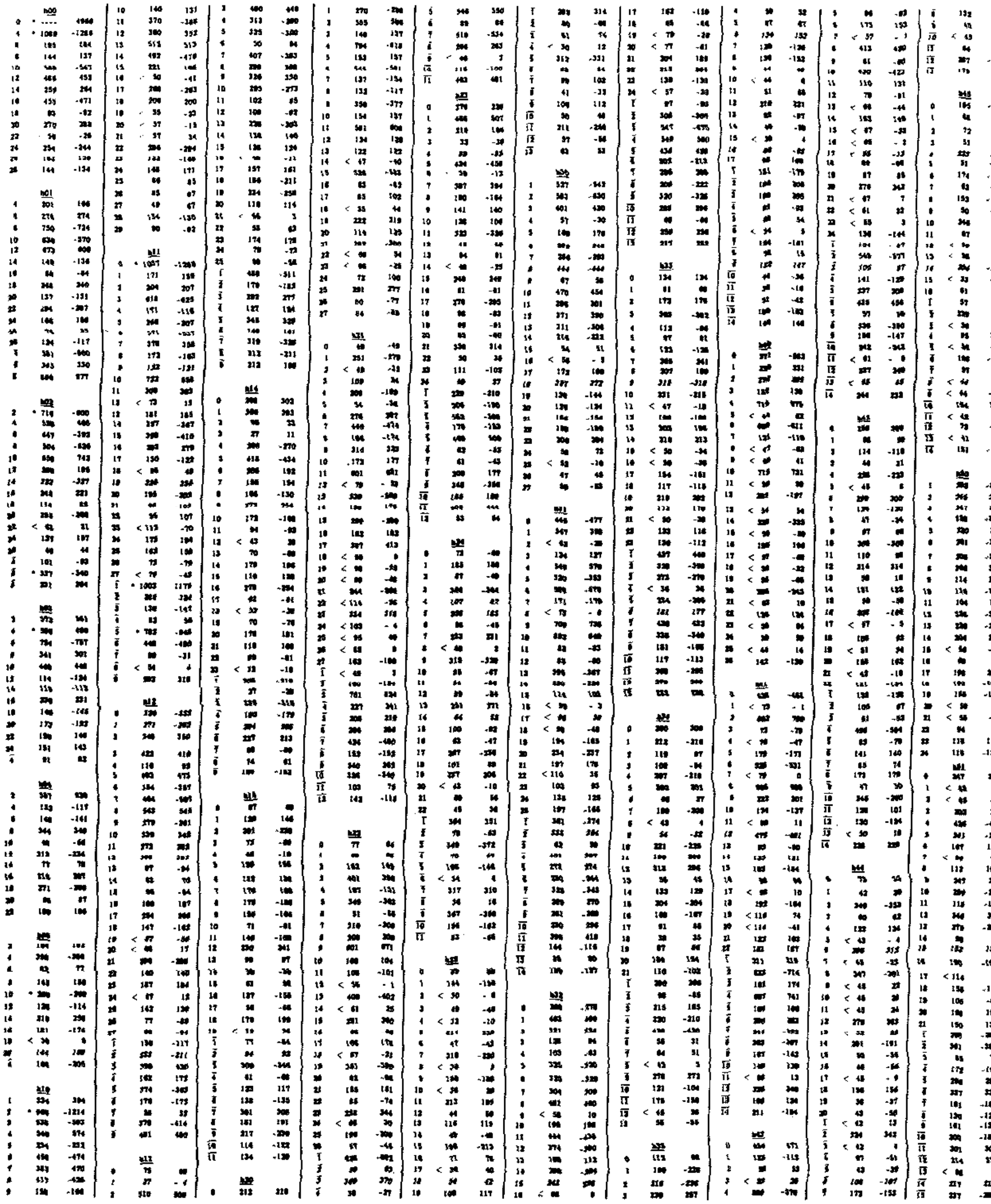

Table 4. (continued)

[illegible]

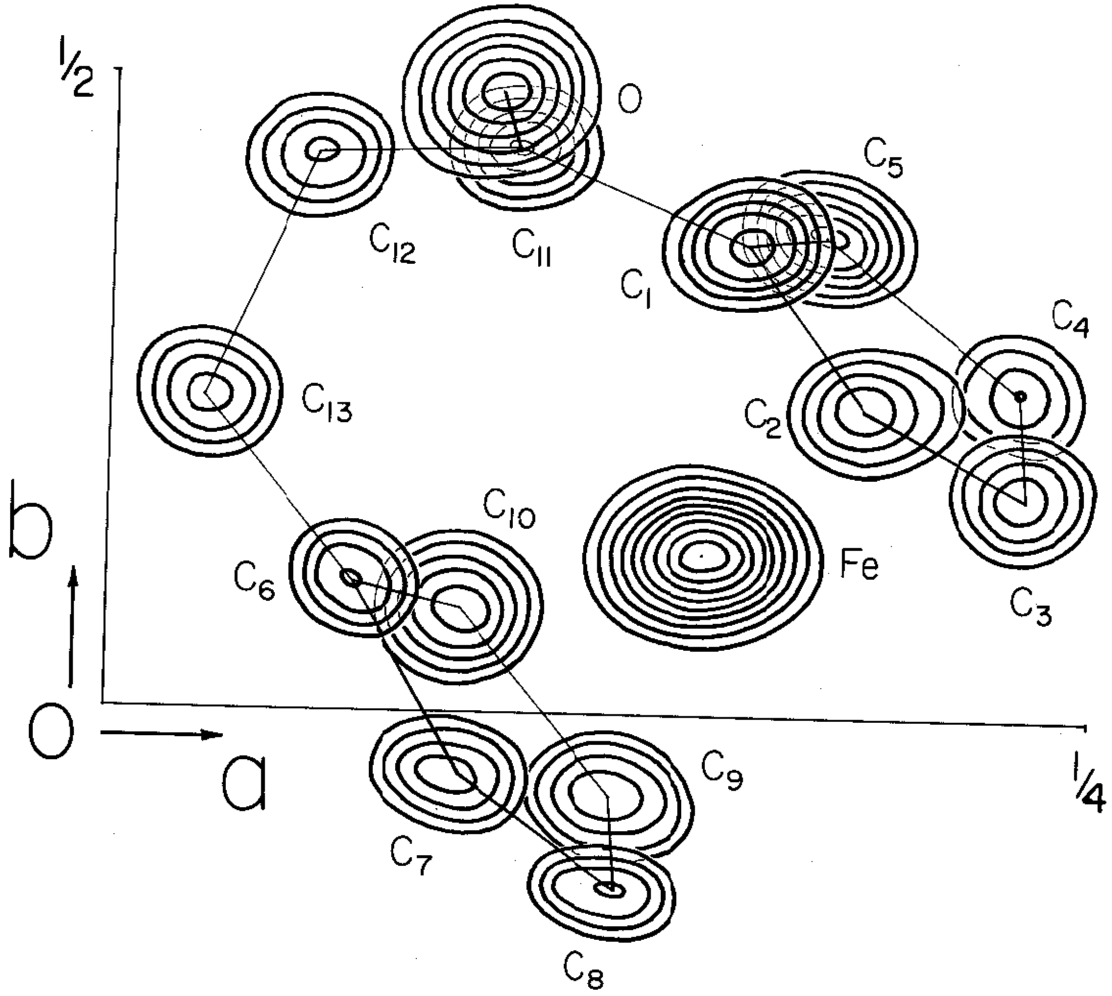

Figure 5. Composite three-dimensional electron density map of α-keto-1, 1'-trimethyleneferrocene projected onto (001). The contours are drawn at 4, 5, 6, ... e. Å^{-2} except for the iron atom, where the contours are at 5, 10, 15, ... e. Å^{-2}.

taken as close to the center of electron density as possible. A three-dimensional difference Fourier summation was also performed with the same intervals and over the same ranges. The structure factor calculation from which the ΔF's were derived did not include the hydrogen atom parameters. Figure 6 shows the resulting electron density map.

3. Discussion

i. Bond angles and interatomic distances.

The bond angles and interatomic distances for α-keto-1,1'-trimethyleneferrocene were calculated from the final refined atomic coordinates using a 220 computer program written by the author (see Appendix, part II). Figure 7 shows the calculated molecular dimensions. The interatomic distances from this determination are compared in table 5 with those found for ferrocene (24-26), dibenzoylferrocene (27), and 1,1'-tetramethylethyleneferrocene (13). It is interesting to note that even though the two rings of the bridged ketone are not coplanar, the average Fe-C and ring C-C bond distances agree quite well with those determined for the compounds listed in table 5. Furthermore, the internal agreement among the ten ring C-C bond lengths is very good, the spread being less than 0.04 Å. These observations would seem to indicate that the bridge pulls the 1 and 1' carbon atoms closer together than they are in ferrocene, thus tilting the rings without causing appreciable ring bond distortions. It also appears that

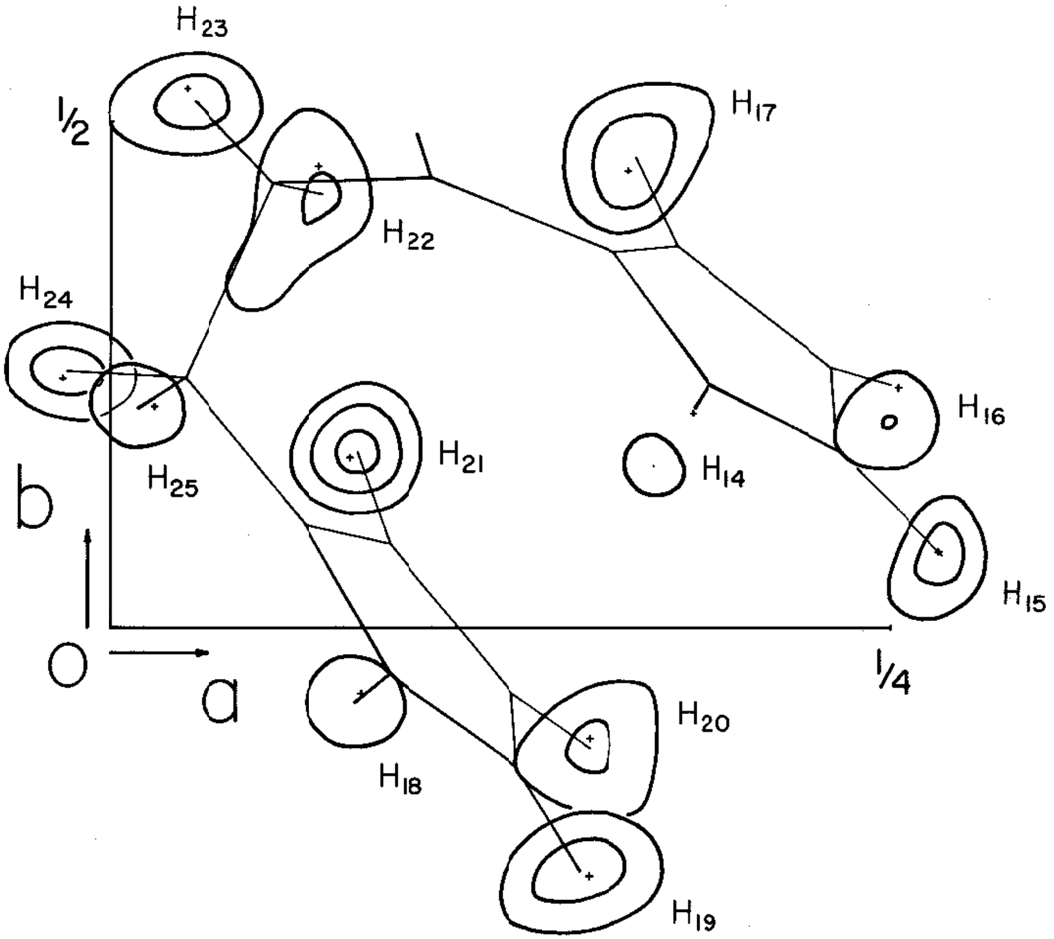

Figure 6. Composite three-dimensional difference Fourier map of α-keto-1,1'-trimethyleneferrocene projected onto (001). The contours are drawn at 0.4, 0.6 and 0.8 e. $\mathring{A}^{-2}$. The assumed positions of the hydrogen atoms during the last least-squares refinement are indicated by crosses.

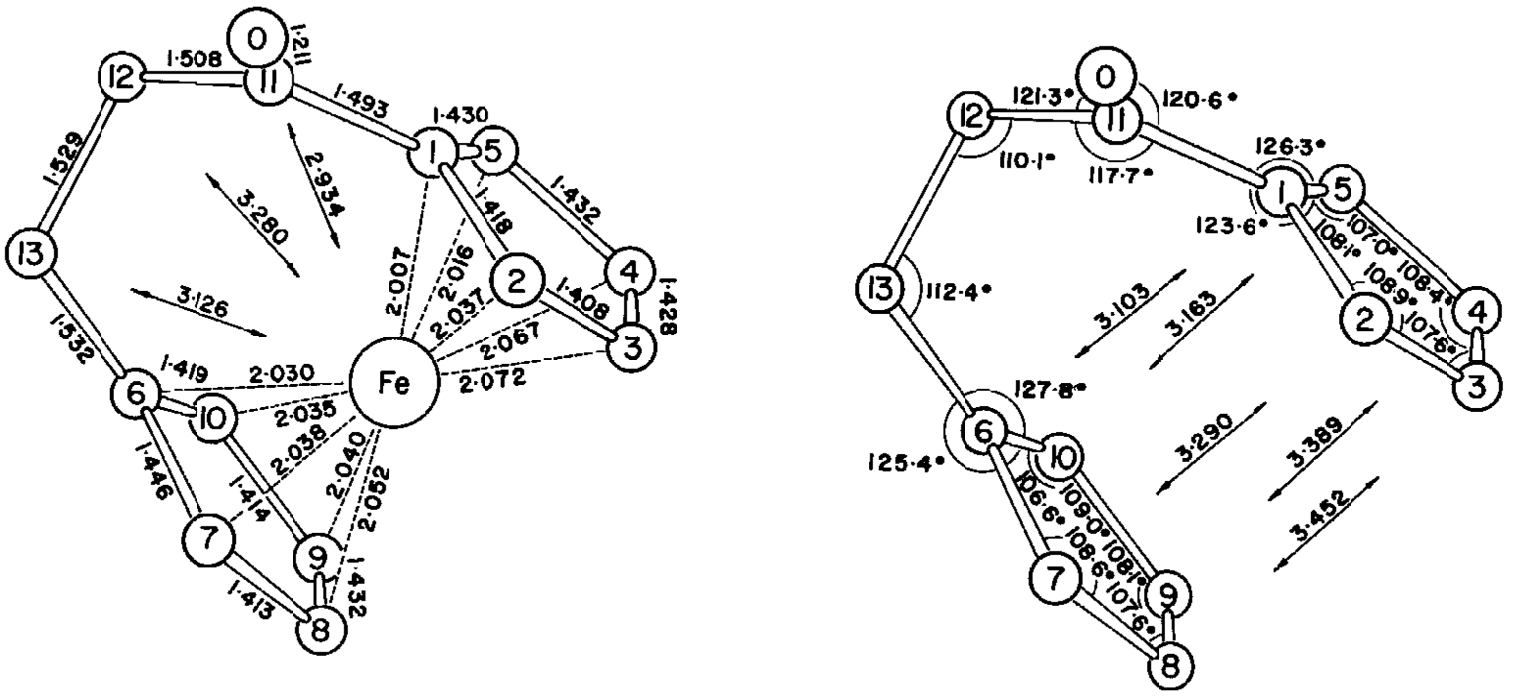

Figure 7. Molecular dimensions of α-keto-1, 1'-trimethyleneferrocene. The average standard deviations for the interatomic distances are ± 0.006 Å for Fe-C, ± 0.009 Å for C-O and ± 0.010 Å for C-C. The average standard deviation in the bond angles is ± 0.3°.

Table 5. Comparison of the average interatomic distances and their standard deviations for α-keto-1, 1'-trimethyleneferrocene, ferrocene, dibenzoylferrocene and 1, 1'-tetramethylethyleneferrocene. All distances are in Angstrom units. The standard deviations have been multiplied by 10^3.

Compound	Method	Ref.	Fe-Ring C	Ring C-C	Ring C-C'	C=O	C_α-C_1
α-Keto-1, 1'-trimethyleneferrocene	X-ray		2.040(6)	1.428(10)	3.275(10)	1.211(9)	1.493(10)
Ferrocene	X-ray	24	2.045(10)	1.403(20)	3.32(30)*		
Ferrocene	e. d.	25	2.064(13)	1.440(29)	3.32(60)*		
Ferrocene	e. d.	26	2.03 (20)	1.43(30)	3.25(30)*		
Dibenzoylferrocene	X-ray	27	2.05(20)	1.41(30)		1.21(10)	1.52(20)
1, 1'-Tetramethylethyleneferrocene	X-ray	13	2.052(20)	1.45(40)	3.26(40)		

* Spacing between the best planes through the two rings.

there is little strain in the trimethylene bridge since the bond lengths and angles are quite close to the expected values (22). By contrast, in 1,1'-tetramethylethyleneferrocene the middle bond of the two-carbon bridge is stretched (*) to approximately 1.61 Å (13).

ii. Spatial conformation of the cyclopentadienyl rings.

The best plane through each of the cyclopentadienyl rings and through the carbonyl group was calculated by the least-squares method using a 220 computer program written by the author (see Appendix, part II). The results of these calculations are shown in table 6. As may be seen, the ring atoms do not deviate significantly from coplanarity, which is further evidence that the bridge does not cause distortions in the rings.

The most obvious effect of the trimethylene bridge is to tilt the two cyclopentadienyl rings so they are no longer parallel. The dihedral angle between the planes (defined as the acute angle formed by the normals to the planes of the two rings) is 9.8°. In the two-carbon bridged derivative of ferrocene, 1,1'-tetramethylethyleneferrocene (13), the planes are tilted about 23°.

In a crystal of ferrocene the iron atoms lie at centers of symmetry; therefore, the rings are staggered by exactly 36°. By contrast the rings of the bridged ketone are more nearly eclipsed, being

---

[*] The lengthening of this bond may not be significant for the standard deviation given by Burke for the C-C bonds is about 0.04 Å. If it is a real effect it may be due in part to steric hindrance between the adjacent methyl groups on the bridge.

Table 6. Best planes through the cyclopentadienyl rings and through the carbonyl group. The values m_i are the direction cosines of the normal to the best plane with respect to the orthogonal axes a, b, c*. Atoms indicated by asterisks were not included in the calculation of the plane.

Direction cosines		Atom	Deviation
m_a	0.613	C_1	-0.005 Å
m_b	0.731	C_2	-0.001
m_{c*}	0.300	C_3	0.006
		C_4	-0.010
		C_5	0.009
		* C_{11}	0.301
		* Fe	1.640
		* Origin	-4.748
m_a	0.722	C_6	-0.006
m_b	0.622	C_7	0.003
m_{c*}	0.303	C_8	0.001
		C_9	-0.004
		C_{10}	0.006
		* C_{13}	-0.123
		* Fe	-1.640
		* Origin	-1.741
m_a	0.246	C_1	-0.012
m_b	0.929	C_{11}	0.039
m_{c*}	-0.276	C_{12}	-0.012
		O	-0.012
		* Origin	2.870

staggered by only 11.8°[*]. In 1,1'-tetramethylethyleneferrocene (13), this angle is 9 to 10°.

iii. Thermal ellipsoids.

The magnitudes and orientations of the thermal ellipsoids for each of the heavy atoms were calculated by the method of Rollett and Davies (28) and Waser (29) using a program written by Hebert (30) for the 220 computer. These results are listed in table 7. There are sizable anisotropies in the thermal motions; the major and minor axes of the ellipsoids for all of the atoms except the oxygen atom and C_7 are generally oriented along the c* and a axes of the crystal[**]. This would seem to indicate that the entire molecule vibrates in a direction approximately parallel to c*. Superimposed on this vibration are the motions of the individual atoms. The principal axis of the oxygen thermal ellipsoid lies in the ab plane and is inclined at an angle of 51° to the normal of the best plane through the carbonyl group (table 6). The anisotropy of the ring carbon atoms may be seen clearly from the molecular plane electron density maps shown in figures 8 and 9. These Fourier sections were taken through the best planes of the cyclopentadienyl rings (table 6). The calculations were performed using a

---

[*] The degree of staggering is defined here as the angle between the lines from the centroid of each ring to the carbon attached to the bridge after the lines have been projected onto an "average" plane. The "average" plane is taken such that its normal bisects the acute angle formed by the normals to the best planes through the two rings.

[**] Since only c axis data were used in the refinement of the temperature parameters, the thermal anisotropy may be an artifice which arises from systematic errors in the data.

Table 7. Magnitudes and direction cosines of the principal axes of the thermal ellipsoids for α-keto-1,1'-trimethyleneferrocene. The direction cosines, m, are taken with respect to the orthogonal axes a, b, c*. The root mean square deviation, μ, is given by $(B/8\pi^2)^{\frac{1}{2}}$.

	Axis i	B_i	μ(Å)	m_{ia}	m_{ib}	m_{ic*}
Fe	1	2.93	0.192	-0.346	0.061	0.926
	2	2.39	0.174	0.925	-0.136	0.379
	3	1.61	0.143	0.148	0.989	-0.005
O	1	6.20	0.279	0.879	0.468	0.099
	2	4.49	0.239	0.257	-0.602	0.763
	3	2.64	0.183	-0.397	0.647	0.639
C_1	1	3.78	0.219	-0.271	-0.165	0.940
	2	2.78	0.188	0.846	-0.509	0.179
	3	1.53	0.139	0.457	0.844	0.292
C_2	1	4.30	0.232	-0.610	0.055	0.772
	2	2.72	0.186	-0.437	0.808	-0.407
	3	2.08	0.162	0.659	0.587	0.489
C_3	1	4.70	0.243	-0.502	-0.152	0.836
	2	3.41	0.208	0.035	0.980	0.197
	3	1.87	0.154	0.863	-0.128	0.512
C_4	1	5.48	0.264	0.034	0.021	0.999
	2	2.98	0.194	-0.684	0.728	-0.012
	3	1.97	0.158	0.727	0.685	-0.018
C_5	1	4.14	0.230	-0.595	0.358	0.701
	2	3.02	0.196	0.700	-0.205	0.704
	3	1.45	0.135	0.392	0.911	-0.118
C_6	1	4.72	0.244	-0.074	-0.105	0.990
	2	3.09	0.198	0.767	-0.640	0.012
	3	1.51	0.138	0.635	0.761	0.146
C_7	1	4.19	0.231	0.854	-0.509	0.122
	2	3.32	0.205	-0.003	0.182	0.983
	3	1.99	0.159	0.517	0.841	-0.139
C_8	1	6.11	0.278	0.138	-0.003	0.994
	2	2.99	0.194	0.975	-0.169	-0.108
	3	1.16	0.121	0.168	0.986	-0.016
C_9	1	5.32	0.260	0.801	0.090	-0.567
	2	4.26	0.232	0.535	-0.546	0.660
	3	1.74	0.148	0.264	0.832	0.494

Table 7. (continued)

	Axis i	B_i	μ(Å)	m_{ia}	m_{ib}	m_{ic*}
C_{10}	1	4.05	0.226	-0.618	-0.122	0.758
	2	2.70	0.185	-0.637	0.655	-0.424
	3	1.81	0.152	0.458	0.746	0.497
C_{11}	1	3.80	0.219	0.483	-0.193	0.868
	2	2.86	0.190	0.874	0.107	-0.446
	3	1.61	0.143	-0.001	0.975	0.220
C_{12}	1	3.95	0.224	-0.339	-0.383	0.849
	2	3.26	0.203	0.756	0.431	0.514
	3	1.75	0.149	-0.558	0.817	0.127
C_{13}	1	4.96	0.251	0.053	-0.321	0.947
	2	3.05	0.197	-0.211	0.922	0.319
	3	2.31	0.171	0.974	0.217	0.047

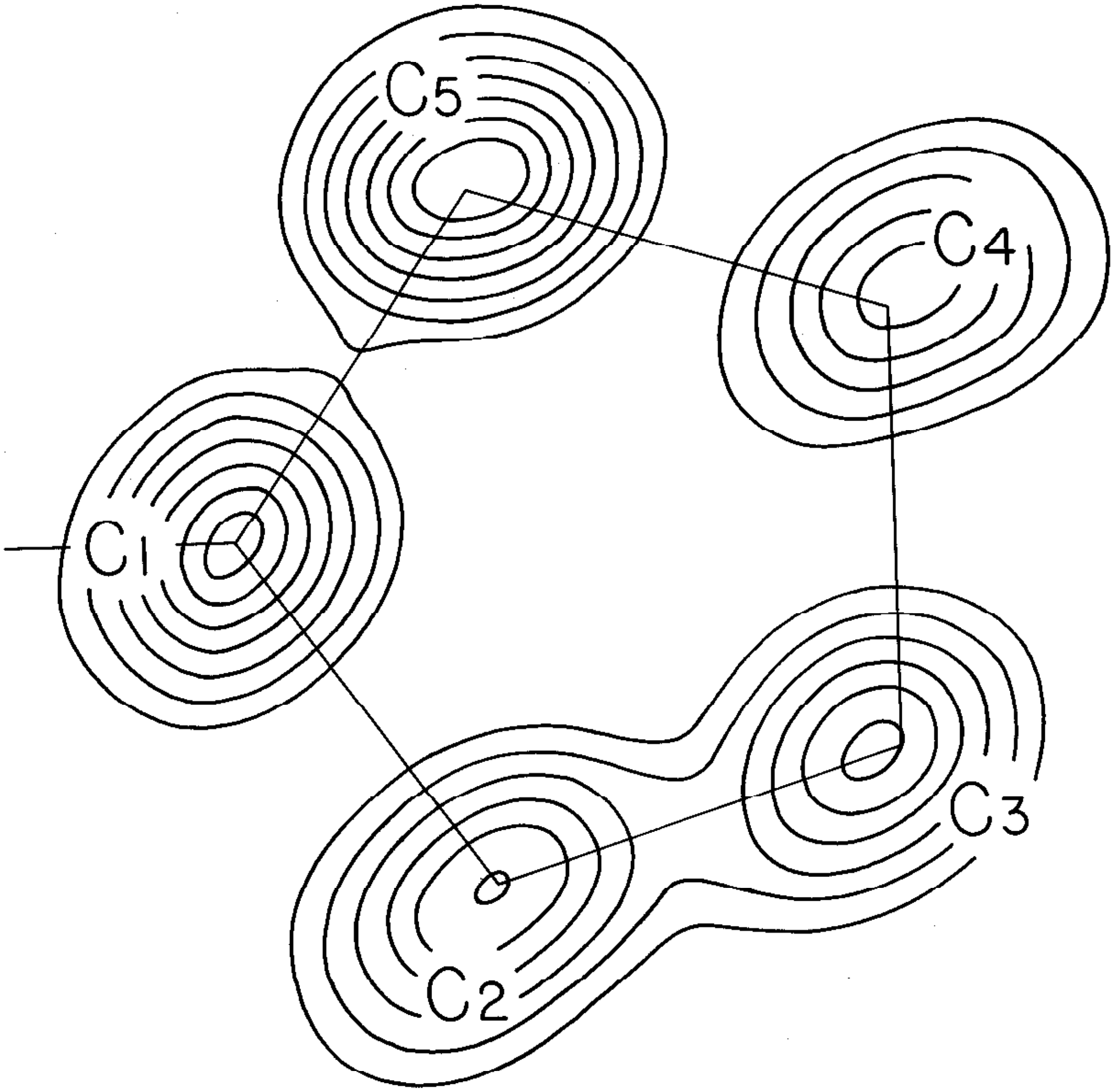

Figure 8. Electron density map in the best plane (table 6) of the cyclopentadienyl ring C_1-C_5 of α-keto-1, 1'-trimethyl-eneferrocene. The contours are drawn at intervals of 2, 3, 4 ... e. Å^{-2}. The orientation is as in figure 5.

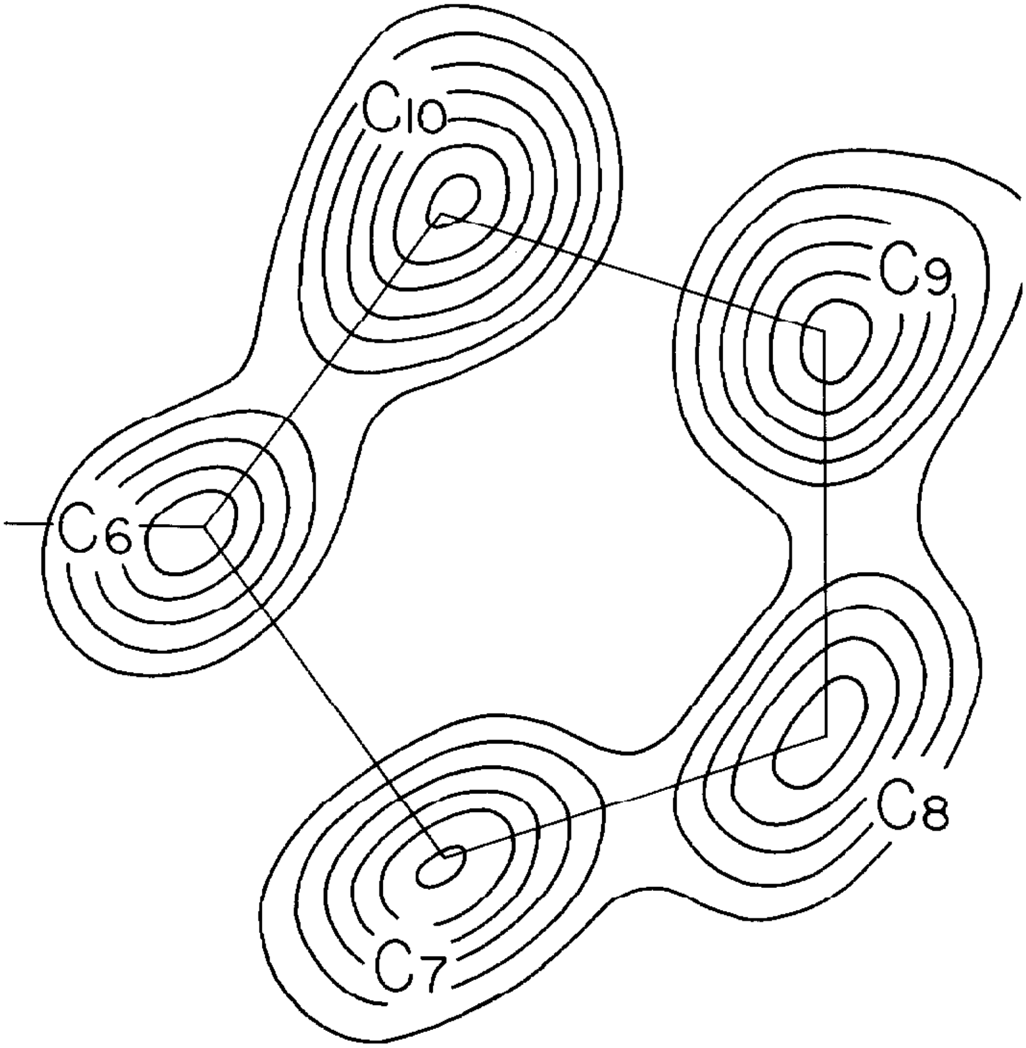

Figure 9. Electron density map in the best plane (table 6) of the cyclopentadienyl ring C_6-C_{10} of α-keto-1, 1'-trimethyleneferrocene. The contours are drawn at intervals of 2, 3, 4 ... e. $\AA^{-2}$. The orientation is as in figure 5.

program written for the 220 computer by Duchamp (31). The principal anisotropy shown by these electron density maps is due to the motion of the molecule as a whole. Superimposed upon this vibration there appears to be a tangential motion of the ring carbon atoms which are not attached to the bridge.

iv. Molecular packing.

The molecular packing of α-keto-1, 1-trimethyleneferrocene is shown in figure 10. The intermolecular distances less than 3.7 Å were calculated using a 220 program written by Barker (32) to generate the coordinates of the nearest symmetry-related molecules from the heavy atom coordinates in table 2. The results of this calculation are given in table 8. No calculation of the intermolecular H-H or H-heavy atom distances was run since the coordinates of the hydrogen atoms are only assumed.

v. Mechanistic implications.

The crystal structure of α-keto-1, 1'-trimethyleneferrocene has been presented here as a possible model for the configuration of the carbonium ion generated in the solvolysis of α-acetoxy-1, 1'-trimethyleneferrocene. If indeed the ketone in the crystal and the carbonium ion in solution are quite similar, it is difficult to explain the marked stability of the latter as observed by Hill and Richards. Stabilization by the iron atom would seem to be ruled out in this model since the distance from the iron atom to the α-carbon, as shown in

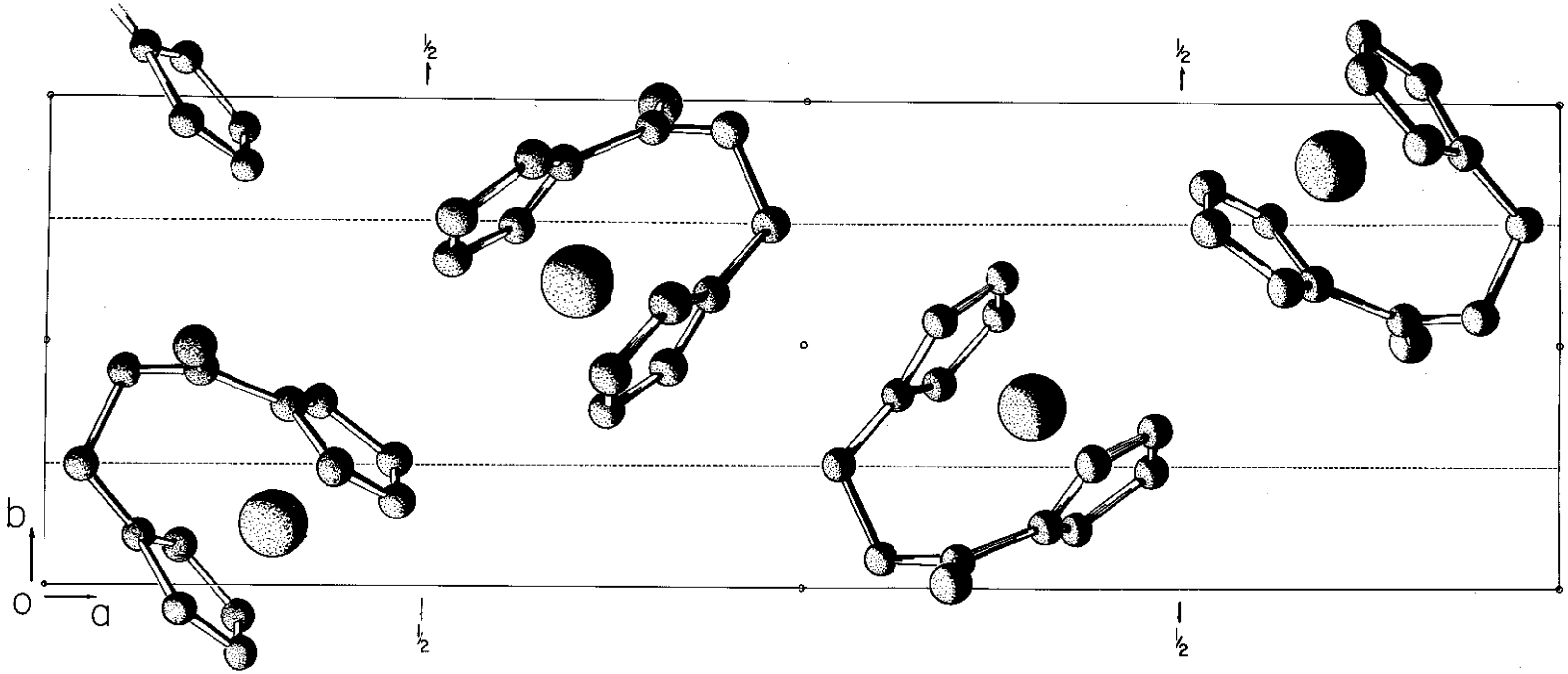

Figure 10. The structure of α-keto-1, 1'-trimethyleneferrocene as viewed along [001].

Table 8. Intermolecular distances less than 3.7 Å for α-keto-1,1'-trimethyleneferrocene. The atoms referred to in the first column belong to the reference molecule at x, y, z.

From	To	In molecule at	D(Å)
C_{11}	C_8	$x, 1 + y, z$	3.439
O	C_{13}	$\bar{x}, 1 - y, 1 - z$	3.501
O	C_5	$x, y, 1 + z$	3.532
O	C_{12}	$\bar{x}, 1 - y, 1 - z$	3.559
O	C_{10}	$x, y, 1 + z$	3.585
C_{10}	C_{13}	$\bar{x}, \bar{y}, \bar{z}$	3.606
C_4	C_9	$\frac{1}{2} - x, \frac{1}{2} + y, \bar{z}$	3.624
C_{12}	C_8	$x, 1 + y, z$	3.637
C_{12}	C_{12}	$\bar{x}, 1 - y, \bar{z}$	3.642
C_6	C_6	$\bar{x}, \bar{y}, \bar{z}$	3.668

figure 7, is too long (2.9 Å) for an appreciable Fe-C interaction. In addition, the vacant p orbital of the carbonium ion, if taken to be normal to the plane of the carbonyl group, is tilted at an angle of about 59° with respect to an orbital from the iron atom to the α-carbon atom. Nor would it seem possible that appreciable stability could be derived from conjugation of the carbonium ion with the adjacent cyclopentadienyl ring; the α-carbon is bent about 0.3 Å out of the plane of the ring and its p orbital (in the carbonium ion) is inclined at an angle of about 42° to the orbitals of the ring π system.

The stability of the carbonium ion does not seem to be explainable in terms of the structure of the ketone, and it may be necessary to introduce distortions in the molecular framework of the ion. From a study of a scale model of the ketone, it seems possible to twist the C=O bond into coplanarity with the ring and at the same time to bring the α-carbon atom a little closer to the iron atom, but only at the expense of increasing the peripheral iron-ring distances significantly. In the solvolyses of the other compounds studied by Hill and Richards it is probable that the ring bearing the α-carbon atom shifts slightly in its plane, as shown, in order to provide more effective stabilization of the carbonium ion. But, because of its rigid structure, a similar shift in the bridged carbonium ion does not seem possible.

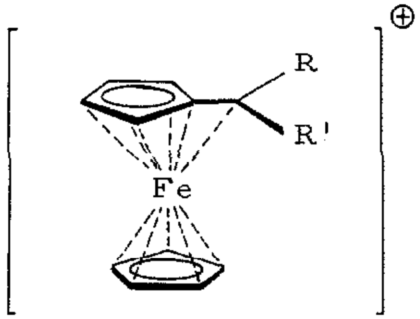

In conclusion it may be said that the iron participation hypothesis of Hill and Richards is a useful one and appears to be valid for many α-metallocenyl cations. However, the factors which influence the stability of the carbonium ion from the solvolysis of α-acetoxy-1,1'-trimethyleneferrocene are still open to speculation.

References to Part I.

1. T. J. Kealy and P. L. Pauson, Nature, 168, 1039 (1951).
2. S. A. Miller, J. A. Tebboth and J. F. Tremain, J. Chem. Soc., 632 (1952).
3. R. B. Woodward and E. Csendes, unpublished results (1953); M. Rosenblum, Ph. D. Dissertation, Harvard University, Cambridge (1953).
4. K. L. Rinehart, Jr., and R. J. Curby, Jr., J. Am. Chem. Soc., 79, 3290 (1957).
5. K. Schlögl, M. Peterlik and H. Seiler, Monatsh., 93, 1309 (1962); C. A., 59, 3951h (1963).
6. K. L. Rinehart, Jr., D. E. Bublitz and D. H. Gustafson, J. Am. Chem. Soc., 85, 970 (1963).
7. K. Schlögl and M. Peterlik, Monatsh., 93, 1328 (1962); C. A., 59, 3953g (1963).
8. E. A. Hill, Ph. D. Dissertation, California Institute of Technology, Pasadena (1961).
9. L. M. Jackman, "Applications of Nuclear Magnetic Resonance Spectroscopy in Organic Chemistry," Pergamon Press, New York, N. Y., 1959, pp. 122-124.
10. J. H. Richards and E. A. Hill, J. Am. Chem. Soc., 81, 3484 (1959); E. A. Hill and J. H. Richards, ibid., 83, 3840 (1961); E. A. Hill and J. H. Richards, ibid., 83, 4216 (1961).

11. M. J. Buerger, "X-Ray Crystallography," John Wiley and Sons, Inc., New York, 1942, pp. 221-295.

12. M. J. Buerger, "Photography of the Reciprocal Lattice," Murray Printing Co., Cambridge, Mass., ASXRED Monograph 1, 1944.

13. M. E. Burke, private communication (1963).

14. A. Hybl, Ph. D. Dissertation, California Institute of Technology, Pasadena (1961).

15. R. S. Deverill, private communication (1962).

16. L. Pauling, "Nature of the Chemical Bond," Cornell University Press, Ithaca, N. Y., 1960, p. 260.

17. K. Hoogsteen, "Crystallographic Fourier Summation Program for the Burroughs 220 Computer," California Institute of Technology, Pasadena (1960).

18. R. E. Marsh, "Structure-factor Least-squares Program for Monoclinic Space Groups," California Institute of Technology, Pasadena (1960).

19. J. Berghuis, I. M. Haanappel, M. Potters, B. O. Loopstra, C. H. MacGillavry and A. L. Veenendaal, Acta Cryst., 8, 478 (1955).

20. J. A. Hoerni and J. A. Ibers, ibid., 7, 744 (1954).

21. L. H. Thomas and K. Umeda, J. Chem. Phys., 26, 293 (1957).

22. "Tables of Interatomic Distances and Configuration in Molecules and Ions," The Chemical Society (London), (1958).

23. E. W. Hughes, J. Am. Chem. Soc., 63, 1737 (1941).

24. J. D. Dunitz, L. E. Orgel and A. Rich, Acta Cryst., 9, 373 (1956).

25. A. F. Berndt, Ph. D. Dissertation, California Institute of Technology, Pasadena (1957).

26. E. A. Seibold and L. E. Sutton, J. Chem. Phys., 23, 1967 (1955).

27. Y. T. Struchkov and T. L. Khotsyanova, Kristallografia, 2, 376 (1957).

28. J. S. Rollett and D. R. Davies, Acta Cryst., 8, 125 (1955).

29. J. Waser, ibid., 8, 731 (1955).

30. K. Hebert, private communication (1963).

31. D. J. Duchamp, "Molecular Plane Fourier Program," California Institute of Technology, Pasadena (1962).

32. D. Barker, "Program to Generate Equivalent Positions," California Institute of Technology, Pasadena (1962).

II. The Chloranil-Hexamethylbenzene Complex, A Refinement

1. Introduction

When one allows a hot, concentrated benzene solution of equal molar quantities of chloranil and hexamethylbenzene (I) to cool, purple-red acicular crystals of an intermolecular complex,

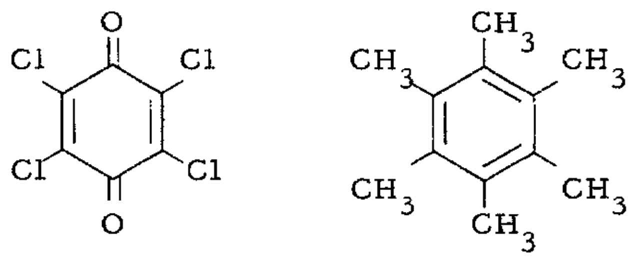

I

$C_6Cl_4O_2 \cdot C_6(CH_3)_6$, are obtained. These crystals show pronounced pleochroism, the maximum light absorption being parallel to the needle axis (a axis). This indicates that the molecules are probably stacked in columns of alternating chloranil and hexamethylbenzene molecules parallel to the a axis.

The crystal structure of the complex between chloranil and hexamethylbenzene has been investigated by Harding and Wallwork (1). They found the space group to be $P2_1/c$, with unit-cell dimensions $a = 7.30$ Å, $b = 8.64$ Å, $c = 15.26$ Å and $\beta = 106°$. There are two complexes in the unit cell with each molecule lying on a center of symmetry. They reported extreme non-planarity for the chloranil and hexamethylbenzene molecules and explained the puckering in terms of steric interactions and polarization bonding between the two molecules. Since then, Donohue and Trueblood (2) and Nyburg (3) have expressed surprise at this and other features of the reported structure and have suggested that, in view of the small number of observed reflections (only 185), the reported non-planarity might not be significant. A refinement of this structure using the data of Harding and Wallwork was initiated in order to see if their data might not be consistent with a more reasonable structure.

2. Refinement of the Structure

Using the observed structure factors listed in table 2 of Harding and Wallwork, several cycles of least-squares refinement of the positional parameters were carried out. The calculations were performed on the Burroughs 220 computer using the monoclinic structure factor and least-squares program written by Marsh (see Part I, p. 17). The weights were taken inversely proportional to the square of the form factor of carbon.* Individual isotropic temperature parameters were adjusted only approximately, with the restriction that chemically equivalent atoms have identical parameters. In order to place the data on an absolute scale, it was found

---

*A number of pronounced and persistent discrepancies between calculated and observed structure factors among the weak reflections discouraged the author from the usual scheme of assigning weights inversely proportional to the observed structure factors.

necessary to multiply the observed structure factors by 4.25.

The atomic parameters and their standard deviations before and after refinement are listed in table 1. The standard deviations after refinement are about 0.06 Å for the positions of the oxygen and carbon atoms and 0.02 Å for the chlorine atoms.* The standard deviations in the temperature factors are about 2.0 for the light atoms and 0.7 for the chlorine atoms. In the last least-squares refinement cycle no coordinate shift was as much as one-third of its standard deviation. The final R factor was 0.14 compared with the value 0.27 obtained from the parameters of Harding and Wallwork.

3. Discussion

The best planes through the chloranil and hexamethylbenzene rings were calculated using the 220 computer program written by the author (see Appendix, part II). Two calculations were run, the first using the atomic coordinates of Harding and Wallwork** and the other the refined coordinates; the results are shown in table 2. As may be seen, the two rings are more nearly planar after refinement than they were before. The two molecules are closely parallel, the calculated dihedral angle being 2.1°.

---

* These values are in approximately the expected ratio whereas, as Donohue and Trueblood (2) point out, the standard deviations given by Harding and Wallwork are greater for the chlorine atoms than for the lighter atoms. The latter authors have acknowledged (4, 6) that the standard deviations which they reported were calculated incorrectly.

** It is clearly more appropriate to include all twelve atoms of the chloranil molecule in the calculation of the best plane than, as Harding and Wallwork did, to consider only the six carbon atoms.

Table 1. Atomic parameters for the chloranil-hexamethylbenzene complex before and after refinement. The isotropic temperature factors are expressed in the form $T = \exp(-B \sin^2 \Theta / \lambda^2)$. A value of 5.04 for B was used by Harding and Wallwork for the carbon and chlorine atoms. The standard deviations have been multiplied by 10^3. No temperature factor or standard deviations were reported for the oxygen atom. The atoms are numbered as in figure 1.

	Before refinement			After refinement			
	x	y	z	x	y	z	B
C_1	0.076(3)	-0.147(3)	0.040(2)	0.071(5)	-0.140(6)	0.028(2)	1.0
C_2	0.075(3)	-0.007(3)	0.093(2)	0.056(7)	-0.024(5)	0.093(3)	1.0
C_3	-0.016(3)	0.132(3)	0.043(2)	-0.011(6)	0.124(5)	0.063(3)	1.0
Cl_4	-0.020(3)	0.253(3)	0.142(2)	-0.024(2)	0.260(2)	0.142(1)	5.5
Cl_5	0.123(3)	-0.333(3)	0.069(2)	0.141(2)	-0.335(2)	0.071(1)	5.5
O_6	0.083	-0.053	0.173	0.095(4)	-0.058(4)	0.181(2)	3.4
C_7	0.554(3)	-0.127(3)	0.052(2)	0.576(6)	-0.132(6)	0.057(3)	1.9
C_8	0.528(3)	0.019(3)	0.094(2)	0.542(8)	0.007(5)	0.098(3)	1.9
C_9	0.478(3)	0.145(3)	0.047(2)	0.479(6)	0.130(6)	0.037(3)	1.9
C_{10}	0.428(3)	0.307(3)	0.083(2)	0.446(6)	0.302(7)	0.086(3)	6.0
C_{11}	0.615(3)	-0.275(3)	0.110(2)	0.654(6)	-0.265(8)	0.116(4)	6.0
C_{12}	0.594(3)	0.029(3)	0.199(2)	0.590(7)	0.034(8)	0.202(4)	6.0

Table 2. Best planes through the molecules of the chloranil-hexamethylbenzene complex before and after refinement. The values m_i are the direction cosines of the normals to the best planes with respect to the orthogonal axes a, b, c*. The origin was not included in the least-squares calculations.

Before refinement				After refinement			
Direction cosines		Atom	Deviation	Direction cosines		Atom	Deviation
m_a	0.967	C_1	-0.094 Å	m_a	0.961	C_1	-0.087 Å
m_b	0.248	C_2	-0.218	m_b	0.270	C_2	-0.050
$m_c{}^*$	0.060	C_3	-0.033	$m_c{}^*$	0.066	C_3	-0.019
		Cl_4	0.051			Cl_4	-0.001
		Cl_5	0.065			Cl_5	0.009
		O_6	0.078			O_6	0.029
		Origin	0.000			Origin	0.000
m_a	0.967	C_7	0.041	m_a	0.961	C_7	-0.015
m_b	0.243	C_8	0.044	m_b	0.275	C_8	0.045
$m_c{}^*$	0.073	C_9	-0.009	$m_c{}^*$	0.029	C_9	-0.028
		C_{10}	0.112			C_{10}	-0.023
		C_{11}	0.095			C_{11}	-0.029
		C_{12}	-0.129			C_{12}	0.014
		Origin	-3.530			Origin	-3.508

The bond distances and angles before and after refinement were calculated and the results are shown in figure 1. These molecular dimensions show no significant deviations from the expected values, the extreme value 1.71 Å, calculated for a pair of C-CH_3 bonds, being only two standard deviations from the normal distance of 1.54 Å. The intermolecular distances after refinement are shown on the packing diagram in figure 2. The closest approaches, 3.32 Å, are between oxygen and chlorine atoms of chloranil molecules in adjacent stacks.

On the basis of this refinement it appears that the experimental data of Harding and Wallwork are compatible with planar molecules having normal dimensions and it is not necessary to postulate, as they have done, a zigzag arrangement of polarization bonds to explain this structure. This refinement was recently published (5); in reply Wallwork and Harding wrote:

> The refinement of the crystal structure of the chloranil-hexamethylbenzene complex by Jones and Marsh (ref. 5, this thesis) confirms the suggestion already made (ref. 4, this thesis) that the molecular distortions originally reported (ref. 1, this thesis) are probably not significant. They were mistakenly interpreted as being significant in the original work because the standard deviations of atomic positions were incorrectly calculated. In spite of the improvement in R and molecular planarity brought about by

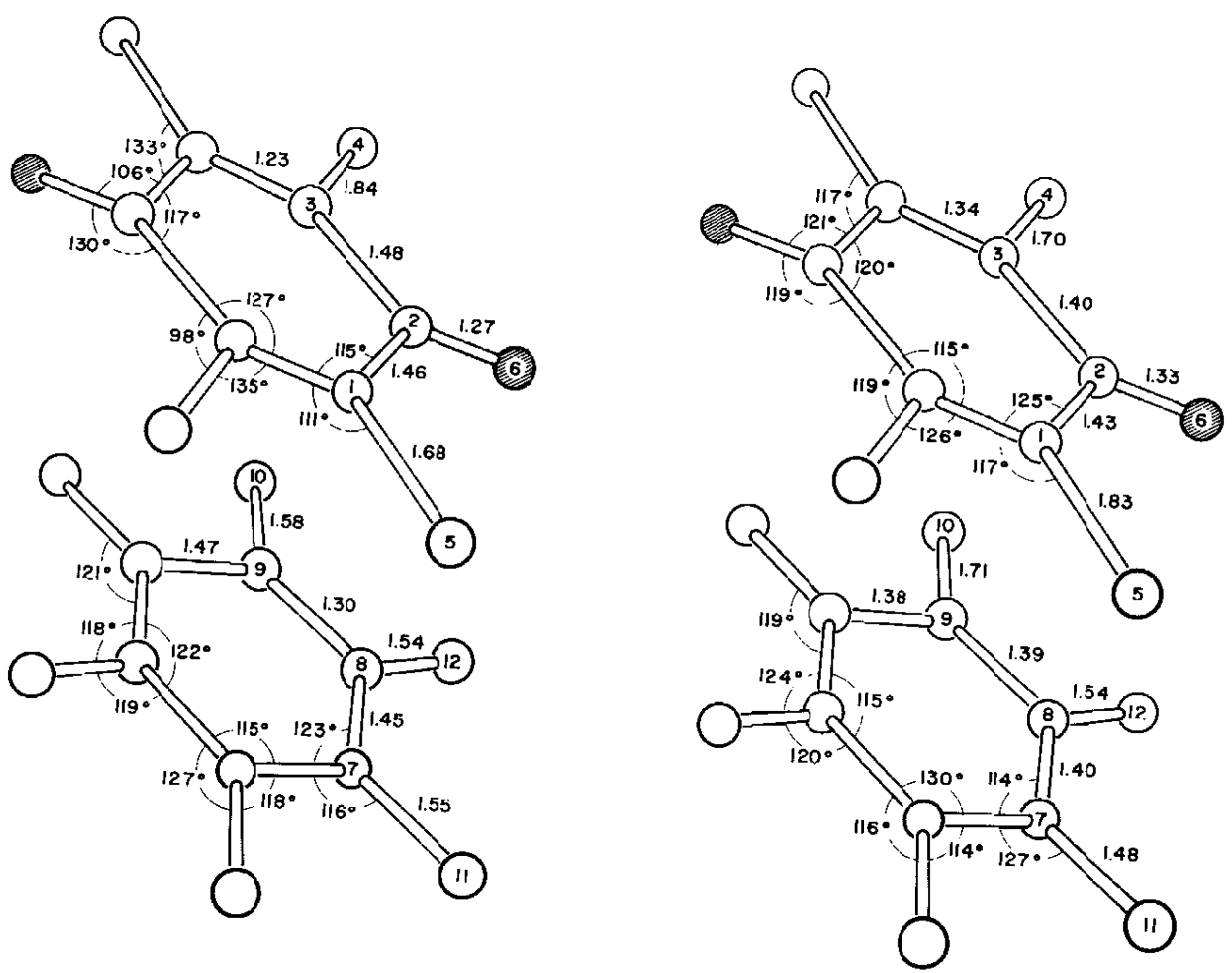

Before refinement

After refinement

Figure 1. Molecular dimensions for the chloranil-hexamethylbenzene complex before and after refinement.

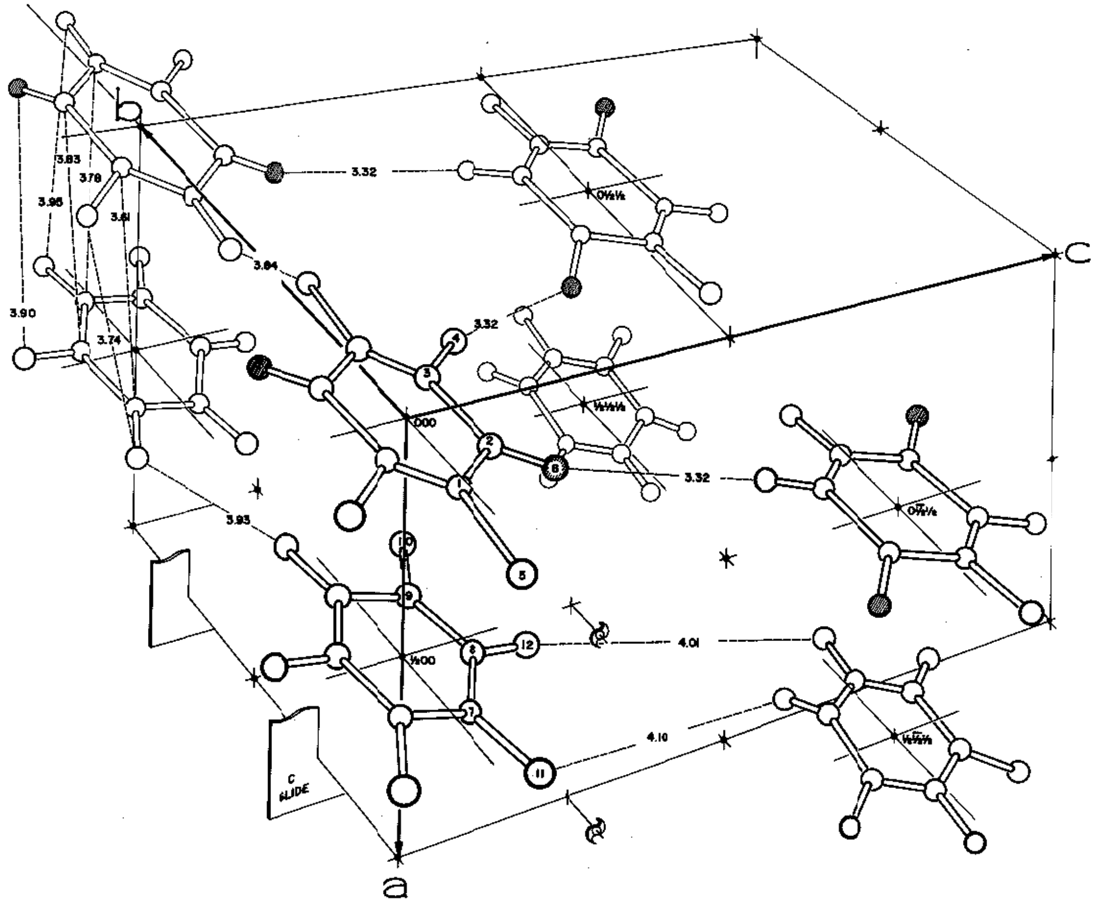

Figure 2. The molecular packing and intermolecular distances for the chloranil-hexamethylbenzene complex. The oxygen atoms are shaded.

the recent refinement it is clear that the present X-ray data are not sufficient to establish accurate atomic positions. New and more extensive data are now being obtained at about -100° C, and these will be used in a further refinement of the structure.

References to Part II

1. T. T. Harding and S. C. Wallwork, Acta Cryst., 8, 787 (1955).
2. J. Donohue and K. N. Trueblood, ibid., 9, 965 (1956).
3. S. C. Nyburg, "X-ray Analysis of Organic Structures," Academic Press, New York, 1961, p. 287.
4. S. C. Wallwork, J. Chem. Soc., 494 (1961).
5. N. D. Jones and R. E. Marsh, Acta Cryst., 15, 809 (1962).
6. S. C. Wallwork and T. T. Harding, ibid., 15, 810 (1962).

III. Two Phenazine Derivatives from Pseudomonas Aureofaciens.

1. Introduction

Recent investigations by Haynes and coworkers (1), Kluyver (2), Olson (3) and the author have led to the isolation and identification of two phenazine derivatives from cultures of the soil bacterium Pseudomonas aureofaciens. The major constituent of extracts of this bacterium is a golden colored (hence the name aureofaciens) compound, $C_{13}H_8O_2N_2$, which has been shown to be 1-phenazinecarboxylic acid (I).

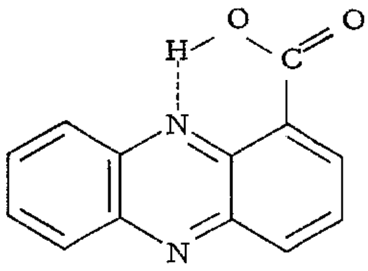

I

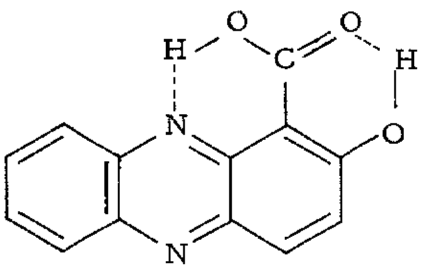

II

One of several minor constituents is an orange compound, $C_{13}H_8O_3N_2$, which was only very recently shown by Olson to be 2-hydroxy-1-phenazinecarboxylic acid (II). The structure of II was concurrently and independently determined by the author using X-ray diffraction techniques.

2-Hydroxy-1-phenazinecarboxylic acid, although orange when crystalline, forms a blood-red solution in weak base. Olson has found that the red color does not begin to appear until nearly two equivalents of base have been added to the yellow neutral solution of II in 2:1 dioxane-water. It is probable, therefore, that the highly colored species is not the carboxylate anion but rather the keto dianion (III). This is confirmed by the fact that 1-phenazinecarboxylic acid (I) remains light yellow in base while 2-hydroxyphenazine changes from light yellow to dark red-orange (4). In neutral solution and in the solid, II probably exists in the enol form.

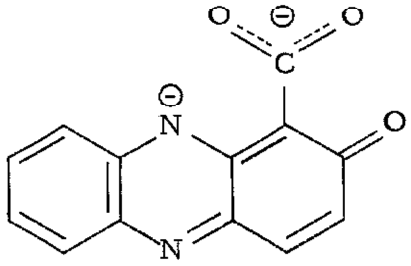

III

In the purification of the orange pigment (II) Olson experienced some difficulty separating it from the 1-phenazinecarboxylic acid (I) which is present in the crude extracts. Chromatography was of no use; however, he was able eventually to separate the two components by repeated extraction of the solid mixture with 10% sodium hydroxide solution. The yellow 1-phenazinecarboxylate anion is apparently much less soluble in base than the red keto dianion of II.

The structure of II was determined by Olson from ultraviolet and infrared spectra and from the synthesis outlined below.

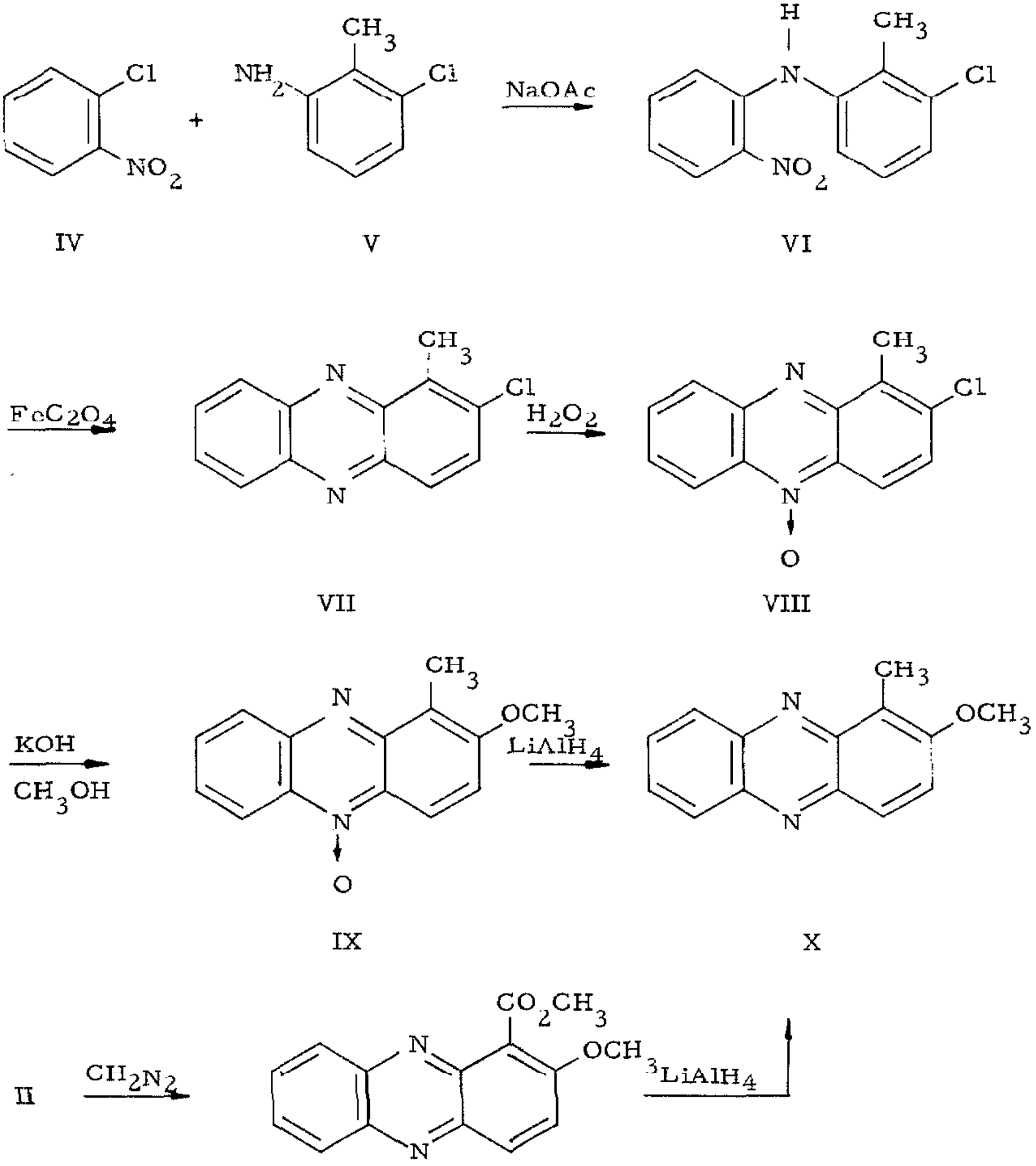

3-Chloro-2-methyl-2'-nitrodiphenylamine (VI) was prepared by heating a mixture of o-chloronitrobenzene (IV), 3-chloro-2-methylaniline (V) and sodium acetate. The product was reduced with ferrous oxalate to give 1-methyl-2-chlorophenazine (VII) which was oxidized with hydrogen peroxide to give an N-oxide, presumably 1-methyl-2-chlorophenazine-5-oxide (VIII). The oxide was then refluxed with potassium hydroxide in methanol to give 1-methyl-2-methoxyphenazine-5-oxide (IX), which was then reduced with lithium aluminum hydride to 1-methyl-2-methoxyphenazine (X). The latter was found to be identical in all respects with the product formed from the methylation of II with diazomethane, followed by reduction with lithium aluminum hydride. Thus II is shown unequivocally to be 2-hydroxy-1-phenazinecarboxylic acid.

At the time that the author's investigation of II was begun, its molecular structure had tentatively been identified as 2-hydroxy-1-phenazinecarboxaldehyde-10-oxide (XI), which has the same empirical formula as II. This erroneous identification was corrected by Olson shortly before the crystal structure was solved by the author.

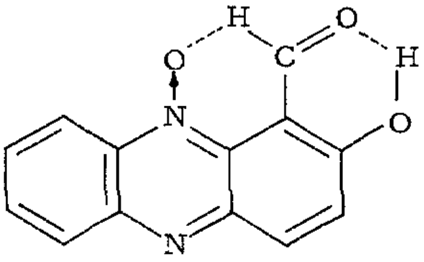

XI

In the course of this investigation the crystal structure of 1-phenazinecarboxylic acid was also determined, albeit unintentionally. The two-dimensional structure of the latter is reported here because it provided experience which was useful in the more difficult determination of the crystal structure of II.

2. Determination and refinement of the structures.

i. Preliminary crystallographic measurements.

About 5 mg. of an orange compound purported to be a fairly pure sample of an undetermined phenazine pigment, $C_{13}H_8O_3N_2$, was obtained from E. S. Olson. The sample was dissolved in a small volume of warm acetic anhydride in an Erlenmeyer flask and was set aside to crystallize. The first crystals appeared at the surface of the solution in the form of elongated orange plates; however, as the solution evaporated further, clusters of slender orange needles began to appear at the bottom of the flask. The crystals were collected on a micro-Buchner funnel and were washed with a small volume of fresh acetic anhydride followed by a few drops of ether.

A cursory microscopic examination of the two types of crystals suggested they might be different habits of the same crystal structure.* In order to determine if this was the case goniometric measurements were taken from a crystal of each habit. One of the plates with several good faces was mounted with its elongated direction parallel to the optical goniometer rotation axis. Figure 1 shows a typical cross section of one of the plates with the faces indexed; the goniometric measurements are listed in table 1. One of the needle-like crystals was then mounted with the needle axis parallel to the goniometer rotation axis. The faces on the needle were not as well defined as those on the plates; therefore, the measurements listed in table 2 are only approximate. Figure 2 shows a typical cross section of one of the needles with the faces indexed and the positions of the crystallographic axes indicated. The goniometric measurements taken on the plate and the needle clearly show that they were not simply two different habits of the same crystal structure.

The first X-ray diffraction pattern observed from these crystals was a 20° oscillation photograph** taken from one of the

---

* Actually, as will be shown later, the two crystal forms are different compounds. The needles are 1-phenazinecarboxylic acid (I) and the plates are 2-hydroxy-1-phenazinecarboxylic acid (II). The orange color of the former was misleading since in pure form I is bright yellow. That the crystals of I were contaminated with II may be seen from the fact that both gave red solutions in base, whereas pure I gives no such color test. Nor could the two compounds have been distinguished from their melting points. Both began to decompose (presumably decarboxylation) near 200°; the remainder of I melted at 225.5-230° (lit. (4) m. p. 239°) while II melted at 222-223.5° (lit. (3) m. p. 225-266°).

** Unless otherwise noted, copper K_{α} (nickel filtered) radiation excited at 45 kv. and 15 ma. was used for all photographs.

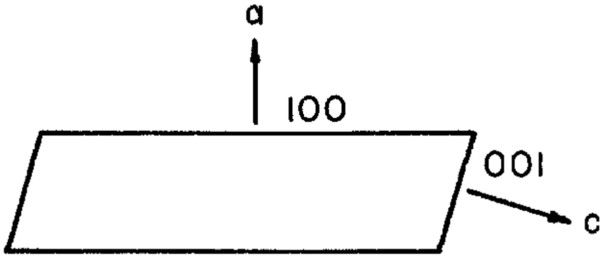

Figure 1. Typical cross section of a plate (2-hydroxy-1-phenazinecarboxylic acid) crystallized from acetic anhydride. The faces are indexed and the positions of the crystallographic axes are indicated.

Table 1. Goniometric measurements taken on a crystal of the type shown in figure 1.

Longitude	Latitude	Index
61° 37'	0° 02'	$00\bar{1}$
134° 38'	359° 56'	100
241° 38'	0° 00'	001
314° 37'	0° 08'	$\bar{1}00$

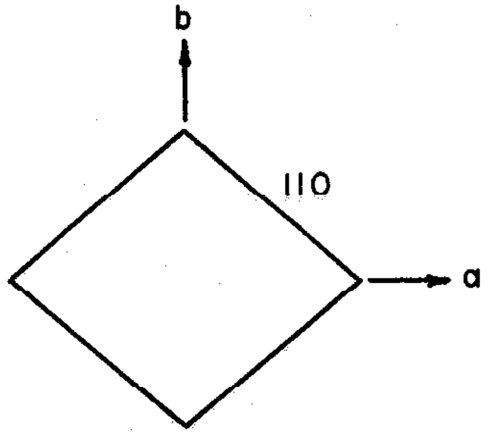

Figure 2. Typical cross section of a needle (1-phenazinecarboxylic acid) crystallized from acetic anhydride. The faces are indexed and the positions of the crystallographic axes are indicated.

Table 2. Goniometric measurements taken on a crystal of the type shown in figure 2.

Longitude	Latitude	Index
356° 01'	0° 09'	$\bar{1}10$
76° 21'	0° 01'	110
175° 49'	359° 57'	$1\bar{1}0$
256° 10'	0° 03'	$\bar{1}\bar{1}0$

plates rotated parallel to its elongated direction (b axis). Measurements from this photograph gave a value of 5.89 Å for b. Using the equi-inclination Weissenberg technique a set of layer-line photographs, h0ℓ to h3ℓ inclusive, was obtained. From the h0ℓ photograph the values a = 21.6 Å, c = 8.38 Å and β = 107° were measured. The positions of the a and c axes on the film were chosen such as to make these axes normal to the crystal faces (see figure 1). More precise unit cell parameters were later determined for this compound (2-hydroxy-1-phenazinecarboxylic acid); these have the values

a = 21.777 ± 0.002 Å, β = 107.02 ± 0.02°,
b = 5.896 ± 0.001 Å,
c = 8.416 ± 0.001 Å.

These lattice constants were obtained from Straumanis-type, zero-layer Weissenberg photographs taken at room temperature using crystals mounted about the b and c axes. An optical comparator was used to measure the relative positions of a total of 129 reflections from the h0ℓ and hk0 photographs; the Bragg angle was then calculated for each reflection. The lattice parameters were calculated using the Burroughs 220 computer program written by the author (see Appendix, part I). The estimated uncertainties in the lattice parameters are about ten times the calculated standard deviations. The corrections for absorption and eccentricity were found to be negligible.

The density of one of the plates was determined to be about

1.53 g. cm.$^{-3}$ by flotation in a mixture of chloroform and carbon tetrachloride. Assuming four molecules in the unit cell the calculated density for $C_{13}H_8O_3N_2$ (m. w. 240.2) is 1.54 g. cm.$^{-3}$

The systematic extinctions from the b axis photographs and from an hk0 precession photograph taken with unfiltered molybdenum radiation gave the following conditions limiting possible reflections: $hk\ell$, no conditions; $h0\ell$, h = 2n and 0k0, k = 2n. The crystals, therefore, probably belong to the centrosymmetric, monoclinic space group $C_{2h}^{5} - P2_1/a$. Because the molecules have no center of symmetry, they must lie in general symmetry positions in the unit cell.

Another 20° oscillation photograph was taken, this time from one of the needles with its axis aligned parallel to the rotation axis of the camera. Measurements taken from this film gave a value of 3.87 Å for the c axis. This same crystal was used to collect the set of photographs hk0 to hk3 inclusive by the equi-inclination Weissenberg technique. The hk0 film gave the measured values $1/a^* = 18.2$ Å and b = 14.3 Å. An $h0\ell$ photograph was then taken with unfiltered molybdenum radiation using the precession technique. Measurements from this film gave a β-angle of 99.5°. The a axial length then becomes 18.5 Å. More precise lattice constants were determined later; these have the values $1/a^* = 18.222 \pm 0.002$ Å and $b = 14.338 \pm 0.002$ Å. These values were obtained by the method outlined above from 172 reflections on an hk0 Straumanis-type, Weissenberg photograph. The author has been unable to mount one of these needles to obtain precision data around another axis.

The density of one of the needles was determined by flotation in a mixture of carbon tetrachloride and chloroform to be about 1.54 g. cm.$^{-3}$ Assuming four molecules in the unit cell and the empirical formula $C_{13}H_8O_3N_2$, the calculated density is 1.57 g. cm.$^{-3}$ *

The systematic extinctions observed on the photographs taken with the needle-like crystal were the same as those observed for the plate, hence the space group $C_{2h}^5 - P2_1/a$ may be assigned.

Because the crystals of the two habits were the same color, had nearly the same densities and unit cell volumes, crystallized in the same space group, had similar melting points and gave the same color test, the author came to the conclusion at this point that they were polymorphic forms of the same compound. Polymorphism is not an uncommon occurrence in crystals of organic compounds. The infrared spectra of these two crystal forms would have shown instead that they were different compounds, but at this stage of the investigation there was not sufficient sample available to obtain spectra.

---

*Since the needles have been shown to be 1-phenazinecarboxylic acid (I), the correct empirical formula is $C_{13}H_8O_2N_2$ (m. w. 224.21). The correct calculated density is 1.47 g. cm.$^{-3}$ The density of one of the needles has been subsequently redetermined and the value 1.51 g. cm.$^{-3}$ was obtained. The discrepancy between the observed and calculated densities is probably due to the fact that the needles were quite small, making it difficult to tell when they were suspended.

ii. The two-dimensional structure of 1-phenazinecarboxylic acid.

Because of their short axis (3.87 Å) and more favorable morphology, it was decided to determine the structure of the needle-like crystals. The same crystal from which the unit cell parameters were obtained was used to collect the hk0 intensity data. Three separate packs of three films each were taken, the exposure times being 2, 16, and 50 hours. A graduated intensity scale was also prepared from this same crystal.

The intensities from the hk0 photographs were estimated visually by comparing them to the intensity scale with the aid of a large magnifying glass. An average film factor was used to scale the readings from the several photographs. Lorentz and polarization corrections were then applied to the data using the Burroughs 220 computer program written by Hybl (ref. 14, part I).

The most obvious features of an hk0 photograph from this crystal were the regions of intense reflections surrounded by areas of relatively weak reflections. In order to visualize more readily the intensity distribution, a weighted hk0 reciprocal lattice net was constructed. This net, shown in figure 3, was plotted from the corrected intensities, the radius of each spot being proportional to $|F|$ and the area to $|F|^2$. The plot clearly shows the Fourier transform of a six-membered ring lying nearly flat in the unit cell with one of the

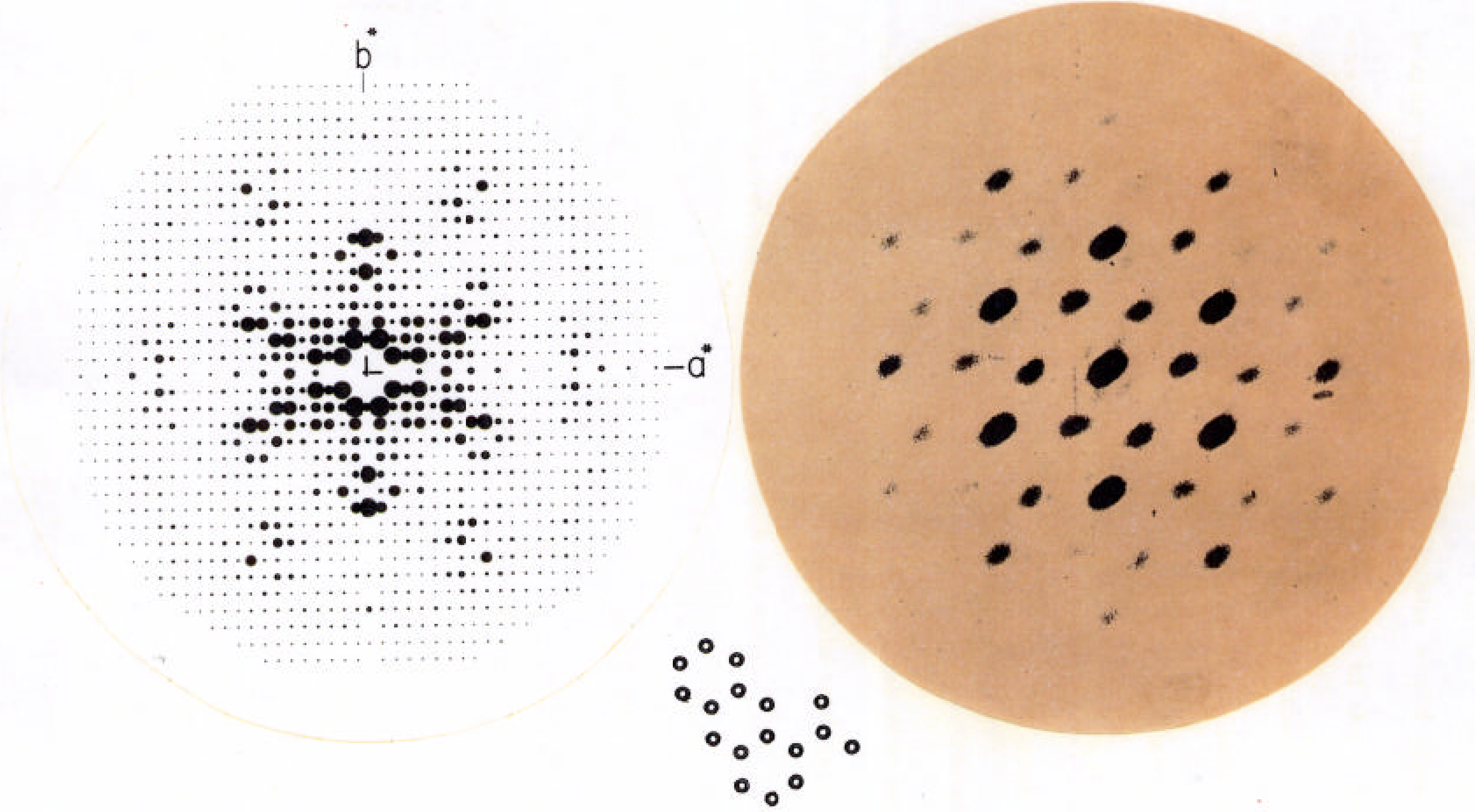

Figure 3. Weighted hk0 reciprocal lattice net (left) for 1-phenazinecarboxylic acid compared to the optical transform (enlarged approximately 40X) of the molecule. The drawing of the mask (actual size) from which the transform was obtained indicates the orientation of the molecule.

2.8 Å interatomic vectors roughly parallel to the b^* reciprocal lattice vector. That the hk0 photographs would show this pattern was quite expected, since the 3.87 Å axis of the unit cell confines the molecules to lie nearly flat in a plane normal to [001]. The weighted reciprocal lattice does not, however, indicate a unique orientation for the phenazine ring system. In theory the patches of high intensity on the weighted reciprocal lattice net should appear to be elongated in the direction normal to the line joining the ring centers, due to the increased resolution of the transform parallel to the line of centers. However, because of the mm symmetry of the hk0 reciprocal lattice net, it is impossible to determine the direction of elongation of the regions of high intensity. There were, then, three possible orientations for the rings, each at an angle of 120° from the other two, as shown below. However, orientations 2 and 3 are equivalent because of the pgg symmetry of the hk0 projection of the unit cell.

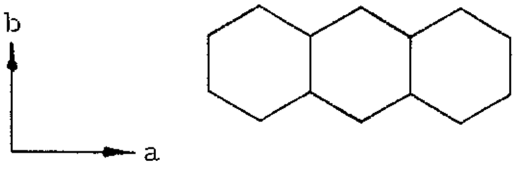

1

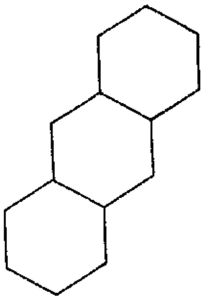

2

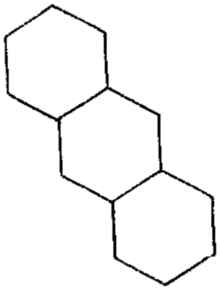

3

Later, after the structure had been determined, the optical diffraction pattern of the molecule was photographed for comparison with the weighted reciprocal lattice net. Both the optical transform and the mask from which it was obtained are shown in figure 3. The optical transform was prepared using an apparatus similar to that of Taylor, Hinde and Lipson (5). The mask was constructed from stiff cardboard on a scale of 0.13" = 1 Å, the holes being 5/64" in diameter for all atoms (6). The apparent elongation of the maxima normal to the line of ring centers of the molecule may be clearly seen in this optical transform.

In order to choose between the two possible orientations of the phenazine ring system and to determine the position of the molecule in the asymmetric unit, the (001) Patterson vector map was examined. For simplicity, only the rings were considered, especially since the positions of the substituents were unknown. Also, all of the ring atoms were considered to be equivalent. In this projection, the molecules lie at $x, y; \bar{x}, \bar{y}; \frac{1}{2} + x, \frac{1}{2} - y$ and $\frac{1}{2} - x, \frac{1}{2} + y$. The asymmetric unit of the Patterson projection will, therefore, contain the peaks of the intermolecular vector sets centered at $(2x, 2y)$, $(\frac{1}{2} - 2x, \frac{1}{2})$ and $(\frac{1}{2}, \frac{1}{2} - 2y)$. These arrays of peaks may overlap, of course. It was useful for the interpretation of the vector map to introduce the further simplification that the atoms of each ring may be represented by a single "atom" at the center of the ring. That this approximation is valid may be seen from an examination of the set of vectors between two six-membered rings, as shown below.

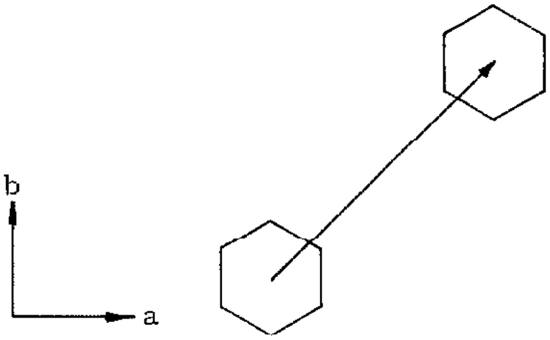

ρ

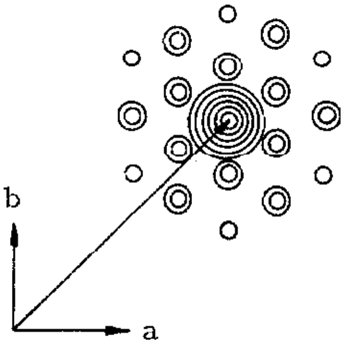

P

The relative position of the two rings is immaterial as long as they have the same orientation. There are 36 vectors in this set, six of which are superimposed on the vector joining the centers of the two rings. Since all of the other peaks of the set are small compared to this peak, the set of 36 vectors may be approximated by the single vector joining the centers. In a similar manner, the set of 196 intermolecular vectors between the atoms of two phenazine ring systems, where each of the individual six-membered rings has the same orientation, may be approximated by the set of 9 vectors joining the ring centers.

Figure 4 shows both of the possible orientations of the phenazine nucleus with respect to the glide line which is parallel to the b axis in the hk0 projection. The intermolecular vector array, P, which is shown for each orientation is independent of the distance of

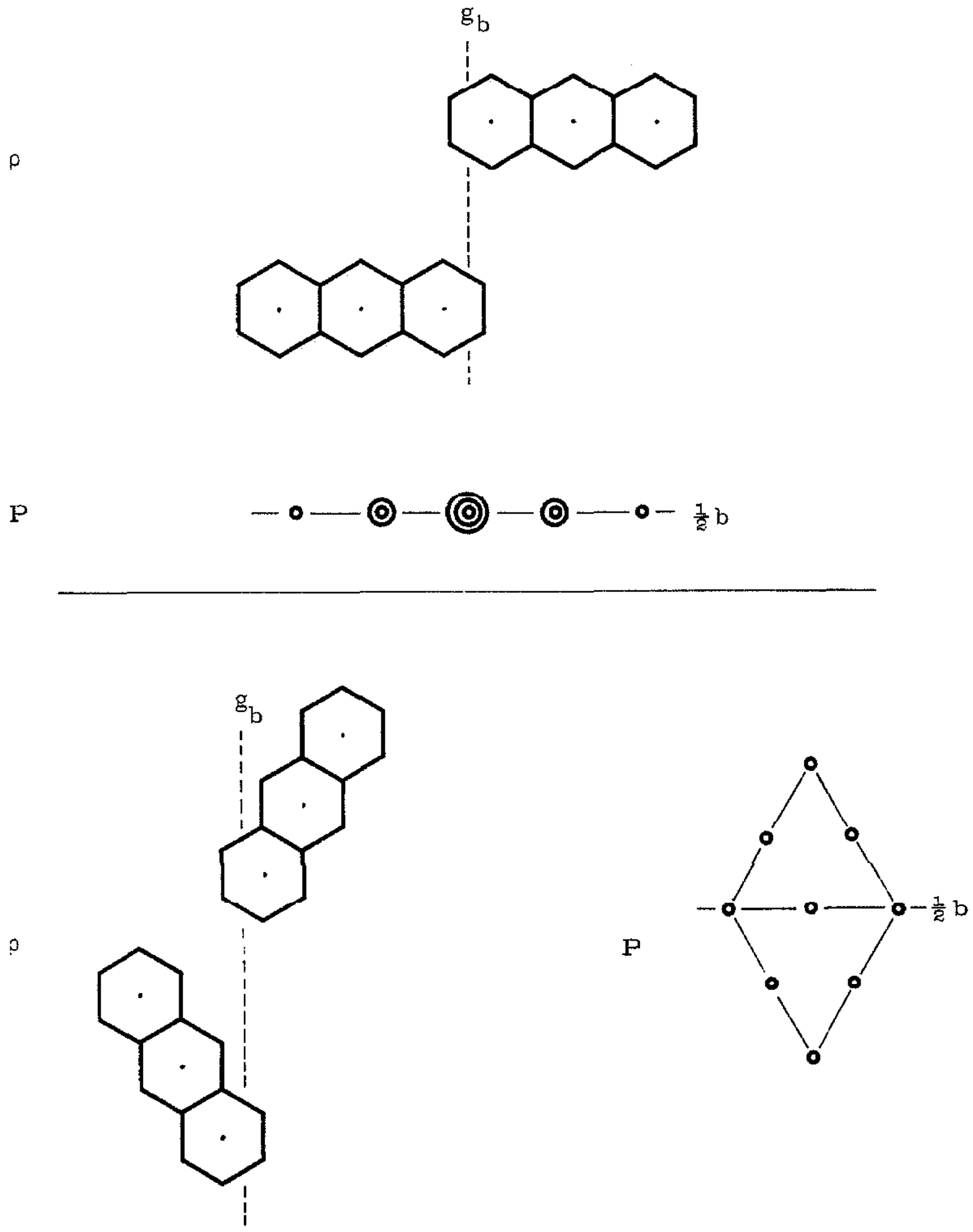

Figure 4. The Patterson intermolecular vector array for two molecules related by a glide line parallel to the b axis, shown for each of the two possible orientations of the phenazine ring system.

the molecule from the g glide. When the ring system lies normal to g, the nine intermolecular vectors form five peaks in a straight line at $y = \frac{1}{2}$. The peaks, which are separated by 2.4 Å, have the relative magnitudes 1: 2: 3: 2: 1. In the other orientation, the intermolecular vectors form a diamond-shaped array of 9 peaks of approximately equal magnitude. Each of the peaks is separated from the closest neighboring peaks by 2.4 Å and the center line of the array is at $y = \frac{1}{2}$. For two phenazine nucleii related by a glide line parallel to the a axis, the vector peak arrays will be the same as above, except that they will be centered at $x = \frac{1}{2}$.

The (001) Patterson projection, shown in figure 5, was calculated from the expression given earlier (see equation 2, Part I) using the Burroughs 220 computer Fourier program written by Hoogsteen. The summations were carried out at intervals of 0.01 a and 0.01 b. The map was not sharpened because the only program available (Duchamp (7)) to do this calculation on the 220 computer uses a modification function which deemphasizes the intermolecular vectors. The problem was to find on this map one of the two vector arrays shown in figure 4. Several fits were obtained but were rejected because of packing considerations. At this point it was observed that if the phenazine nucleus was oriented parallel to the a axis, F(020) would calculate much larger than observed. From this evidence, the orientation shown at the top of figure 4 was dismissed from

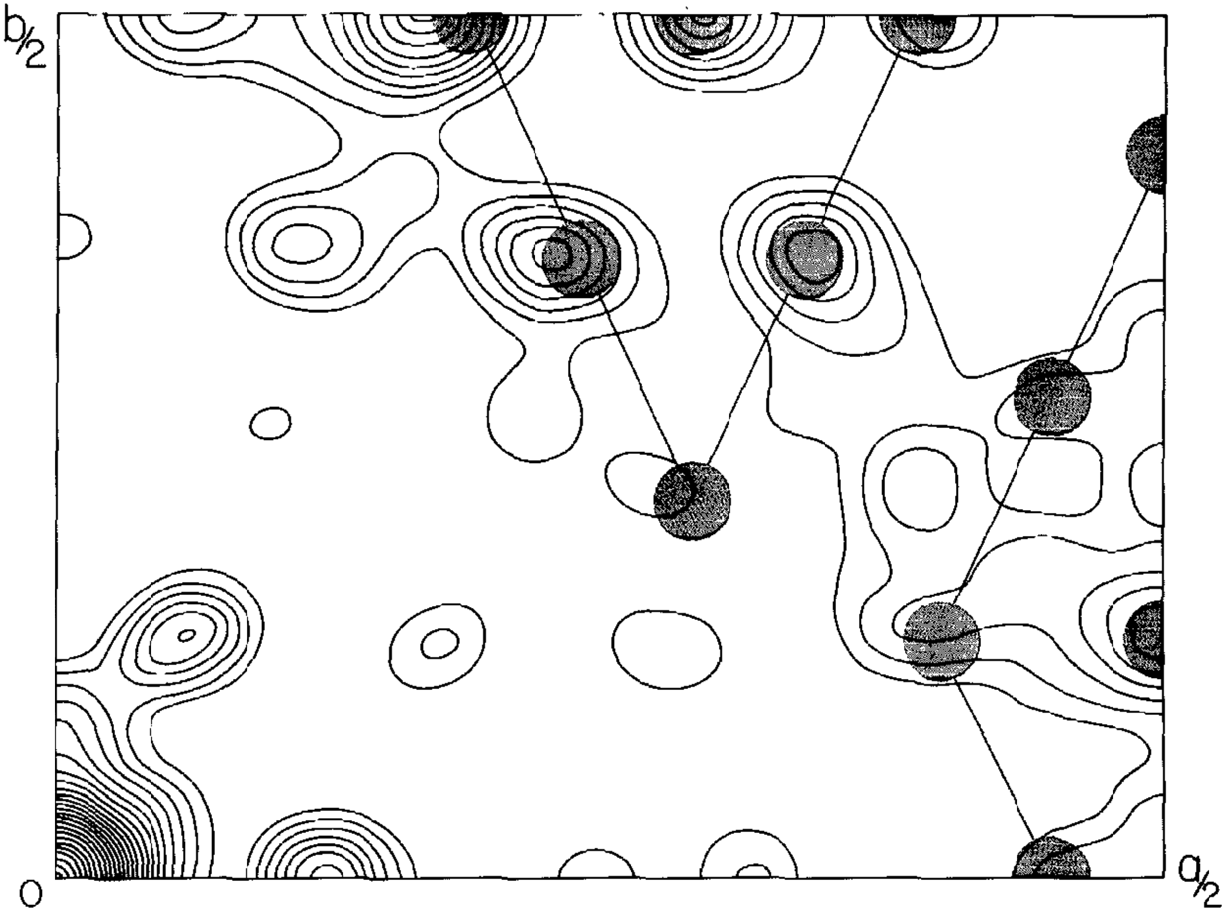

Figure 5. The (001) Patterson projection of 1-phenazinecarboxylic acid with the peaks from vectors between molecules related by glide lines shaded. The contours are drawn at arbitrary but equal levels.

further consideration. This considerably simplified the problem and a reasonable fit, shown by the shaded circles in figure 5, was quickly located.

The atomic coordinates for the ring atoms were derived from the vectors which had been tentatively identified and a structure factor calculation was run using the program written for the monoclinic space groups by Marsh (see Part I, p. 17). The isotropic temperature factor was taken to be 3.0 Å^2 for all atoms. Although the R factor was quite high (over 0.55), the agreement between the observed and calculated structure factors was generally good. An electron density projection onto (001) was then calculated from 49 of the phased hk0 structure factors using the Hoogsteen program with the same summation intervals as before. This map clearly showed the positions of the 14 ring atoms and also contained, adjacent to C_1, a group of three large, but poorly resolved, peaks which looked very much like a carboxyl group.* The only other positive regions on the map were two small peaks, either of which might possibly have been a hydroxyl group.

At this time the author was still under the mistaken impression that the needle-like crystals being investigated were the unknown

---

* About this time Olson showed that the unknown pigment was not 2-hydroxy-1-phenazinecarboxaldehyde-10-oxide (X) as was originally believed, but rather contained a hydroxyl and a carboxyl group.

phenazine pigment, $C_{13}H_8O_3N_2$. Because of this, numerous attempts were made to refine the structure by the least-squares technique, including in the calculations the carboxyl group and an oxygen atom at one or the other of the positions indicated by the Fourier map. After every few cycles of least-squares a new electron density map was calculated. Although the ring and carboxyl atoms were better resolved on each successive map, both of the other peaks remained relatively small. It soon became clear that there was no hydroxyl group in this molecule.

The first structure factor calculation run after the hydroxyl group was removed from the trial model gave a value for R of 0.27. Several cycles of least-squares refinement, where the weights were taken inversely proportional to the form factor of carbon and the individual isotropic temperature factors were allowed to shift, brought R down to 0.20. The weighting function was changed at this point to the $1/F_{obs}$ scheme (see equation 8, Part I). After three more cycles of least-squares, R was 0.15. The weighting function was then changed to the $1/F_{obs}^2$ scheme (see equation 9, Part I) and anisotropic temperature factors were included for the heavy atoms. The hydrogen atoms, whose coordinates were determined assuming C-H and O-H distances of 1.0 Å, were also included in the calculations with isotropic temperature parameters equal to those for the heavy atoms to which they are attached. After six more least-squares refinement cycles, during which the hydrogen atom positions were readjusted manually, all the parameter shifts were less than one-third of their standard deviations. The refinement in two-dimensions was considered complete at this point with R = 0.094. A total of 325 reflections were included in the final structure factor calculation, of which 197 contributed to the least-squares sums. Because of the large temperature motion of the molecule many "less than" reflections had been recorded; however, only four of these calculated larger than the threshold value. Table 3 lists the final heavy atom parameters and their standard deviations and table 4 gives the assumed hydrogen atom parameters. The standard deviations for the heavy atom parameters were obtained from the diagonal terms of the inverse matrix. The final observed and calculated hk0 structure factors are listed in table 5.

The observed structure factors and their calculated signs were used in the Hoogsteen program to obtain the final (001) electron density map shown in figure 6. A difference Fourier map projected onto (001) was also calculated and is shown in figure 7. As will be discussed later, O_{16} of the carboxyl group is clearly hydrogen bonded to N_{13}.

iii. The two-dimensional structure of 2-hydroxy-1-phenazinecarboxylic acid.

The h0ℓ intensity data from one of the plate-like crystals were recorded photographically using the multiple-film

Table 3. Final heavy atom parameters and their standard deviations for 1-phenazinecarboxylic acid in the (001) projection. The temperature factors are expressed in the form $T = \exp(-B_{11} h^2 - B_{22} k^2 - B_{12} hk)$. The atoms are numbered as in figure 6. All values have been multiplied by 10^4.

	x	y	B_{11}	B_{22}	B_{12}
C_1	2215(15)	900(20)	38(10)	78(21)	9(22)
C_2	2125(17)	- 50(23)	49(13)	88(25)	6(26)
C_3	1482(14)	-516(16)	41(10)	42(13)	18(17)
C_4	927(13)	- 86(15)	36(9)	37(13)	1(15)
C_5	992(12)	883(17)	30(8)	42(13)	11(15)
N_6	442(11)	1300(13)	34(8)	47(12)	- 6(14)
C_7	511(15)	2220(18)	41(11)	58(18)	3(20)
C_8	- 77(16)	2701(19)	40(10)	58(17)	19(19)
C_9	1(18)	3626(20)	56(14)	59(19)	33(24)
C_{10}	648(19)	4108(20)	61(16)	66(19)	10(26)
C_{11}	1212(15)	3691(19)	40(10)	53(16)	-14(18)
C_{12}	1155(13)	2720(16)	32(9)	36(13)	4(15)
N_{13}	1717(10)	2297(13)	30(7)	40(11)	6(13)
C_{14}	1629(13)	1388(17)	34(10)	48(15)	0(18)
C_{15}	2905(15)	1361(24)	36(11)	99(25)	32(24)
O_{16}	2973(10)	2273(14)	40(8)	78(14)	-21(15)
O_{17}	3350(10)	936(15)	43(8)	98(17)	30(17)

Table 4. Assumed hydrogen atom parameters for 1-phenazinecarboxylic acid. The temperature factors are expressed in the form $T = \exp(-B \sin^2\theta / \lambda^2)$. The atoms are numbered as in figure 7.

	x	y	B
$H_{18}(C_2)$	0.259	-0.042	6.2
$H_{19}(C_3)$	0.144	-0.120	5.8
$H_{20}(C_4)$	0.048	-0.046	5.6
$H_{21}(C_8)$	-0.057	0.230	5.0
$H_{22}(C_9)$	-0.046	0.398	5.8
$H_{23}(C_{10})$	0.071	0.478	6.1
$H_{24}(C_{11})$	0.170	0.403	5.2
$H_{25}(O_{16})$	0.248	0.228	5.9

Table 5. Observed and calculated hk0 structure factors for 1-phenazinecarboxylic acid. The three columns in each group contain the values of h, $10|F_{obs}|$ and $10F_{calc}$. Reflections indicated by an asterisk were omitted from the least-squares calculations due to extinction effects. "Less than" reflections were included in the least-squares sums only if they calculated larger than the threshold value.

h00

0	* ----	4646
4	123	153
6	316	330
8	191	-213
10	119	118
12	42	- 35
14	37	23
16	61	- 64
18	152	150
20	62	46
22	< 26	- 6

h10

2	* 549	-669
3	253	-259
4	* 481	-559
5	138	-164
6	203	224
7	217	-218
8	157	-155
9	64	54
10	44	35
11	93	- 88
12	38	24
13	28	20
14	< 30	30
15	114	-121
16	196	218
17	71	- 85
18	< 31	- 29
19	42	29
20	< 34	- 6
21	39	45
22	34	26
23	20	13

h20

0	233	249
1	* 591	-685
2	211	-190
3	290	322
4	242	-266
5	127	-133
6	374	-392
7	391	-434
8	46	30
9	97	96
10	61	- 68
11	< 26	10
12	74	79
13	64	- 70
14	67	60
15	54	- 44
16	117	-130
17	138	149
18	49	- 48
19	< 36	10
20	< 34	7
21	< 30	- 9
22	25	22

h30

1	336	361
2	85	86
3	260	- 266
4	312	- 348
5	122	113
6	307	-318
7	38	- 28
8	355	368
9	434	467
10	162	-177
11	100	93
12	44	- 45
13	29	22
14	30	28
15	123	116
16	68	- 69
17	50	- 51
18	< 38	17
19	< 36	17
20	< 33	10
21	< 29	- 4
22	< 24	- 26

h40

0	118	-113
1	204	200
2	161	-153
3	82	62
4	65	54
5	116	97
6	119	-110
7	294	309
8	70	- 67
9	< 24	6
10	176	194
11	99	- 78
12	< 28	9
13	66	- 68
14	< 31	- 2
15	< 32	17
16	50	38
17	50	40
18	48	- 35
19	35	- 29
20	< 32	2
21	32	21
22	< 23	1

h50

1	196	195
2	170	164
3	120	-137
4	76	- 73
5	< 20	5
6	< 21	3
7	32	- 21
8	202	198
9	234	-237
10	42	53
11	34	36
12	< 29	- 27
13	64	73
14	< 31	15
15	< 32	- 18
16	39	42
17	< 31	16
18	< 36	- 25
19	< 34	- 2
20	< 31	- 12
21	27	- 27
22	< 21	10

h60

0	517	-575
1	136	138
2	49	58
3	84	98
4	92	91
5	< 22	- 23
6	78	- 80
7	34	- 21
8	73	69
9	92	91
10	39	31
11	58	- 53
12	48	- 30
13	< 31	- 10
14	32	31
15	45	56
16	< 30	- 10
17	78	- 82
18	65	- 62
19	< 33	- 27
20	< 29	9
21	24	8

h70

1	94	91
2	311	323
3	45	- 40
4	158	166
5	41	36
6	52	- 57
7	67	- 65
8	< 27	- 21
9	56	- 46
10	< 29	11
11	56	48
12	< 31	7
13	39	- 25
14	< 32	- 12
15	< 32	- 17
16	69	- 71
17	< 36	- 13
18	< 34	- 8
19	< 31	8
20	< 27	- 4
21	< 21	- 5

h80

0	553	563
1	306	322
2	54	54
3	55	- 56
4	64	58
5	40	- 45
6	65	49
7	84	83
8	< 28	- 3
9	62	- 59
10	82	88
11	< 31	- 12
12	84	- 47
13	45	49
14	< 32	- 20
15	31	35
16	< 37	- 10
17	45	- 44
18	55	54
19	< 28	- 8
20	< 24	2

h90

1	< 26	- 22
2	41	- 46
3	59	68
4	57	65
5	< 28	- 27
6	94	90
7	150	-163
8	216	-238
9	91	-103
10	44	46
11	< 32	12
12	< 32	- 2
13	< 32	- 11
14	< 38	31
15	80	- 75
16	78	75
17	< 32	3
18	29	- 34
19	< 25	- 6
20	< 20	2

h10, 0

0	28	4
1	63	- 59
2	26	- 11
3	60	70
4	< 29	- 22
5	95	- 89
6	166	-180
7	239	-275
8	76	- 56
9	< 32	- 8
10	67	53
11	90	83
12	< 39	11
13	54	41
14	< 37	- 20
15	< 35	- 1
16	38	- 30
17	< 30	10
18	< 26	5
19	< 21	9

h 11, 0

1	<' 30	30
2	< 30	7
3	< 30	25
4	43	- 35
5	< 31	- 34
6	< 31	- 24
7	59	- 60
8	55	- 58
9	306	384
10	50	- 51
11	70	68
12	< 36	10
13	< 37	- 38
14	< 35	31
15	62	57
16	< 30	- 2
17	28	- 16
18	< 21	- 11

h 12, 0

0	38	- 20
1	77	66
2	54	- 41
3	< 33	- 38
4	< 33	- 15
5	67	72
6	103	-105
7	133	152
8	39	- 30
9	67	- 66
10	83	85
11	< 37	- 23
12	50	47
13	< 34	29
14	< 32	- 5
15	29	14
16	48	61
17	< 21	- 7

h 13, 0

1	< 33	- 7
2	45	49
3	55	- 49
4	39	33
5	< 32	- 32
6	< 32	2
7	63	- 47
8	82	67
9	37	- 38
10	< 36	- 4
11	< 34	22
12	38	12
13	< 30	17
14	< 28	- 1
15	49	- 52
16	32	- 32

h 14, 0

0	139	152
1	67	- 71
2	< 39	27
3	49	36
4	< 38	- 8
5	61	66
6	< 37	13
7	< 36	- 22
8	< 35	- 4
9	< 34	- 11
10	33	28
11	< 31	0
12	< 29	- 2
13	26	- 27
14	< 22	0

h 15, 0

1	42	43
2	66	- 58
3	< 36	6
4	< 36	1
5	< 36	- 14
6	< 34	24
7	< 33	- 11
8	< 32	- 23
9	< 30	- 3
10	< 28	- 1
11	< 26	- 13
12	33	30

h 16, 0

0	< 33	- 25
1	< 33	- 9
2	< 33	8
3	< 32	- 11
4	< 32	3
5	< 31	22
6	< 30	- 2
7	< 28	7
8	< 27	14
9	29	- 26
10	< 22	- 12

h 17, 0

1	< 28	5
2	< 28	0
3	< 27	- 6
4	< 26	16
5	< 25	16
6	< 24	- 5
7	< 23	- 1
8	29	- 39

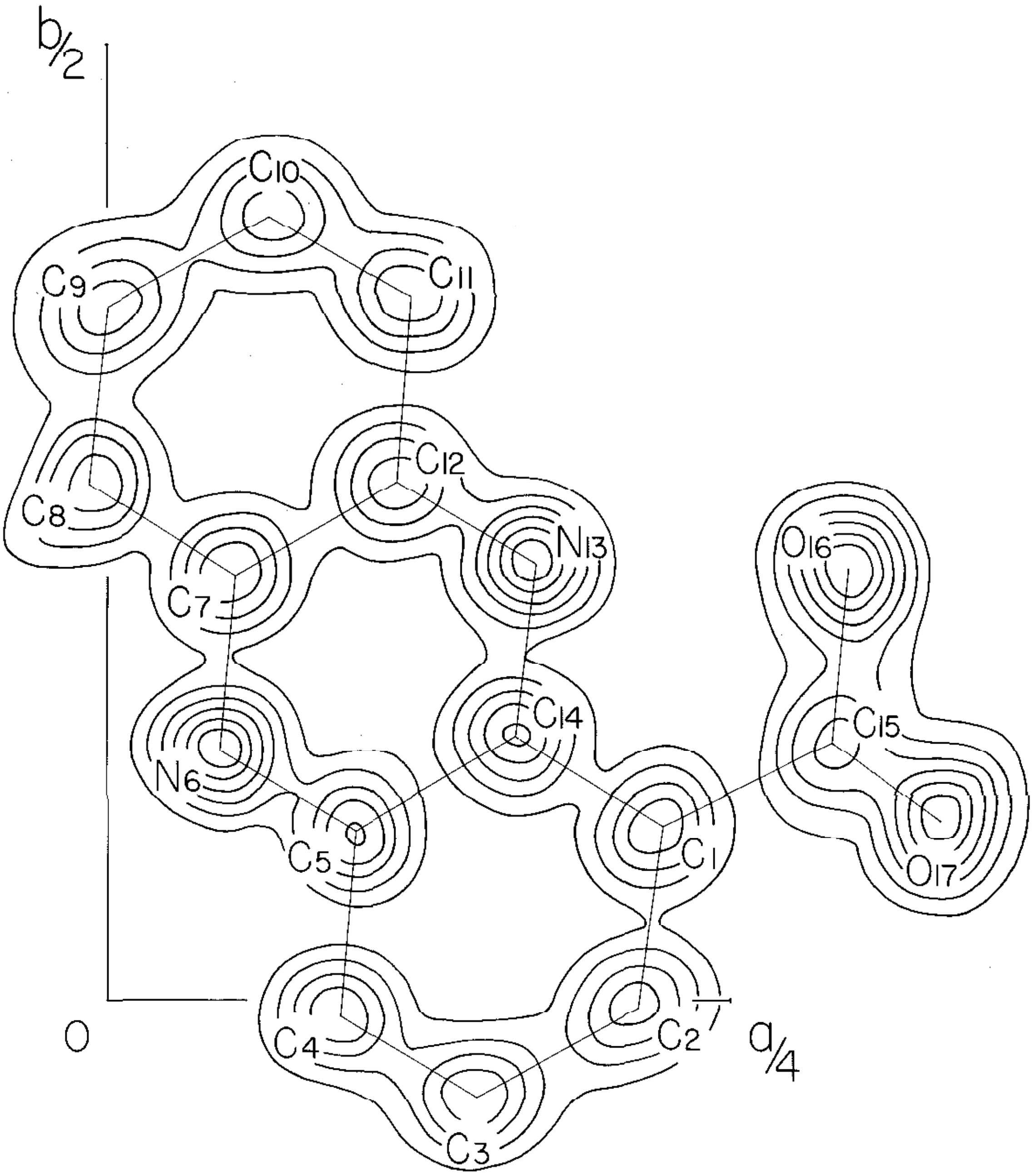

Figure 6. Final (001) electron density map of 1-phenazinecarboxylic acid. The contours are drawn at 2, 3, 4, ... e. Å^{-2}.

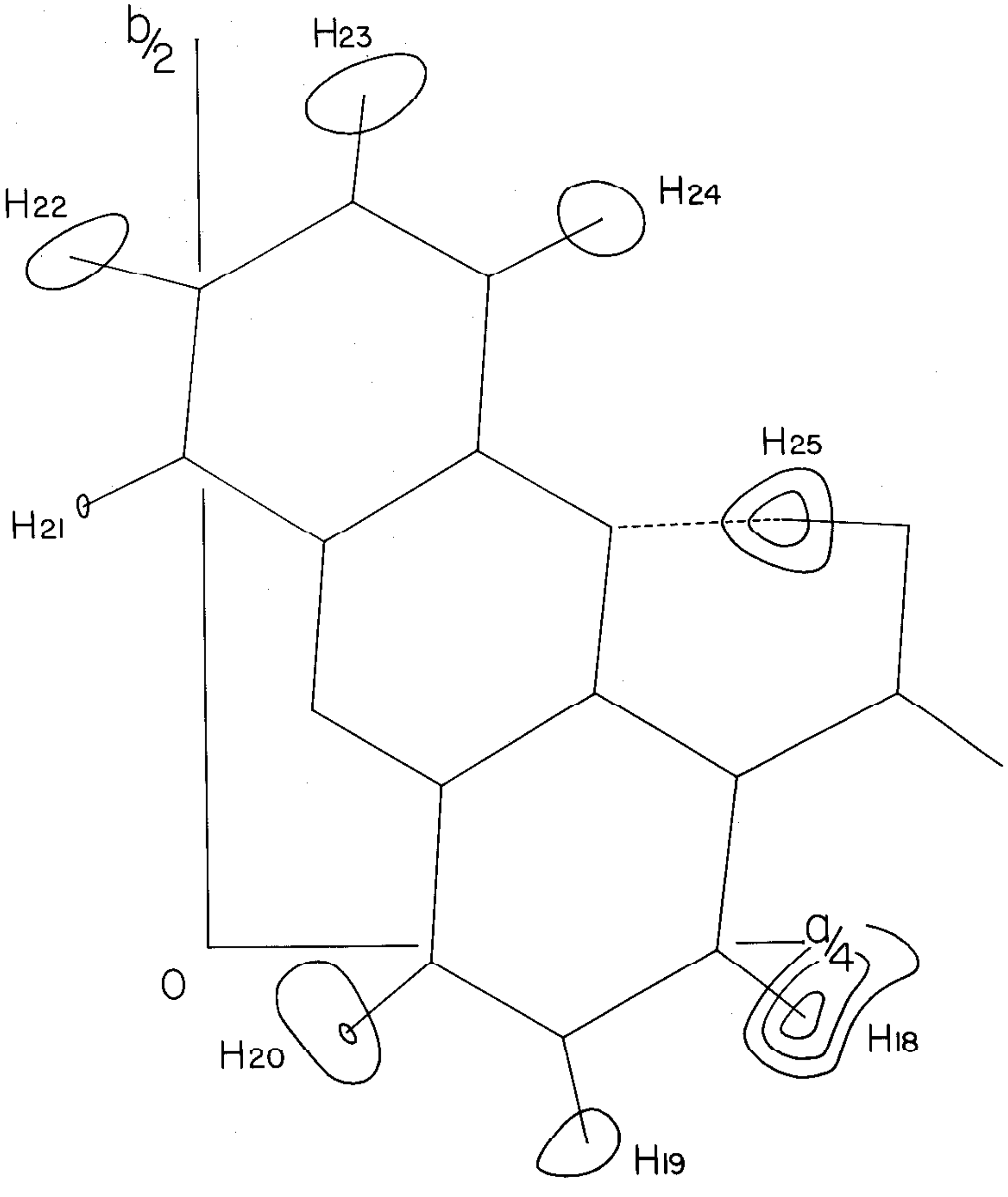

Figure 7. The (001) difference Fourier map for 1-phenazinecarboxylic acid, showing the hydrogen bond (dotted line) between O_{16} and N_{13}. The contours are drawn at 0.3, 0.5, and 0.7 e. $Å^{-2}$.

Weissenberg technique. The intensities of the reflections were estimated visually by comparison with a graduated intensity scale prepared from the same crystal. The readings from the several photographs were then scaled together using a film factor which was the average of the individual film factors. Lorentz and polarization corrections were applied to the data using the Hybl program for the Burroughs 220 computer.

As was the case with 1-phenazinecarboxylic acid, the photographs from the hydroxy derivative showed patches of intense reflections surrounded by areas of relatively weak reflections. The weighted $h0\ell$ reciprocal lattice net, which was plotted from the corrected intensity data with the radius of each spot being proportional to $|F|$ and the area to $|F|^2$, is shown in figure 8. Because the length of the b axis is about 5.9 Å, it was expected that the planes of the molecules in the unit cell would not be parallel to (010) but rather would be inclined somewhat. In projection, then, certain of the bond lengths would appear to be shortened and the rings would lose their hexagonal symmetry. The regions of intense reflections on the weighted $h0\ell$ reciprocal lattice net would, therefore, be expected to appear at higher values of $\sin\theta$ than they would if the molecule lay parallel to (010). With this in mind, an examination of the weighted $h0\ell$ reciprocal lattice net indicated a possible shape and orientation for the six-membered rings of the phenazine system. Because the

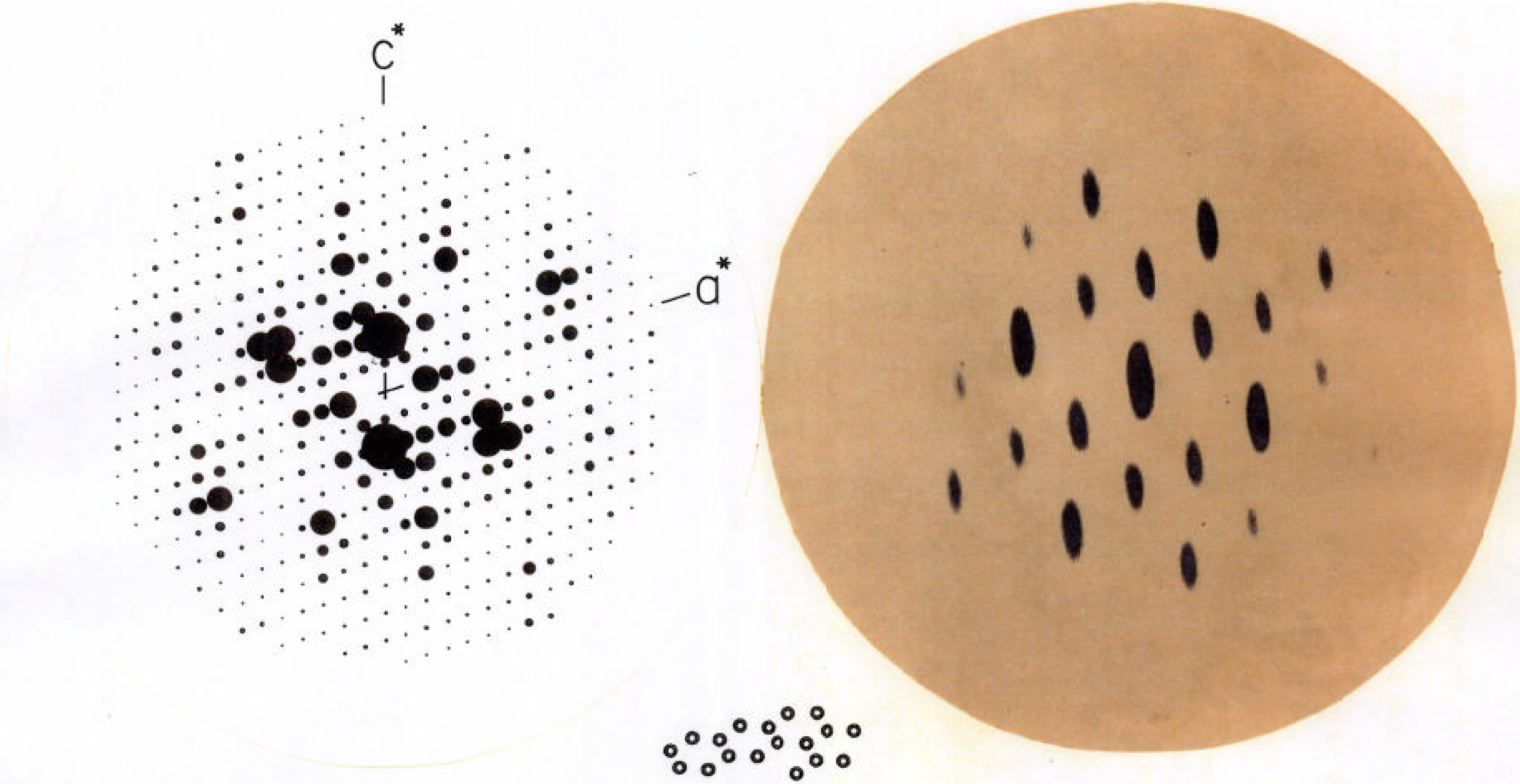

Figure 8. Weighted $h0\ell$ reciprocal lattice net (left) for 2-hydroxy-1-phenazinecarboxylic acid compared to the optical transform (enlarged approximately 40X) of the molecule. The drawing of the mask (actual size) from which the transform was obtained indicates the orientation of the molecule.

$h0\ell$ net contains no symmetry other than a center, it was possible to observe the apparent elongation, roughly normal to a^*, of the intense regions. This would indicate that the molecules lie in the unit cell with the ring center-ring center vectors approximately parallel to a^*, as had been surmised earlier from the shape and symmetry of the unit cell and from the exceptionally strong 002 reflection.

Later, after the structure of this compound had been determined, the optical diffraction pattern of the molecule was photographed by the technique described previously. It is shown for comparison in figure 8, along with a drawing of the mask from which the pattern was obtained.

In order to further confirm the shape and orientation of the individual rings in the phenazine nucleus, and in the hope of locating the position of the molecule in the asymmetric unit, two (010) Patterson projections were calculated, the second of which had the origin peak removed and was sharpened. The Patterson expression in the $h0\ell$ projection is

$$\begin{aligned} P(UOW) = \frac{2}{A}\Big\{\sum_{0}^{\infty} h \sum_{0}^{\infty} \ell \big[(|F(h0\ell)|^2 + |F(\bar{h}0\ell)|^2)\cos 2\pi hU \cos 2\pi \ell W \\ - (|F(h0\ell)|^2 - |F(\bar{h}0\ell)|^2)\sin 2\pi hU \sin 2\pi \ell W\big]\Big\} \quad . \end{aligned} \tag{1}$$

The vector maps were both calculated from equation 1 in intervals of 0.01a and 0.02c using the Burroughs 220 computer program written by Hoogsteen. The sharpened $|F_{obs}|^2$'s for the second map, shown in figure 9, were calculated using the computer program written by Duchamp (7). The latter program evaluates the expression

$$|F_{obs}|_s^2 = M[k[F_{obs}]^2 - \sum_i n_i f_i^2 \exp(-2B \sin^2\theta/\lambda^2)] \qquad (2)$$

where M is a modification function of the form

$$M = (\frac{2\sin\theta}{\lambda})^4 \exp(-4.4 \sin^2\theta/\lambda^2) \qquad (3)$$

which is taken from Waser and Schomaker (8). This modification function emphasizes the intramolecular vectors (about 1.5 Å) while giving lower weight to the longer intermolecular vectors. The overall scale factor, k, and the overall isotropic temperature factor, B, were determined by the technique of Wilson (9). The two vector maps were quite similar, except that the peaks around the origin of the sharpened map were clearly distinguishable. Peaks in the sharpened Patterson map representing vectors between atoms in the same ring are shown shaded in figure 9 and the bond vectors are indicated by dotted lines. The shape and orientation of the six-membered rings of the phenazine nucleus, as derived from this map, were found to agree closely with those obtained from the weighted h0ℓ reciprocal lattice net.

The next problem was to find the location of the molecule in the asymmetric unit. Because of the presence of the glide plane in

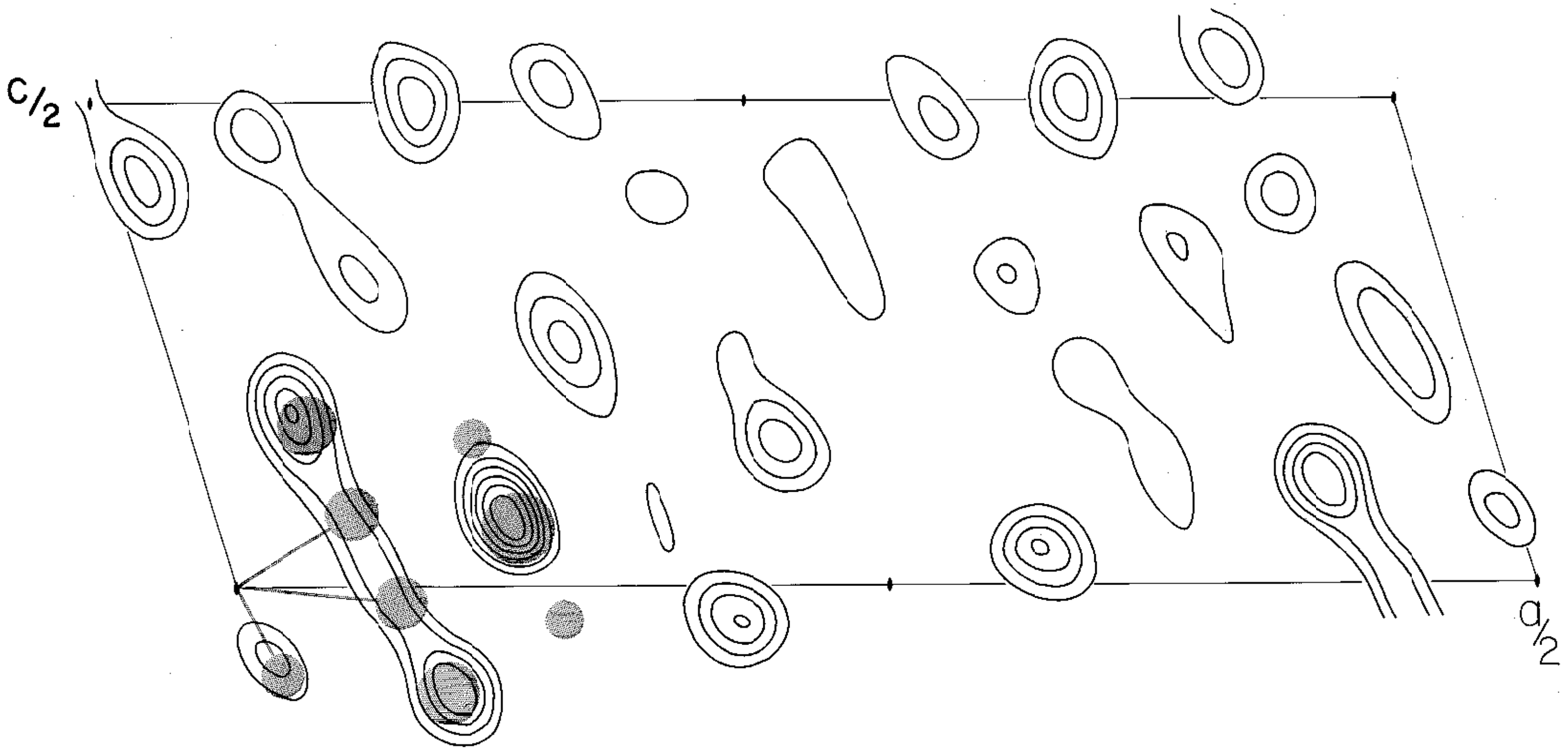

Figure 9. The (010) Patterson projection of 2-hydroxy-1-phenazinecarboxylic acid. Peaks representing vectors between atoms in the same ring are shaded and the bond vectors are indicated by dotted lines. The contours are drawn at arbitrary but equal levels.

the space group $P2_1/a$, one may choose an apparent unit cell in the h0ℓ projection which is halved along a. This cell contains two molecules and has the symmetry p2, requiring that the phenazine nucleii of the two molecules be parallel. As is seen in figure 4, the set of intermolecular vectors between two parallel phenazine ring systems may be approximated by a set of five peaks in a straight line with relative weights approximately in the ratios 1: 2: 3: 2: 1. If the two molecules in the apparent unit cell are centered at (x, y) and (1-x, 1-y), the vector array will be centered at (1 - 2x, 1 - 2y). From packing considerations it was clear that the row of peaks roughly parallel to a^* at the top of figure 9 contained the vectors being sought. However, the heights of these peaks were not in the expected ratios* and at least two locations, and possibly a third, seemed plausible.

Since the shape and orientation of the phenazine nucleus were known, it was decided to attempt to determine its position in the asymmetric unit simply by moving it in small increments over the region of possible locations, performing a structure factor calculation at each point. In order to carry out this calculation, a molecular search routine was written by the author to generate the atomic coordinates for the monoclinic structure factor program. A new set of coordinates for the 14 atoms in the phenazine nucleus was calculated

---

* The approximation of the phenazine nucleus being represented by three "atoms" at the centers of the rings begins to break down as more substituents are added.

at each point of a 15 x 10 grid, the grid points being separated by 0.01a and 0.02c, respectively. The origin of the grid was taken at $x = 0.18$ and $z = 0.16$. Approximately 60 h0ℓ structure factors were calculated at each point, but only the value of R (see equation 7, Part I) was printed for each calculation. The lowest value of R (0.66) was calculated when the phenazine nucleus was centered at the point $x = 0.25$ and $y = 0.26$. This location was very close to one of the three derived earlier from the (010) vector map. The calculation was then run again with the phenazine ring system centered at this point, this time printing the observed and calculated structure factors.

An (010) electron density map was calculated from about 30 of the phased structure factors, using the Hoogsteen computer program. The summations were carried out in intervals of 0.01a and 0.02c. This map showed all the ring atoms, albeit poorly resolved, and three peaks which appeared to be a carboxyl group on the α position of the phenazine nucleus. There were several other smaller peaks on the map, any one of which might have been a hydroxyl oxygen atom.*

At this point a large number of structure factor calculations and least-squares refinement cycles were run on several of the possible structures derived from the h0ℓ electron density map. The observations in each case were weighted inversely proportional to the

---

* Although the correct structure of this compound had been recently shown by Olson to be 2-hydroxy-1-phenazinecarboxylic acid, this evidence was purposely ignored in order to show that the structure could be solved without the aid of prior chemical knowledge.

form factor of carbon and an isotropic temperature factor of 3.5 for B, as derived from the Wilson plot, was used for all atoms. After structure factors were calculated for each new structure, another (010) electron density map was calculated. Although one of the first structures tried was essentially correct, this was not immediately recognized because the agreement between the observed and calculated structure factors was not as good as was expected (R = 0.53). However, the other structures gave even poorer agreement and the author soon returned to the correct structure. The least-squares refinement of this structure progressed very slowly, possibly because of the poor resolution of the atoms in the (010) projection. After about a dozen least-squares cycles, R had dropped only to 0.37. Another (010) electron density map calculated at this point indicated that the molecule should be shifted slightly toward the origin, approximately parallel to a^*. This improved the calculations somewhat but another dozen least-squares cycles, during which the isotropic temperature parameters were allowed to shift, were required to bring R down to 0.26. The weighting scheme was then changed to the $1/F_{obs}$ function (see equation 8, Part I) and, after five more cycles, R was 0.18. Anisotropic temperature factors were introduced for all the atoms and the weighting scheme was changed to the $1/F^2_{obs}$ function (see equation 9, Part I). Seven more least-squares cycles dropped R to 0.145. At this point the shifts were all very small and the refinement in the $h0\ell$ projection was considered complete. A total of 216 reflections were included in the final $h0\ell$ structure factor calculation, of which 172 contributed to the least-squares sums. Of the latter, 17 were "less than" reflections which calculated larger than the threshold value.

The observed $h0\ell$ structure factors with their calculated signs were used in a final (010) electron density map, shown in figure 10. As will be explained later, the origin has been shifted by -0.25a in this drawing.

iv. The three-dimensional structure of 2-hydroxy-1-phenazinecarboxylic acid.

During the preliminary work on this structure a purer sample (m. p. 223.5-225.5°; lit. (3) m. p. 225-266°) of 2-hydroxy-1-phenazinecarboxylic acid was supplied the author by E. S. Olson. The red-orange powder was recrystallized slowly from acetic anhydride to give a variety of shapes and sizes of the plate-like crystal habit. It was relatively easy to select and mount crystals for the b axis and c axis intensity photographs.

The intensity data for reflections $h0\ell$ to $h5\ell$, inclusive, and for reflections hk0 to hk5, inclusive, were recorded photographically using the multiple-film Weissenberg technique. Two packs of

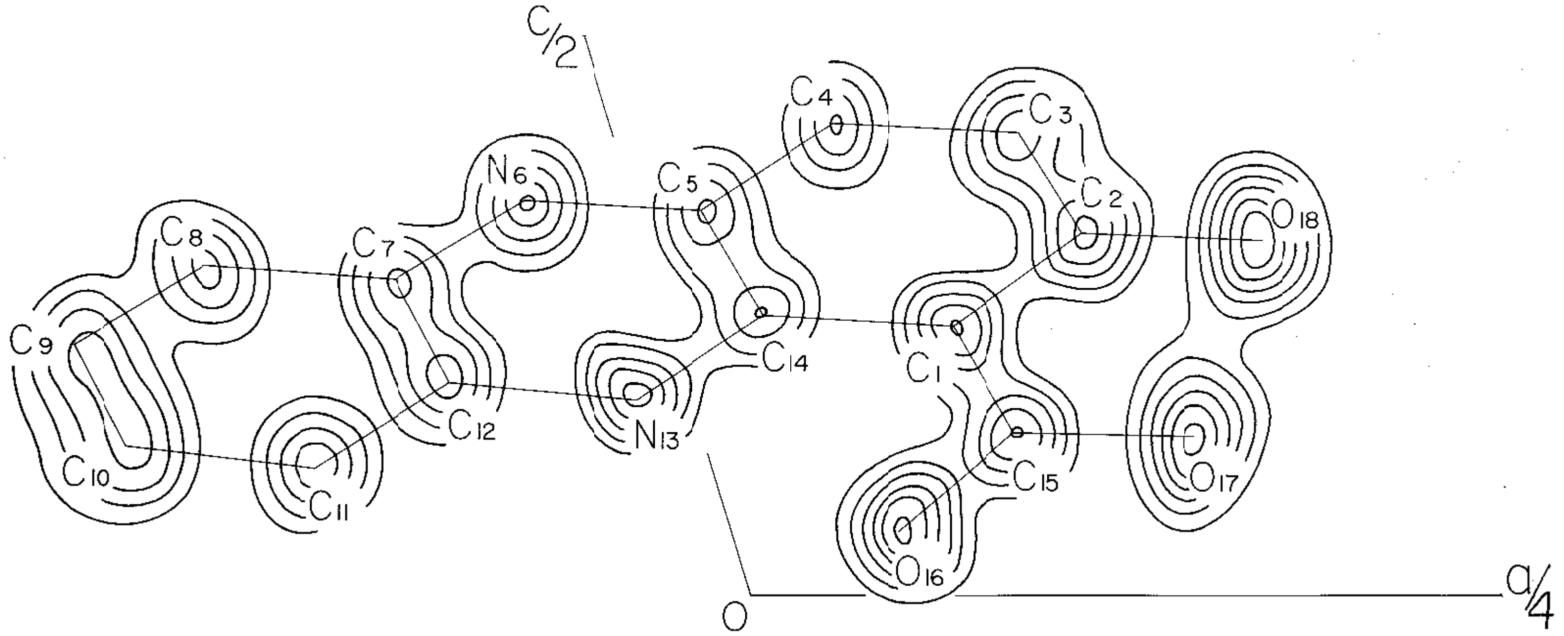

Figure 10. Final (010) electron density map for 2-hydroxy-1-phenazinecarboxylic acid. The contours are drawn at 3, 4, 5 ... e. Å^{-2}.

three films each were exposed for each layer, the first for 6 to 16 hours and the second for 48 to 120 hours. The long exposure times were necessary because the crystals were rather small. Since the spot shapes on the photographs from the two axes were similar, only a single graduated intensity scale was prepared, this from the crystal mounted to rotate about the b axis.

The intensities of all the reflections on these photographs were estimated visually by comparing them to the graduated intensity scale with the aid of a magnifying glass. The measured intensities were scaled within each layer using an average film factor calculated for each set of photographs. Lorentz and polarization corrections were applied to the intensity data using the program written by Hybl for the Burroughs 220 computer. Layer scale factors were then calculated using the least-squares scaling program written by Deverill (see p. 12, Part I).

In order to determine the y coordinates for the atoms, a set of relative y coordinates was calculated from the refined x and z coordinates and from a table of expected bond lengths (ref. 22, Part I). Another molecular search program was written to generate the atomic coordinates as the model was moved in increments of 0.02b over the region of possible locations. The magnitude of R was calculated at each point, using approximately 150 values of $F(hk\ell)$ in the monoclinic structure factor program. The lowest value of R (0.46) was calculated when the phenazine nucleus was centered at $y = 0.54$. From packing considerations, this seemed to be a permissible location.

The first three-dimensional structure factor calculation, using isotropic temperature factors from a previous two-dimensional calculation, gave the disappointing value of 0.50 for R. Several cycles of least-squares calculations were run, with the weights taken inversely proportional to the form factor of carbon, but the structure did not refine significantly. At this point it was noticed that the agreement between the observed and calculated structure factors was reasonably good for those reflections with h even but was poor for those reflections with h odd. This suggested that the origin had been taken at the wrong location in the $h0\ell$ projection. In this projection, the location of the origin is ambiguous, since it is impossible to distinguish between centers of symmetry and screw axes. Because $h0\ell$ reflections are present only with h even in the space group $P2_1/a$, it was possible to refine the structure in projection with the origin taken at a screw axis rather than at a center of symmetry. After 0.25 had been subtracted from all the x coordinates, the three-dimensional structure began to refine. Four least-squares cycles dropped R to 0.26. The anisotropic temperature parameters B_{11}, B_{33} and B_{13} from the final $h0\ell$ refinement were then included in the calculation for all the atoms. After three more cycles R had dropped only to 0.24, the slow rate of convergence probably being due to the block diagonal matrix approximation which is used in the Marsh program. Since it appeared that further refinement using this program would be a slow process, the work was discontinued at this point, to be resumed later when a full matrix least-squares program becomes available. The partially refined heavy atom parameters and their standard deviations, which were calculated by the least-squares program from the diagonal elements of the inverted matrices, are listed in table 6. The average uncertainties in the positional parameters are 0.013 Å for the carbon atoms, 0.010 Å for the nitrogen atoms and 0.009 Å for the oxygen atoms.

The observed structure factors and their calculated signs were used in the molecular plane Fourier program written by Duchamp (ref. 31, Part I) to calculate the electron density in the plane of the molecule. The atoms in this map, which is shown in figure 11, are surprisingly well resolved considering the level of refinement; even some of the hydrogen atoms may be seen!

3. Discussion of the structure of 1-phenazinecarboxylic acid.

i. Bond lengths and intermolecular distances.

Although it is usually difficult to obtain meaningful bond lengths and intermolecular distances from a structure solved only in projection, one can at least determine the minimum values

Table 6. Partially refined heavy atom parameters and their standard deviations for 2-hydroxy-1-phenazinecarboxylic acid. The temperature factors are expressed in the form $T = \exp(-B_{11}h^2 - B_{33}\ell^2 - B_{13}h\ell)$ and are taken from the final $h0\ell$ refinement. The atoms are numbered as in figure 11. All values have been multiplied by 10^4.

	x	y	z	B_{11}	B_{33}	B_{13}
C_1	930(5)	4374(18)	2427(13)	20(3)	121(18)	22(11)
C_2	1460(5)	5777(19)	3204(13)	21(2)	189(22)	68(13)
C_3	1367(6)	7734(22)	4117(14)	32(3)	186(24)	58(15)
C_4	764(6)	8316(22)	4233(14)	20(3)	357(35)	56(17)
C_5	216(5)	6817(19)	3408(13)	22(3)	270(28)	70(15)
N_6	- 355(4)	7434(17)	3566(11)	25(2)	229(21)	28(12)
C_7	- 858(5)	6020(19)	2795(13)	24(3)	208(25)	29(14)
C_8	-1468(7)	6669(26)	2986(17)	24(4)	294(33)	- 3(17)
C_9	-1994(7)	5299(25)	2202(17)	62(7)	360(42)	136(28)
C_{10}	-1916(7)	3292(25)	1317(16)	30(4)	376(40)	76(21)
C_{11}	-1312(6)	2716(24)	1154(15)	20(3)	239(27)	36(14)
C_{12}	- 783(6)	4155(20)	1897(13)	24(3)	203(24)	54(15)
N_{13}	- 186(4)	3592(17)	1769(12)	19(2)	197(19)	3(11)
C_{14}	323(6)	4912(20)	2513(13)	28(3)	213(26)	76(16)
C_{15}	1043(5)	2452(19)	1449(12)	18(2)	161(20)	16(11)
O_{16}	576(4)	1196(14)	612(10)	26(2)	271(19)	40(11)
O_{17}	1636(4)	2015(16)	1434(10)	23(2)	351(23)	99(12)
O_{18}	2054(4)	5358(16)	3198(10)	23(2)	249(19)	47(11)

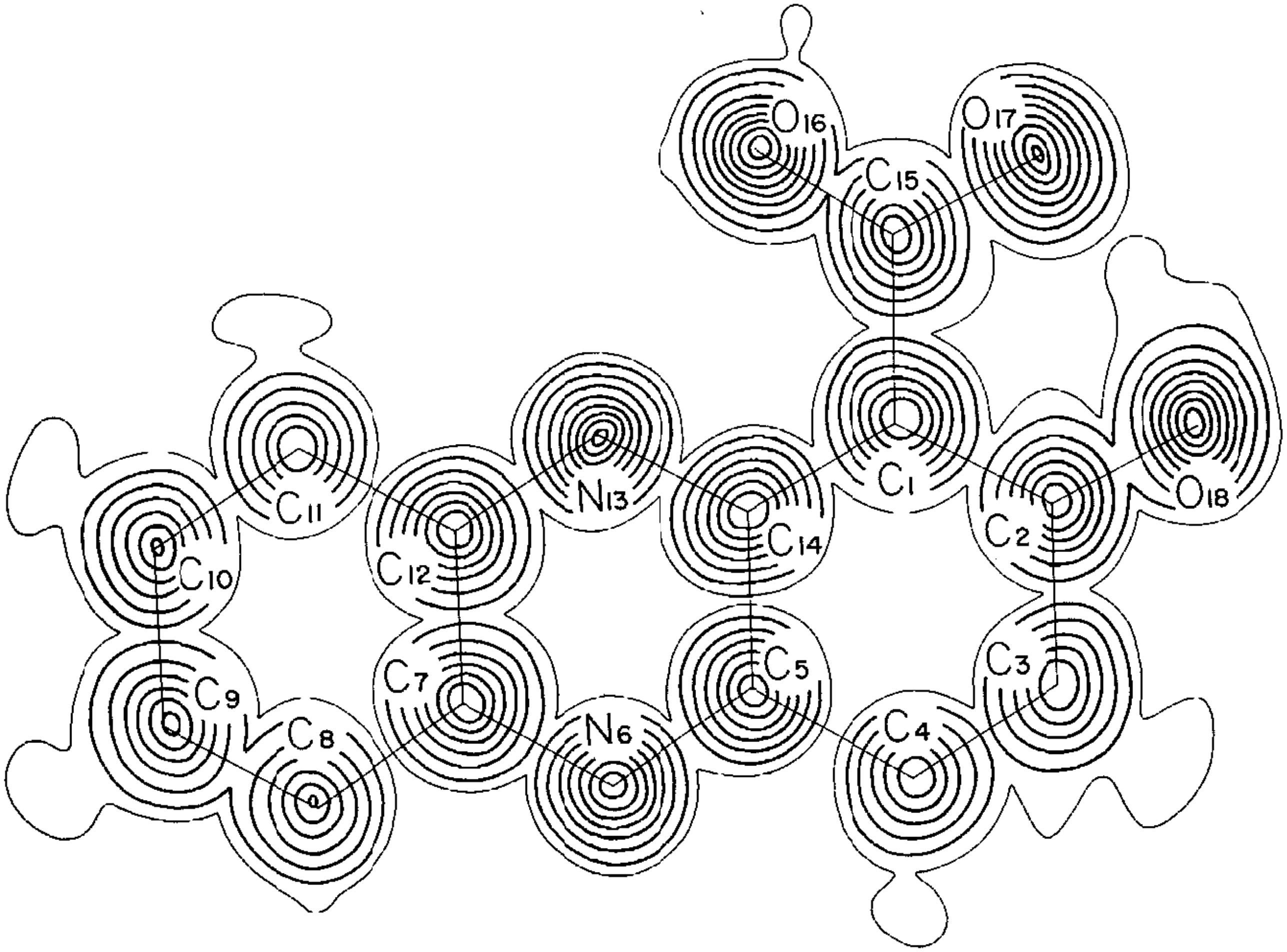

Figure 11. Electron density map in the best plane (table 10) of a molecule of 2-hydroxy-1-phenazinecarboxylic acid. The first light contour is drawn at 0.5 e. Å^{-3} and the heavy contours are drawn at 1, 2, 3 ... e. Å^{-3}.

of these parameters. The projected bond lengths, when compared to the expected values, may allow one to estimate the angle of tilt of the molecule , as has been done for 1-phenazinecarboxylic acid in the (001) projection. Table 7 lists the projected bond lengths, which were calculated on the Burroughs 220 computer, using the program written by the author (see Appendix, part II). These bond distances indicate that the molecule is tilted 20-25° from the plane of the projection, about an axis roughly parallel to a line drawn from N_{13} through the middle of the C_5-N_6 bond.

The projected intermolecular distances less than 3.6 Å are listed in table 8. These were calculated using the Burroughs 220 computer program written by Barker (ref. 32, Part I).

ii. Hydrogen bonding.

The absence of an O-H stretching frequency peak above 3000 $cm.^{-1}$ in the infrared spectrum (in chloroform) of 1-phenazinecarboxylic acid indicates that the molecule is internally hydrogen bonded in solution. As may be seen from the (001) difference Fourier map shown in figure 7, the compound is also intramolecularly hydrogen bonded in the crystalline state. It is interesting that the molecule forms this type of bond rather than a hydrogen bonded dimer as do most carboxylic acids (10). Empirically, one might expect the latter to be the preferred bonding scheme, since oxygen is more

Table 7. Bond distances in the (001) projection of 1-phenazinecarboxylic acid.

Bond	D(Å)	Bond	D(Å)
$C_1 - C_2$	1.37	$C_{11} - C_{12}$	1.39
$C_2 - C_3$	1.36	$C_{12} - N_{13}$	1.20
$C_3 - C_4$	1.20	$N_{13} - C_{14}$	1.31
$C_4 - C_5$	1.39	$C_{14} - C_1$	1.30
$C_5 - N_6$	1.20	$C_5 - C_{14}$	1.38
$N_6 - C_7$	1.32	$C_7 - C_{12}$	1.40
$C_7 - C_8$	1.29	$C_1 - C_{15}$	1.44
$C_8 - C_9$	1.33	$C_{15} - O_{16}$	1.31
$C_9 - C_{10}$	1.38	$C_{15} - O_{17}$	1.02
$C_{10} - C_{11}$	1.20	$O_{16} - N_{13}$	2.32

Table 8. Intermolecular distances less than 3.6 Å in the (001) projection of 1-phenazinecarboxylic acid. The atoms in the first column belong to the reference molecule at x, y. Symmetry related distances are not listed.

From	To	In molecule at	D(Å)
C_4	N_6	$\bar{x}, \bar{y}$	3.08
C_9	O_{17}	$-\frac{1}{2} + x, \frac{1}{2} - y$	3.37
C_9	C_{10}	$\bar{x}, 1 - y$	3.46
C_4	C_4	$\bar{x}, \bar{y}$	3.46
C_{10}	O_{17}	$\frac{1}{2} - x, \frac{1}{2} + y$	3.46
C_{10}	C_{10}	$\bar{x}, 1 - y$	3.51
C_3	O_{16}	$\frac{1}{2} - x, -\frac{1}{2} + y$	3.51
C_{11}	O_{17}	$\frac{1}{2} - x, \frac{1}{2} + y$	3.56

electronegative than nitrogen. It is possible that packing considerations and the close proximity of N_{13} to O_{16} dictate the presence of the intramolecular bond. In projection the N_{13}-O_{16} distance is 2.32 Å (table 7), but, because of the tilt of the molecule and because O_{16} may not lie exactly in the plane of the molecule, this distance may be somewhat longer, perhaps 2.4-2.6 Å. The C_{15}-O_{16}-H_{25} angle, as measured from figure 7, is probably not larger than 90°, compared to the usual angle of 100-110°.

iii. Thermal ellipses.

The magnitudes and orientations of the thermal ellipses in the (001) projection of 1-phenazinecarboxylic acid are listed in table 9. These values were calculated from the temperature parameters given in table 3 using the Burroughs 220 computer program written by Hebert (ref. 30, Part I). As may be seen from the plotted ellipses, shown in figure 12, there are sizeable anisotropies in the thermal motions of the peripheral carbon and oxygen atoms. The principal mode of vibration in the (001) plane appears to be a torsion motion about an axis located roughly on the midpoint of a line joining N_6 and C_{12}. The presence of a large, nearly isotropic temperature motion at C_2 is perplexing, but a possible explanation is given below.

Table 9. Magnitudes and direction cosines of the principal axes of the thermal ellipses for 1-phenazinecarboxylic acid in the (001) projection. The direction cosines, m, for the major axis are taken with respect to the a and b crystal axes. The root mean square deviation, μ, is given by $(B/8\pi^2)^{\frac{1}{2}}$.

	Axis i	B_i	μ(Å)	m_{1a}	m_{1b}
C_1	1	6.55	0.288	0.285	0.958
	2	4.88	0.249		
C_2	1	7.36	0.306	0.339	0.941
	2	6.46	0.286		
C_3	1	5.85	0.272	0.932	0.364
	2	3.13	0.199		
C_4	1	4.81	0.247	0.999	0.018
	2	3.03	0.196		
C_5	1	4.31	0.234	0.837	0.547
	2	3.04	0.196		
N_6	1	4.65	0.243	0.928	0.372
	2	3.70	0.217		
C_7	1	5.47	0.263	0.966	0.260
	2	4.75	0.245		
C_8	1	6.04	0.277	0.792	0.610
	2	3.99	0.225		
C_9	1	8.33	0.325	0.894	0.448
	2	3.97	0.224		
C_{10}	1	8.24	0.323	0.983	0.181
	2	5.30	0.259		
C_{11}	1	5.68	0.268	0.881	0.474
	2	3.94	0.224		
C_{12}	1	4.27	0.232	0.984	0.175
	2	2.90	0.192		
N_{13}	1	4.10	0.228	0.935	0.355
	2	3.16	0.200		
C_{14}	1	4.51	0.239	1.000	0.008
	2	3.98	0.225		

Table 9 (continued)

	Axis i	B_i	μ (Å)	m_{1a}	m_{1b}
C_{15}	1	8.82	0.334	0.382	0.924
	2	4.02	0.226		
O_{16}	1	7.08	0.299	0.530	0.848
	2	4.61	0.242		
O_{17}	1	8.83	0.334	0.443	0.896
	2	4.90	0.249		

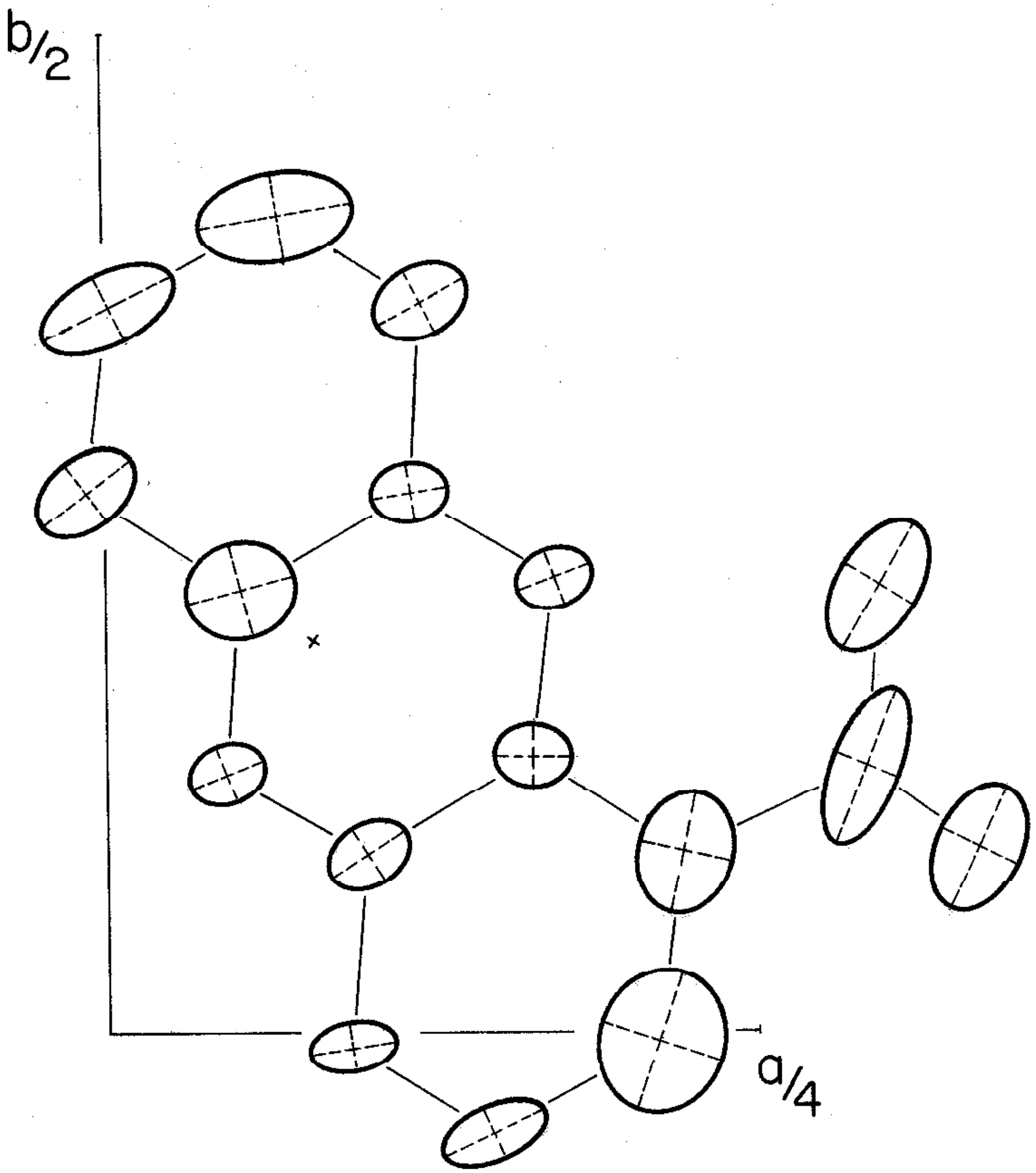

Figure 12. Temperature factor ellipses for 1-phenazinecarboxylic acid in the (001) projection. The ellipses are plotted on a relative scale from the data in table 9. The approximate location of the torsion axis is indicated by a cross.

iv. Conclusion.

It seems probable that the crystal used in this structure determination contains a small amount of 2-hydroxy-1-phenazinecarboxylic acid, as indicated by the evidence presented earlier (see footnote, p. 62). If this is true, the molecules of the hydroxy acid would be expected to replace the 1-phenazinecarboxylic acid molecules in random sites throughout the crystal. A quite similar situation has been reported by Curti, Riganti and Locchi (11). These investigators studied solid solutions of phenazine and N-oxyphenazine and found that one would readily replace the other, the unit cell parameters changing gradually as the ratio of the components was varied between the extremes of pure crystalline phenazine on the one hand and pure crystalline N-oxyphenazine on the other. Thus it is possible that the anomalous temperature factor at C_2 (see figure 12) and the rather large "hydrogen" peak at H_{18} (see figure 7) may both be explained by the presence of a small amount of 2-hydroxy-1-phenazinecarboxylic acid.

The author recently obtained a sample of pure 1-phenazinecarboxylic acid which was recrystallized slowly from acetic anhydride to give extremely fine, fibrous needles. There was very little resemblance between these crystals and the crystal which was used in this structure determination; however, the fibrous crystals have not yet been examined with X-rays.

That it was possible to determine the structure of 1-phenazinecarboxylic acid from one small, impure crystal is testimony to the power of X-ray diffraction analysis in the determination of the structures of organic compounds. This probably could not have been done by any other physical or chemical technique.

4. Discussion of the structure of 2-hydroxy-1-phenazinecarboxylic acid.

i. Molecular dimensions and planarity.

The interatomic distances and bond angles for 2-hydroxy-1-phenazinecarboxylic acid were calculated from the partially refined positional parameters given in table 6, using the program written by the author for the Burroughs 220 computer. The results of these calculations are shown in figure 13. The average bond lengths are 1.41 ± 0.03 Å for the aromatic C-C bonds and 1.36 ± 0.03 Å for the C-N bonds. These may be compared with the values 1.402 ± 0.009 Å and 1.355 ± 0.009 Å, respectively, as given by Herbstein and Schmidt from their determination of the crystal structure of phenazine (12).

The best plane through the molecule was calculated using the author's computer program with the atoms weighted according to their atomic numbers. Table 10 lists the results of this calculation; within the limits of error the molecule is planar.

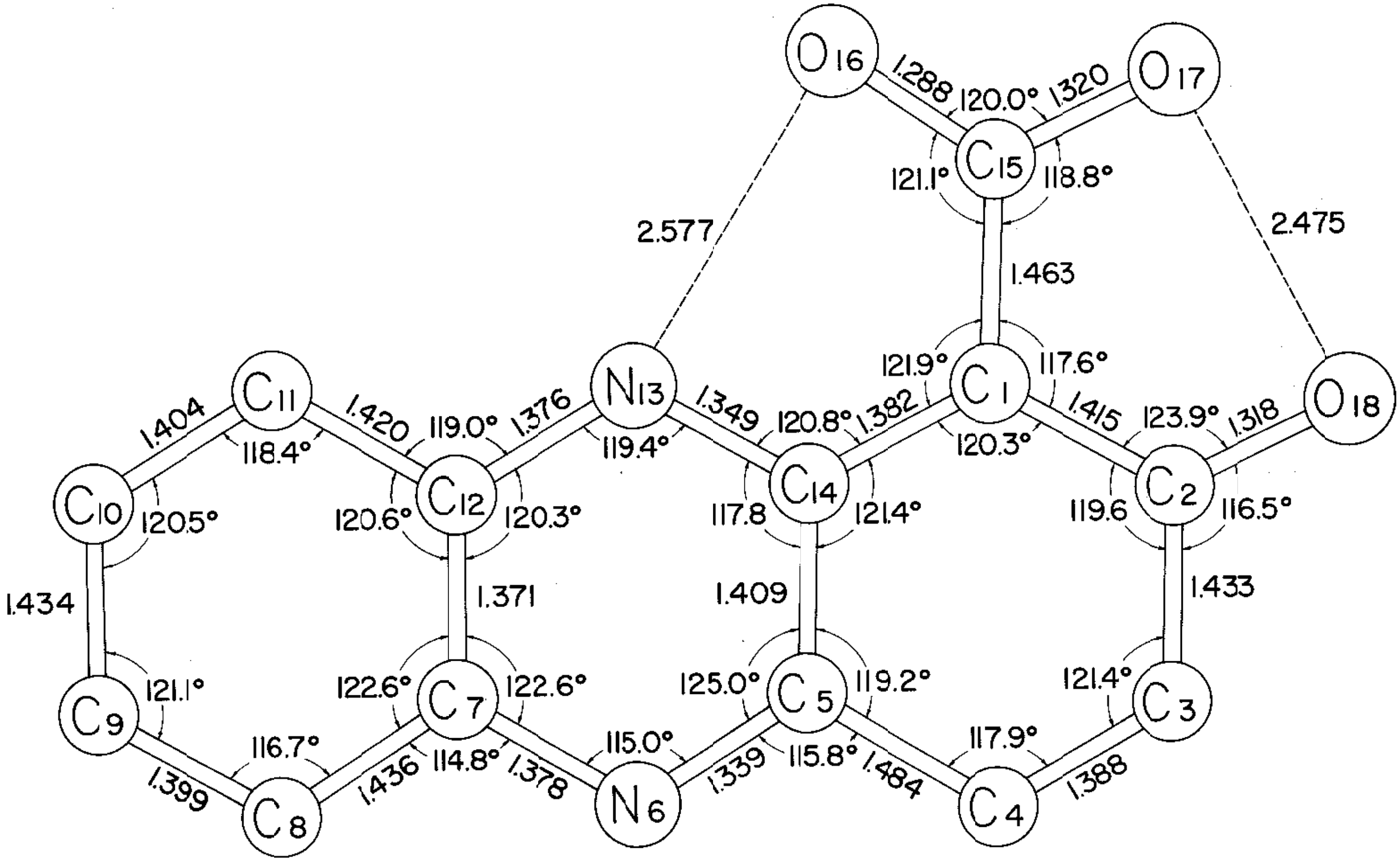

Figure 13. Interatomic distances and bond angles for 2-hydroxy-1-phenazinecarboxylic acid, as calculated from the partially refined coordinates given in table 6. The average standard deviation for the interatomic distances is approximately ± 0.03 Å. The average standard deviation in the bond angles is approximately ± 1.5°.

Table 10. Best plane through a molecule of 2-hydroxy-1-phenazinecarboxylic acid. The values of m_i are direction cosines of the normal to the best plane with respect to the orthogonal axes a, b, c^*.

Direction	cosines
m_a	-0.068
m_b	-0.564
m_{c^*}	0.807

Atom	Deviation
C_1	-0.026 Å
C_2	-0.009
C_3	0.008
C_4	0.034
C_5	0.014
N_6	0.028
C_7	0.007
C_8	0.003
C_9	0.002
C_{10}	-0.053
C_{11}	-0.045
C_{12}	0.008
N_{13}	-0.004
C_{14}	0.004
C_{15}	0.015
O_{16}	0.097
O_{17}	-0.032
O_{18}	-0.057
Origin	-0.030

ii. Molecular packing and hydrogen bonding.

Crystals of 2-hydroxy-1-phenazinecarboxylic acid are quite dense ($\rho = 1.54$ g. cm.$^{-3}$) for an organic compound containing only light elements; by comparison, nicotinic acid (3-carboxypyridine) has a density of 1.47 g. cm.$^{-3}$ (13) and phenazine (α-form) a density of only 1.33 g. cm.$^{-3}$ (12). It was expected, then, that the molecules of this compound would be packed tightly in the crystal structure; this was found to be the case.

Intermolecular distances were calculated from the partially refined positional parameters listed in table 6 using the coordinate generating program written for the Burroughs 220 computer by Barker. The results of these calculations, for distances less than 3.5 Å, are listed in table 11.

The crystal structure may be described as consisting of stacks of "ribbons" of 2-hydroxy-1-phenazinecarboxylic acid molecules. Each ribbon is composed of parallel, coplanar molecules which are related by centers of symmetry 7.24 Å apart, as shown below. Thus, the pattern of the ribbon is repeated every 14.48 Å.

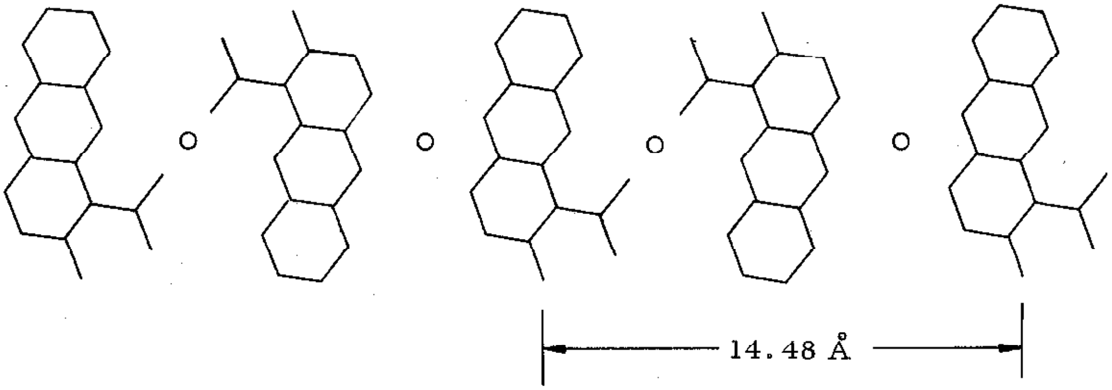

Table 11. Intermolecular distances less than 3.5 Å for 2-hydroxy-1-phenazinecarboxylic acid. The atoms in the first column belong to the reference molecule at x, y, z. Symmetry related distances are not listed.

From	To	In molecule at	D(A)
O_{16}	O_{16}	$\bar{x}, \bar{y}, \bar{z}$	2.798
C_{12}	C_{15}	$\bar{x}, 1 - y, \bar{z}$	3.364
C_4	N_6	$\bar{x}, 2 - y, 1 - z$	3.387
C_{11}	O_{16}	$\bar{x}, \bar{y}, \bar{z}$	3.390
C_4	O_{16}	$x, 1 + y, z$	3.407
N_{13}	O_{16}	$\bar{x}, \bar{y}, \bar{z}$	3.422
C_{11}	O_{17}	$\bar{x}, \bar{y}, \bar{z}$	3.482
C_2	C_9	$\bar{x}, 1 - y, 1 - z$	3.490

The ribbons are then stacked normal to the a^* axis, very nearly in the (012) or (01$\bar{2}$) planes. The distance between the best planes through adjacent ribbons is about 3.31 Å (the (012) interplanar spacing). The stacks of ribbons which are alternately parallel to (012) and to (01$\bar{2}$) are equivalent because of the 2_1 axes parallel to b. One consequence of this packing arrangement may be seen in the 012 reflection, which is at least twice as intense as any other reflection recorded.

The hydrogen bonding in the crystal is entirely within the ribbons; there are no hydrogen bonds between adjacent ribbons or between adjacent stacks of ribbons. The presence of a small peak near O_{18} in the molecular plane electron density map (figure 11) seems to confirm the spectral evidence (3) that O_{18} is hydrogen bonded to O_{17}. The O_{18}-O_{17} distance (figure 13) is 2.48 Å and the C_2-O_{18}-H angle, as measured from figure 11, is probably about 95°. The carboxyl hydrogen atom is not clearly visible on the electron density section and therefore one can only speculate as to its location. However, the close proximity (2.80 Å) of the O_{16} carboxyl atoms across the centers of symmetry has led the author to postulate a novel bifurcated hydrogen bond (see Proposition I).

iii. Conclusion

Although this investigation was undertaken in order to determine the molecular structure of a then unknown natural product, it has resulted in a crystal structure which has several intriguing features of its own. It will be particularly interesting to examine such points as the thermal anisotropies of the atoms in this tightly packed structure and the hydrogen bonding scheme. But the final answers to these and other questions await the further refinement of the structure.

References to Part III.

1. W. C. Haynes, F. H. Stodola, J. M. Locke, T. G. Pridham, H. F. Conway, V. E. Sohns, and R. W. Jackson, J. Bact., 72, 412 (1956).
2. A. J. Kluyver, J. Bact., 72, 406 (1956).
3. E. S. Olson, Ph. D. Dissertation, California Institute of Technology, Pasadena (1964).
4. G. A. Swan and D. G. I. Felton, "Phenazines," Interscience Publishers Inc., New York, 1957, pp. 82-85.
5. C. A. Taylor, R. M. Hinde, and H. Lipson, Acta Cryst., 4, 261 (1951).
6. A. W. Hanson, H. Lipson, and C. A. Taylor, Proc. Roy. Soc., A, 218, 371 (1953).
7. D. J. Duchamp, private communication (1963).
8. J. Waser and V. Schomaker, Rev. Mod. Phys., 25, 671 (1953).
9. A. J. C. Wilson, Nature, 150, 152 (1942).
10. L. Pauling, "Nature of the Chemical Bond," Cornell University Press, Ithaca, N. Y., 1960, pp. 477-484.
11. R. Curti, V. Riganti, and S. Locchi, Acta Cryst., 14, 133 (1961).
12. F. H. Herbstein and G. M. J. Schmidt, ibid., 8, 399 (1955).
13. W. B. Wright and G. S. D. King, ibid., 3, 31 (1950).

APPENDIX

I. A Program for the Calculation of Lattice Parameters.

1. Introduction.

This program was written in basic machine language for the Burroughs 220 digital computer. It provides for calculation, by the least-squares method, of lattice parameters and their estimated standard deviations for all of the several crystal systems. The required input is the Miller index, hkl, the Bragg angle, θ, and the wavelength, λ, for each measured reflection. The data may be given external and/or internal (programmed) weights and provision is made for the standard correction terms for two sources of systematic error, eccentricity and absorption. The output is a list of the observed and calculated Bragg angles, the calculated lattice parameters, and, at the operator's option, the matrix of coefficients of the normal equations and the corresponding inverted matrix.

2. The theory of least-squares.

The following description of the least-squares method is taken in part from Buerger (1). Suppose we have a quantity, Q, which is a linear function of a set of n variables $x_1, x_2, x_3 \ldots\ldots x_n$ with coefficients $a_1, a_2, a_3, \ldots\ldots a_n$,

$$Q = a_1x_1 + a_2x_2 + a_3x_3 + \ldots\ldots + a_nx_n = \sum_{j=1}^{n} a_jx_j \ . \qquad (1)$$

There will, in general, be associated with any physical measurement, q, a random error, ϵ. If q is taken as an observed value of the quantity Q, we may write

$$Q = q + \epsilon = \sum_{j=1} a_j x_j \; . \tag{2}$$

Suppose now that we make a set of m observations, q_m, where $m > n$. We have then a set of m "observational equations"

$$\begin{aligned} q_1 + \epsilon_1 &= \sum_j a_{j1} x_j \\ q_2 + \epsilon_2 &= \sum_j a_{j2} x_j \\ q_3 + \epsilon_3 &= \sum_j a_{j3} x_j \\ &\vdots \qquad \vdots \\ q_m + \epsilon_m &= \sum_j a_{jm} x_j \; . \end{aligned} \tag{3}$$

Because of the errors associated with the measured values of q, solving various sets of n of these equations will lead to slightly different values for the n variables. Since we cannot fit all of the observed data exactly, we must decide upon a criterion for the best fit of the data. According to Legendre's principle, the most acceptable values of the variables are such as to make the sum of the squares of the residuals a minimum; that is,

$$\varepsilon_1^{\ 2} + \varepsilon_2^{\ 2} + \varepsilon_3^{\ 2} + \dots + \varepsilon_m^{\ 2} = \sum_{i=1}^{m} \varepsilon_i^{\ 2} \tag{4}$$

must be a minimum. From equation 3 we see that

$$\varepsilon_i = \left(\sum_j a_{ji} x_j \right) - q_i \tag{5}$$

and therefore we wish to minimize the sum

$$\sum_i \varepsilon_i^{\ 2} = \sum_i \left[\left(\sum_j a_{ji} x_j \right) - q_i \right]^2 . \tag{6}$$

This is a minimum when its partial derivatives with respect to $x_1, x_2 \dots x_n$ are equal to zero; that is, when

$$\frac{\partial \sum_i \varepsilon_i^{\ 2}}{\partial x_1} = 2 \sum_i \left[\left(\sum_j a_{ji} x_j \right) - q_i \right] a_{1i} = 0$$

$$\frac{\partial \sum_i \varepsilon_i^{\ 2}}{\partial x_2} = 2 \sum_i \left[\left(\sum_j a_{ji} x_j \right) - q_i \right] a_{2i} = 0 \tag{7}$$

$$\vdots \qquad\qquad \vdots$$

$$\frac{\partial \sum_i \varepsilon_i^{\ 2}}{\partial x_n} = 2 \sum_i \left[\left(\sum_j a_{ji} x_j \right) - q_i \right] a_{ni} = 0 .$$

Equations 7 may be rewritten

$$\begin{aligned}
\sum_i \sum_j a_{1i}\, a_{ji}\, x_j &= \sum_i a_{1i}\, q_i \\
\sum_i \sum_j a_{2i}\, a_{ji}\, x_j &= \sum_i a_{2i}\, q_i \\
&\vdots \\
\sum_i \sum_j a_{ni}\, a_{ji}\, x_j &= \sum_i a_{ni}\, q_i \, .
\end{aligned} \tag{8}$$

We have now a set of n "normal equations" with n unknowns. They may be solved directly for the set of variables, x_j, if the set of coefficients, a_{ji}, is known. This may be conveniently done by setting up the equations in matrix form

$$\begin{pmatrix}
\sum\limits_i a_{1i}^2 & \sum\limits_i a_{1i}\, a_{2i} & \cdots & \sum\limits_i a_{1i}\, a_{ni} \\
\sum\limits_i a_{2i} a_{1i} & \sum\limits_i a_{2i}^2 & \cdots & \sum\limits_i a_{2i}\, a_{ni} \\
\vdots & \vdots & & \vdots \\
\sum\limits_i a_{ni}\, a_{1i} & \sum\limits_i a_{ni}\, a_{2i} & \cdots & \sum\limits_i a_{ni}^2
\end{pmatrix}
\begin{pmatrix} x_1 \\ x_2 \\ \vdots \\ x_n \end{pmatrix}
=
\begin{pmatrix} \sum\limits_i a_{1i} q_i \\ \sum\limits_i a_{2i} q_i \\ \vdots \\ \sum\limits_i a_{ni} q_i \end{pmatrix} \tag{9}$$

,

or with abbreviated notation

$$Mx = P \, . \tag{10}$$

Inverting the $n \times n$ matrix and multiplying both sides of equation 10 by the inverse, we obtain

$$M^{-1} M\, x = M^{-1} P \, . \tag{11}$$

But $M^{-1}M$ is the identity matrix and therefore

$$x = M^{-1}P \ . \tag{12}$$

3. The least-squares method as applied to the calculation of lattice parameters.

Let us now apply the above technique specifically to the problem of calculating lattice parameters. For the most general triclinic case, the Bragg angle, θ , is a function of the lattice parameters (2)

$$\frac{4}{\lambda^2}\sin^2\theta = h^2a^{*2} + k^2b^{*2} + \ell^2c^{*2} + 2k\ell b^*c^*\cos\alpha^* + 2h\ell a^*c^*\cos\beta^* + 2hka^*b^*\cos\gamma^* + G\sin^2 2\theta + J\left[\frac{\sin^2 2\theta}{\theta} + \frac{\sin^2 2\theta}{\sin\theta}\right] . \tag{13}$$

Correction terms for eccentricity and absorption have been included in equation 13. These will be discussed later. Introducing weights and abbreviating equation 13, we obtain

$$\sqrt{w}\,m = \sqrt{w}\,h^2A + \sqrt{w}\,k^2B + \sqrt{w}\,\ell^2C + \sqrt{w}\,k\ell D + \sqrt{w}\,h\ell E + \sqrt{w}\,hkF + \sqrt{w}\,gG + \sqrt{w}\,jJ \ , \tag{14}$$

where

$A = a^{*2}$; $B = b^{*2}$; $C = c^{*2}$; $D = 2b^{*}c^{*}\cos\alpha^{*}$; $E = 2a^{*}c^{*}\cos\beta^{*}$;

$F = 2a^{*}b^{*}\cos\gamma^{*}$; $g = \sin^{2}2\theta$; $j = \left[\frac{\sin^{2}2\theta}{\theta} + \frac{\sin^{2}2\theta}{\sin\theta}\right]$

$m = \frac{4}{\lambda^{2}}\sin^{2}\theta$.

Equation 14 is one of the set of observational equations, there being one for each observed reflection. The variables A, B, C, D, E, F, G and J are the parameters for which we will solve. We have chosen to write the observational equations as functions of $\sin^{2}\theta$ (rather than $\sin\theta$ or θ) because this results in a linear expression for all crystal systems. In order to minimize the sum of the squares of the residuals in $\sin^{2}\theta$, the quantity

$$\sum_{i} (\sqrt{w_{i}}\,\sin^{2}\theta_{obs} - \sqrt{w_{i}}\,\sin^{2}\theta_{calc})^{2} \qquad (15)$$

must be made a minimum. Finally, differentiating as before, we obtain the set of normal equations, shown in matrix form in table 1. This is the matrix which is set up and inverted by this computer program for the triclinic system.

For efficiency in programming, and with only a negligible increase in calculation time, a full 8 x 8 matrix is set up and inverted for each of the crystal systems. When a whole row and column of the matrix are zero, the corresponding diagonal element is set equal to one before inverting and then reset to zero after

$$\begin{pmatrix} \Sigma w_i h^4_i & \Sigma w_i h^2_i k^2_i & \Sigma w_i h^2_i l^2_i & \Sigma w_i h^2_i k_i l_i & \Sigma w_i h^3_i l_i & \Sigma w_i h^3_i k_i & \Sigma w_i h^2_i g_i & \Sigma w_i h^2_i j_i \\ \Sigma w_i h^2_i k^2_i & \Sigma w_i k^4_i & \Sigma w_i k^2_i l^2_i & \Sigma w_i k^3_i l_i & \Sigma w_i h_i k^2_i l_i & \Sigma w_i h_i k^3_i & \Sigma w_i k^2_i g_i & \Sigma w_i k^2_i j_i \\ \Sigma w_i h^2_i l^2_i & \Sigma w_i k^2_i l^2_i & \Sigma w_i l^4_i & \Sigma w_i k_i l^3_i & \Sigma w_i h_i l^3_i & \Sigma w_i h_i k_i l^2_i & \Sigma w_i l^2_i g_i & \Sigma w_i l^2_i j_i \\ \Sigma w_i h^2_i k_i l_i & \Sigma w_i k^3_i l_i & \Sigma w_i k_i l^3_i & \Sigma w_i k^2_i l^2_i & \Sigma w_i h_i k_i l^2_i & \Sigma w_i h_i k^2_i l_i & \Sigma w_i k_i l_i g_i & \Sigma w_i k_i l_i j_i \\ \Sigma w_i h^3_i l_i & \Sigma w_i h_i k^2_i l_i & \Sigma w_i h_i l^3_i & \Sigma w_i h_i k_i l^2_i & \Sigma w_i h^2_i l^2_i & \Sigma w_i h^2_i k_i l_i & \Sigma w_i h_i l_i g_i & \Sigma w_i h_i l_i j_i \\ \Sigma w_i h^3_i k_i & \Sigma w_i h_i k^3_i & \Sigma w_i h_i k_i l^2_i & \Sigma w_i h_i k^2_i l_i & \Sigma w_i h^2_i k_i l_i & \Sigma w_i h^2_i k^2_i & \Sigma w_i h_i k_i g_i & \Sigma w_i h_i k_i j_i \\ \Sigma w_i h^2_i g_i & \Sigma w_i k^2_i g_i & \Sigma w_i l^2_i g_i & \Sigma w_i k_i l_i g_i & \Sigma w_i h_i l_i g_i & \Sigma w_i h_i k_i g_i & \Sigma w_i g^2_i & \Sigma w_i g_i j_i \\ \Sigma w_i h^2_i j_i & \Sigma w_i k^2_i j_i & \Sigma w_i l^2_i j_i & \Sigma w_i k_i l_i j_i & \Sigma w_i h_i l_i j_i & \Sigma w_i h_i k_i j_i & \Sigma w_i g_i j_i & \Sigma w_i j^2_i \end{pmatrix} \begin{pmatrix} A \\ B \\ C \\ D \\ E \\ F \\ G \\ J \end{pmatrix} = \begin{pmatrix} \Sigma w_i h^2_i m_i \\ \Sigma w_i k^2_i m_i \\ \Sigma w_i l^2_i m_i \\ \Sigma w_i k_i l_i m_i \\ \Sigma w_i h_i l_i m_i \\ \Sigma w_i h_i k_i m_i \\ \Sigma w_i g_i m_i \\ \Sigma w_i j_i m_i \end{pmatrix}$$

Table 1. Normal equations in matrix form for triclinic system. The i's have been omitted from the summations signs for simplicity.

$$\begin{pmatrix} \Sigma w_i (h^2_i + k^2_i)^2 & 0 & \Sigma w_i (h^2_i + k^2_i) l^2_i & 0 & 0 & 0 & \Sigma w_i (h^2_i + k^2_i) g_i & \Sigma w_i (h^2_i + k^2_i) j_i \\ 0 & 0 & 0 & 0 & 0 & 0 & 0 & 0 \\ \Sigma w_i (h^2_i + k^2_i) l^2_i & 0 & \Sigma w_i l^4_i & 0 & 0 & 0 & \Sigma w_i l^2_i g_i & \Sigma w_i l^2_i j_i \\ 0 & 0 & 0 & 0 & 0 & 0 & 0 & 0 \\ 0 & 0 & 0 & 0 & 0 & 0 & 0 & 0 \\ 0 & 0 & 0 & 0 & 0 & 0 & 0 & 0 \\ \Sigma w_i (h^2_i + k^2_i) g_i & 0 & \Sigma w_i l^2_i g_i & 0 & 0 & 0 & \Sigma w_i g^2_i & \Sigma w_i g_i j_i \\ \Sigma w_i (h^2_i + k^2_i) j_i & 0 & \Sigma w_i l^2_i j_i & 0 & 0 & 0 & \Sigma w_i g_i j_i & \Sigma w_i j^2_i \end{pmatrix} \begin{pmatrix} A \\ 0 \\ C \\ 0 \\ 0 \\ 0 \\ G \\ J \end{pmatrix} = \begin{pmatrix} \Sigma w_i (h^2_i + k^2_i) m_i \\ 0 \\ \Sigma w_i l^2_i m_i \\ 0 \\ 0 \\ 0 \\ \Sigma w_i g_i m_i \\ \Sigma w_i j_i m_i \end{pmatrix}$$

Table 2. Normal equations matrix for the tetragonal system.

$$\begin{pmatrix} \Sigma w_i(h^2_i + k^2_i + h_ik_i)^2 & 0 & \Sigma w_i(h^2_i + k^2_i + h_ik_i)l^2_i & 0 & 0 & 0 & \Sigma w_i(h^2_i + k^2_i + h_ik_i)g_i & \Sigma w_i(h^2_i + k^2_i + h_ik_i)j_i \\ 0 & 0 & 0 & 0 & 0 & 0 & 0 & 0 \\ \Sigma w_i(h^2 + k^2_i + h_ik_i)l^2_i & 0 & \Sigma w_i l^4_i & 0 & 0 & 0 & \Sigma w_i l^2_i g_i & \Sigma w_i l^2_i j_i \\ 0 & 0 & 0 & 0 & 0 & 0 & 0 & 0 \\ 0 & 0 & 0 & 0 & 0 & 0 & 0 & 0 \\ 0 & 0 & 0 & 0 & 0 & 0 & 0 & 0 \\ \Sigma w_i(h^2_i + k^2_i + h_ik_i)g_i & 0 & \Sigma w_i l^2_i g_i & 0 & 0 & 0 & \Sigma w_i g^2_i & \Sigma w_i g_i j_i \\ \Sigma w_i(h^2_i + k^2_i + h_ik_i)j_i & 0 & \Sigma w_i l^2_i j_i & 0 & 0 & 0 & \Sigma w_i g_i j_i & \Sigma w_i j^2_i \end{pmatrix} \begin{pmatrix} A \\ 0 \\ C \\ 0 \\ 0 \\ 0 \\ G \\ J \end{pmatrix} = \begin{pmatrix} \Sigma w_i(h^2_i + k^2_i + h_ik_i)m_i \\ 0 \\ \Sigma w_i l^2_i m_i \\ 0 \\ 0 \\ 0 \\ \Sigma w_i g_i m_i \\ \Sigma w_i j_i m_i \end{pmatrix}$$

Table 3. Normal equations matrix for the hexagonal-trigonal system.

$$\begin{pmatrix} \Sigma w_i(h^2_i + k^2_i + l^2_i)^2 & 0 & 0 & 0 & 0 & 0 & \Sigma w_i(h^2_i + k^2_i + l^2_i)g_i & \Sigma w_i(h^2_i + k^2_i + l^2_i)j_i \\ 0 & 0 & 0 & 0 & 0 & 0 & 0 & 0 \\ 0 & 0 & 0 & 0 & 0 & 0 & 0 & 0 \\ 0 & 0 & 0 & 0 & 0 & 0 & 0 & 0 \\ 0 & 0 & 0 & 0 & 0 & 0 & 0 & 0 \\ 0 & 0 & 0 & 0 & 0 & 0 & 0 & 0 \\ \Sigma w_i(h^2_i + k^2_i + l^2_i)g_i & 0 & 0 & 0 & 0 & 0 & \Sigma w_i g^2_i & \Sigma w_i g_i j_i \\ \Sigma w_i(h^2_i + k^2_i + l^2_i)j_i & 0 & 0 & 0 & 0 & 0 & \Sigma w_i g_i j_i & \Sigma w_i j^2_i \end{pmatrix} \begin{pmatrix} A \\ 0 \\ 0 \\ 0 \\ 0 \\ 0 \\ G \\ J \end{pmatrix} = \begin{pmatrix} \Sigma w_i(h^2_i + k^2_i + l^2_i)m_i \\ 0 \\ 0 \\ 0 \\ 0 \\ 0 \\ \Sigma w_i g_i m_i \\ \Sigma w_i j_i m_i \end{pmatrix}$$

Table 4. Normal equations matrix for the cubic system.

inverting. For the monoclinic system, the coefficients of D and F are set equal to zero, and for the orthorhombic system the coefficients of D, E, and F are set equal to zero. For the tetragonal system, the observational equations are of the form

$$\sqrt{w}\,(h^2 + k^2)A + \sqrt{w}\,\ell^2 C + \sqrt{w}\,gG + \sqrt{w}\,jJ = \sqrt{w}\,m\ . \tag{16}$$

The corresponding matrix of normal equations is given in table 2. The form of the hexagonal-trigonal observational equations is

$$\sqrt{w}\,(h^2 + k^2 + hk)A + \sqrt{w}\,\ell^2 C + \sqrt{w}\,gG + \sqrt{w}\,jJ = \sqrt{w}\,m \tag{17}$$

and table 3 gives the normal equations matrix. The cubic observational equations are of the form

$$\sqrt{w}\,(h^2 + k^2 + \ell^2)A + \sqrt{w}\,gG + \sqrt{w}\,jJ = \sqrt{w}\,m\ . \tag{18}$$

Table 4 shows the normal equations matrix for the cubic crystal system.

4. Correction for systematic errors.

It should be noted that the least-squares method gives no indication of the correct form of the observational equation to be used to fit the data, but rather gives only the best fit of the equation employed. It is therefore desirable to include, in the observational equation, correction terms for any important sources of systematic error. There are a number of discussions of sources of error in the determination of lattice parameters (2-7) to which the reader is directed. It is generally agreed that the most important source of systematic error (assuming that film shrinkage has been taken into account) is due to absorption of the primary x-ray beam by the sample. Taylor and Sinclair (5) and Nelson and Riley (7) have shown empirically that the error due to absorption in the measured unit cell edge, d, as a function of the Bragg angle, θ , is given approximately by

$$\frac{\Delta d}{d} = J' \left[\frac{\cos^2\theta}{\theta} + \frac{\cos^2\theta}{\sin\theta} \right] . \tag{19}$$

For the purpose of this program, however, we are concerned with $\Delta(1/d^2)$ which is proportional to the error in $\sin^2\theta$. Since

$$\Delta\left(\frac{1}{d^2}\right) = \frac{-2}{d^3}\,\Delta d = \frac{-2}{d^2}\left(\frac{\Delta d}{d}\right) = \frac{-8\sin^2\theta}{\lambda^2}\left(\frac{\Delta d}{d}\right) , \tag{20}$$

equation 19 may be rewritten

$$\Delta\left(\frac{1}{d^2}\right) = J \left[\frac{\sin^2 2\theta}{\theta} + \frac{\sin^2 2\theta}{\sin\theta} \right] . \tag{21}$$

This is the form of the absorption correction used in this program. It appears that equation 21 holds well for angles greater than 30°. In any event, the correction is likely to be negligible for small organic crystals.

Another source of systematic error arises if the sample is not quite coaxial with the cylindrical film holder. The correction for this eccentricity may easily be shown to have the form

$$\frac{\Delta d}{d} = G' \cos^2\theta \tag{22}$$

which may be rewritten

$$\Delta\left(\frac{1}{d^2}\right) = G \sin^2 2\theta \, . \tag{23}$$

This is the form of the eccentricity correction used in this program. It should be noted that this is not a correction for a sample which wobbles in the beam, for it is assumed that this sort of adjustment is easily made. The eccentricity correction refers to the possibility that the axis of rotation of the shaft is not located at the center of the film holder; it is, therefore, negligible for a well constructed camera.

Although there are undoubtedly other sources of minor systematic errors, only absorption and eccentricity are included, at the operator's option, in the least-squares calculation carried out by this program.

5. Weighting of observations.

This program minimizes the sum of the squares of the residuals in $\sin^2\theta$. Hence an appropriate weighting function may be

$$\sqrt{w} = \frac{1}{\frac{\sigma}{\sin^2\theta}} = \frac{1}{(2\sin\theta\cos\theta)\sigma_\theta} = \frac{1}{(\sin 2\theta)\sigma_\theta} \quad . \tag{24}$$

But σ_θ may be expected to be constant for all values of θ, in which case we may write

$$\sqrt{w} \propto \frac{1}{\sin 2\theta} \quad . \tag{25}$$

This weighting function has been discussed by Hess (8). In addition to the internally programmed weighting function, equation 25, an external weight, $\sqrt{w} = \mathcal{E}$, may be applied to the observed data. The desired combination of the external and internal weights is selected by setting the appropriate program control switches on the computer console.

6. Conversion of reciprocal to direct lattice parameters.

The conversion of reciprocal lattice parameters to direct lattice parameters is straightforward for the higher symmetry crystal systems. However, the expressions are somewhat more complex for the triclinic system. The formulas used in this program for the conversions are given below.

$$a = \frac{\sin\alpha^*}{a^* s^*} \quad , \quad b = \frac{\sin\beta^*}{b^* s^*} \quad , \quad c = \frac{\sin\gamma^*}{c^* s^*} \quad , \tag{26}$$

where

$$s^* = [\sin^2\alpha^* \sin^2\beta^* - \cos^2\alpha^* \cos^2\beta^* + 2\cos\alpha^* \cos\beta^* \cos\gamma^* - \cos^2\gamma^*]^{\frac{1}{2}} ;$$

also,

$$\cos\alpha = \frac{\cos\beta^{*}\cos\gamma^{*} - \cos\alpha^{*}}{\sin\beta^{*}\sin\gamma^{*}}$$

$$\cos\beta = \frac{\cos\alpha^{*}\cos\gamma^{*} - \cos\beta^{*}}{\sin\alpha^{*}\sin\gamma^{*}} \qquad (27)$$

$$\cos\gamma = \frac{\cos\alpha^{*}\cos\beta^{*} - \cos\gamma^{*}}{\sin\alpha^{*}\sin\beta^{*}}$$

7. Calculation of standard deviations.

If absolute weights ($w = 1/\sigma_q^2$) are used in the observational equations, the variances, $\sigma_{x_j}^2$, will be equal to the corresponding diagonal terms of the inverse matrix. That is,

$$\sigma_{x_j}^2 = M_{jj}^{-1} \; . \qquad (28)$$

Usually, however, we have only a relative set of weights and the expression for the variance becomes

$$\sigma_{x_j}^2 = \frac{\sum_i e^2}{m-n} \; [M_{jj}^{-1}] \qquad (29)$$

Equation 29 assumes that the only remaining errors are random observational errors. This means that we must have the correct form and best fit of our observational equation in order to obtain meaningful standard deviations.

The expressions used for calculation of the standard deviations in the lattice parameters are

$$\sigma_a = \frac{a}{2a^{*2}}\,\sigma_A, \qquad \sigma_b = \frac{b}{2b^{*2}}\,\sigma_B, \qquad \sigma_c = \frac{c}{2c^{*2}}\,\sigma_C;$$

also,

$$\sigma_\alpha = \frac{\sigma_D}{2b^* c^* \sin\alpha \sin\beta^* \sin\gamma^*} \tag{30}$$

$$\sigma_\beta = \frac{\sigma_E}{2a^* c^* \sin\beta \sin\alpha^* \sin\gamma^*}$$

$$\sigma_\gamma = \frac{\sigma_F}{2a^* b^* \sin\gamma \sin\alpha^* \sin\beta^*}$$

8. Input.

The data tape input to this program is shown in table 5. Three wavelengths, λ_n, may be used in the calculations if desired. This permits one, for example, to enter $K\alpha_{(\mathrm{mean})}$, $K\alpha_1$, and $K\alpha_2$. Zonal data from two or more axes may be lumped together into one calculation if desired. For example, $h0\ell$ and $hk0$ data may be run together and the calculations will be performed as if $hk\ell$ data had been entered. If one wishes to keep the calculations separate, the $hk\ell$ data words must be divided into blocks with end-word tags, as shown in table 5. The $hk\ell$ data word list begins in cell 1000 and the

Table 5. Input data tape.

Cell	Contents	Remarks
	6 0000 04 0000	
0000	0 00λλ λλ $\lambda\lambda\lambda\lambda_0$	λ_n in Å units; cells 0000 - 0002 must contain λ_n or zero.
1	0 00λλ λλ $\lambda\lambda\lambda\lambda_1$	
2	0 00λλ λλ $\lambda\lambda\lambda\lambda_2$	
	6 0000 04 1000	
1000	0 0±hh ±k k±ℓℓ	First block of hkℓ data.
⋮	⋮	
⋮	4 0±hh ±k k±ℓℓ	
⋮	⋮	p blocks of hkℓ data with a 4 in the sign position of the last word of each block.
⋮	0 0±hh ±k k±ℓℓ	Last block of hkℓ data with a 5 in the sign position.
⋮	⋮	
999 + m (m < 1000)	5 0±hh ±k k±ℓℓ	
	6 0000 04 2000	
2000	λ_n εεθθ.θθ θθθθ	λ_n = 0, 1 or 2; ε = external weight (9.9 ≥ ε ≥ 0.0); θ = Bragg angle in degrees (90° ≥ θ ≥ 0°); these words are in the same order as the corresponding hkℓ words.
⋮	⋮	
1999 + m	λ_n εεθθ.θθ θθθθ	
	6 0000 30 0300	Branch to start of program.

corresponding $\lambda, \mathcal{E}, \theta$ word list begins in cell 2000. It is necessary that the two lists be in the same order and of the same length.

9. Program operation.

Figure 1 is a flow chart of the sequence of operations carried out in this program. The operating time is less than one second per reflection, excluding print-out time. An error halt will occur if the number of parameters is equal to or greater than the number of observations. The program control switches used for this program are listed in table 6.

The operating instructions for this program are as follows:

1) Read in the program tape with the "Hold PZT to Zero" switch in the normal (down) position.
2) Set the selected program control switches.
3) Set up the output for SPO commands.
4) Read in the data tape with the PZT switch down unless $\lambda_n = 2$ for any of the reflections. If there are 2's in the sign positions of any of the data words, set the PZT switch in the up position, press the "S to P" switch, put the "S On" switch on, set rS = 0300 and then read in the data tape. After the data tape has read in and the computer halted in cell 0300, return the PZT switch to the normal position and turn the "S On" switch off.

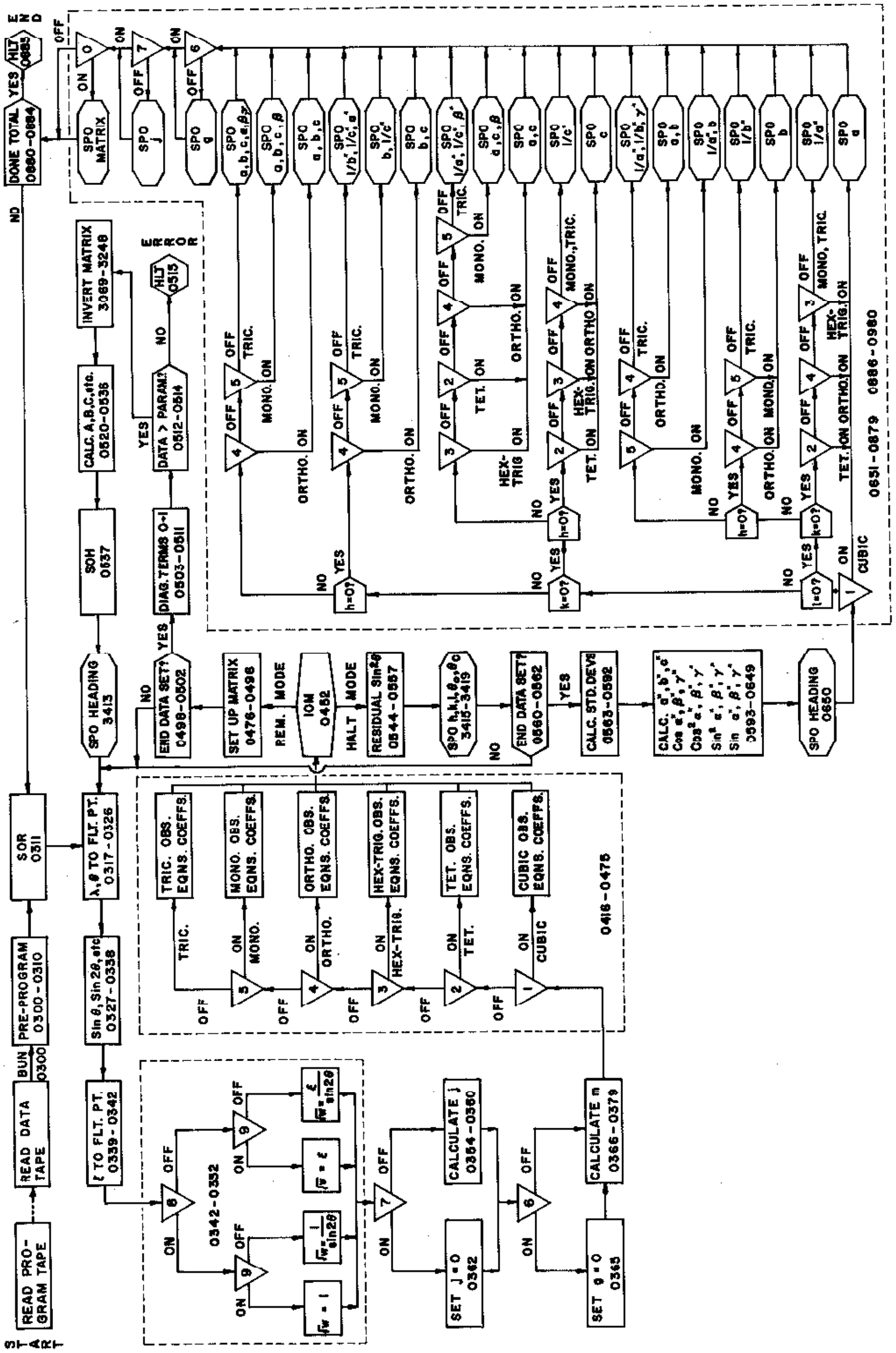

Figure 1. Program flow chart for calculation of lattice parameters by the least-squares method.

Table 6. Program control switch selections.

PCS	Condition	Response
1	On	Cubic system
2	On	Tetragonal system
3	On	Hexagonal system
4	On	Orthorhombic system
5	On	Monoclinic system
1-5	Off	Triclinic system
6	On	Omit eccentricity correction
	Off	Include eccentricity correction
7	On	Omit absorption correction
	Off	Include absorption correction
8	On	$\sqrt{w} = 1$
9	On	
8	On	$\sqrt{w} = \frac{1}{\sin 2\theta}$
9	Off	
8	Off	$\sqrt{w} = \mathcal{E}$
9	On	
8	Off	$\sqrt{w} = \frac{\mathcal{E}}{\sin 2\theta}$
9	Off	
0	On	Print normal and inverse matrices
	Off	Omit matrix print-out

5) The program begins with a BUN to cell 0300. If everything functions normally, the computer will carry out the required calculations and halt with rC = 8421 00 1248. If the number of parameters in the observational equations is equal to or greater than the number of observed data in any input block, the computer will halt with rC = 7777 00 7777. If, because of an input error, a calculated sinθ is greater than one, the computer will halt with rC = 5110 00 0000.

10. Output.

The first group of output is the list of reflections with the observed and calculated Bragg angles in degrees. This list permits one to check quickly for reflections which have been indexed or punched incorrectly.

The second output group is the calculated unit cell parameters. The axial lengths are given in Angstrom units and the axial angles in degrees, along with the standard deviations for each. The values of the eccentricity and absorption corrections will also be printed, along with their standard deviations, depending upon the condition of program control switches 6 and 7.

If program control switch 0 is on, the full 8 x 8 M matrix will be printed by columns, followed by the P vector. The inverse matrix, M^{-1}, will then be printed by columns.

II. A Program for the Calculation of Interatomic Distances, Angles and Best Planes.

1. Introduction.

This program consists of four distinct parts, calculation of orthogonal coordinates, interatomic distances, bond angles and best planes by the least-squares method. Any combination of the four parts of the program may be selected by means of the program control switches. The program was written for the Burroughs 220 digital computer in basic machine language.

The required input is the number of atoms, the fractional atomic coordinates, the lattice parameters, and a designation of any bond angles and best planes to be calculated. The maximum output consists of the orthogonalized coordinates, the interatomic distances less than a designated value, the bond angles, the direction cosines of the best planes with respect to both orthogonal and crystal axes, and the normal deviations of the selected atoms from the best plane.

2. Orthogonalization of coordinates.

The conversion to an orthogonal coordinate system for hexagonal, monoclinic or triclinic unit cells greatly simplifies the equations for the calculations of interatomic distances, bond angles, and least-squares planes. By convention, the orthogonal axes,

$\underset{\sim}{X}$, $\underset{\sim}{Y}$, $\underset{\sim}{Z}$, are related to the crystal axes, $\underset{\sim}{a}$, $\underset{\sim}{b}$, $\underset{\sim}{c}$, as follows: $\underset{\sim}{Y}$ is coincident with $\underset{\sim}{b}$, $\underset{\sim}{Z}$ is coincident with $\underset{\sim}{c}^*$, and therefore $\underset{\sim}{X}$ must lie in the plane of $\underset{\sim}{a}$ and $\underset{\sim}{b}$.

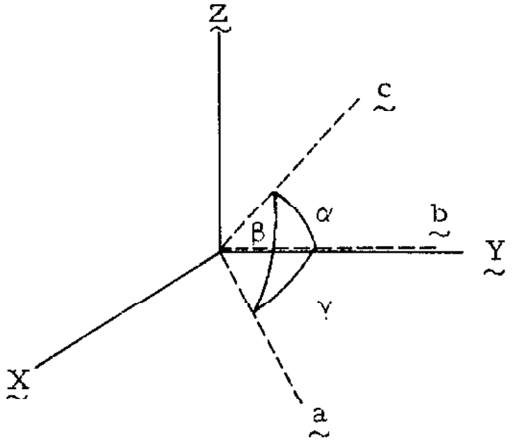

The expressions used in this program for the conversion of crystal coordinates, x, y, z, to orthogonal coordinates, X, Y, Z, are

$$X = ax \sin\gamma + cz \left[\frac{\cos\beta - \cos\alpha \cos\gamma}{\sin\gamma} \right]$$

$$Y = ax \cos\gamma + by + cz \cos\alpha \tag{1}$$

$$Z = cz \left[\frac{1 - \cos^2\alpha - \cos^2\beta - \cos^2\gamma + 2\cos\alpha \cos\beta \cos\gamma}{\sin^2\gamma} \right]^{\frac{1}{2}}$$

3. Interatomic distances.

The distance, d_{ij}, between two atoms, i and j, is calculated by this program from their orthogonal coordinates, using the formula,

$$d_{ij} = [(X_i - X_j)^2 + (Y_i - Y_j)^2 + (Z_i - Z_j)^2]^{\frac{1}{2}} \qquad (2)$$

4. Bond angles.

The angle, θ_{ijk}, formed by three atoms, i, j, and k, is calculated by this program from the law of cosines,

$$\theta_{ijk} = \cos^{-1} \left[\frac{d_{ij}^2 + d_{jk}^2 - d_{ik}^2}{2 d_{ij} d_{jk}} \right] \qquad (3)$$

5. Best planes by the least-squares method.

The calculation, by the least-squares method, of the best plane through a set of atoms has been discussed by Schomaker, Waser, Marsh and Bergman (9) and by Blow (10). Hybl (11) has written a lucid, detailed description of the calculation and is quoted below.

> We define the plane as $m_1X + m_2Y + m_3Z - d = 0$, where m_1, m_2, and m_3 are the direction cosines of the plane normal and d is the distance from the plane to the origin. A Cartesian coordinate system is assumed. The distance d_k from the plane to an atom $P_k(X_kY_kZ_k)$ is then given by $d_k = m_1X_k + m_2Y_k + m_3Z_k - d$. To find the best plane we require that $\sum_k w_k d_k^2 = \sum_k w_k(m_1X_k + m_2Y_k + m_3Z_k - d)^2$ be a minimum subject, as we shall see, to one side condition. The problem of the plane is essentially equivalent to the problem of finding the principal plane of a set of mass points with

the least inertia. To find the principal inertial axes we introduce the side condition that $m_1^2 + m_2^2 + m_3^2 = 1$ by use of the Lagrange multiplier λ. Thus we define

$$F = \sum_k w_k(m_1 X_k + m_2 Y_k + m_3 Z - d)^2 - \lambda(m_1^2 + m_2^2 + m_3^2)$$

The normal equations resulting from the differentiation of the above expression are

$$\tfrac{1}{2}\left(\frac{\partial F}{\partial m_1}\right) = \sum_k w_k X_k(m_1 X_k + m_2 Y_k + m_3 Z_k - d) - \lambda m_1 = 0$$

$$\tfrac{1}{2}\left(\frac{\partial F}{\partial m_2}\right) = \sum_k w_k Y_k(m_1 X_k + m_2 Y_k + m_3 Z_k - d) - \lambda m_2 = 0$$

$$\tfrac{1}{2}\left(\frac{\partial F}{\partial m_3}\right) = \sum_k w_k Z_k(m_1 X_k + m_2 Y_k + m_3 Z_k - d) - \lambda m_3 = 0$$

and

$$-\tfrac{1}{2}\left(\frac{\partial F}{\partial d}\right) = \sum_k w_k(m_1 X_k + m_2 Y_k + m_3 Z_k - d) = 0$$

The last equation can be readily solved for d:

$$d = \frac{\sum_k w_k(m_1 X_k + m_2 Y_k + m_3 Z_k)}{\sum_k w_k} = m_1 \bar{X} + m_2 \bar{Y} + m_3 \bar{Z},$$

where $\bar{X} = \sum_k w_k X_k / \sum_k w_k$ etc. Thus if we make the transformations $x_k = X_k - \bar{X}$, $y_k = Y_k - \bar{Y}$ and $z_k = Z_k - \bar{Z}$, we eliminate d from the first three normal equations which are reduced to

$$(\sum_k w_k x_k^2 - \lambda)m_1 + \sum_k w_k x_k y_k m_2 + \sum_k w_k x_k z_k m_3 = 0$$

$$\sum_k w_k x_k y_k m_1 + (\sum_k w_k y_k^2 - \lambda)m_2 + \sum_k w_k y_k z_k m_3 = 0$$

$$\sum_k w_k x_k z_k m_1 + \sum_k w_k y_k z_k m_2 + (\sum_k w_k z_k^2 - \lambda)m_3 = 0$$

We write this in the matrix form

$$\begin{bmatrix} A_{11}-\lambda & A_{12} & A_{13} \\ A_{12} & A_{22}-\lambda & A_{23} \\ A_{13} & A_{23} & A_{33}-\lambda \end{bmatrix} \begin{bmatrix} m_1 \\ m_2 \\ m_3 \end{bmatrix} = \underline{A} \begin{bmatrix} m_1 \\ m_2 \\ m_3 \end{bmatrix} = 0$$

In order to solve this secular equation, we first expand it to $-\lambda^3 + a\lambda^2 + b\lambda + c = 0$, where $a = (A_{11}+A_{22}+A_{33})$, $b = -(A_{11}A_{22}+A_{11}A_{33}+A_{22}A_{33}) + (A_{12}^2+A_{13}^2+A_{23}^2)$, and $c = A_{11}A_{22}A_{33}+2A_{12}A_{13}A_{23}-(A_{11}A_{23}^2+A_{22}A_{13}^2+A_{33}A_{12}^2)$.

The cubic equation can, of course, be solved directly, but this method is tedious. Since λ is a sum of squares, all solutions of the cubic must be positive and since $\underline{A}$ is a symmetric matrix all three solutions are real. The desired solution is the least of these. Blow (ref. 10, this thesis) has shown that an approximate value to the desired solution $\lambda^{(1)}$ is $\lambda_0^{(1)} = [-b - (b^2-4ac)^{\frac{1}{2}}]/2a$. It is clear that this represents a solution provided by a parabola which approximates to the cubic at small λ. The form of $\lambda_0^{(1)}$ gives the smaller of the two solutions.

This solution may be refined by the Newton-Raphson method (ref. 12, this thesis). The n+1 st refined value is obtained from the n th value by evaluating:

$$\lambda_{n+1}^{(1)} = \lambda_n - \frac{(-\lambda_n^3 + a\lambda_n^2 + b\lambda_n + c)}{(-3\lambda_n^2 + 2a\lambda_n + b)}$$

Because the slope of the cubic at $\lambda_0^{(1)}$ must be steeper than that of the quadratic, refinement by the Newton-Raphson method will always lead to the smallest solution.

Values of m_1, m_2, and m_3 are obtained from substitution of $\lambda^{(1)}$ into matrix $\underline{A}$ and normalizing so that $m_1^2 + m_2^2 + m_3^2 = 1$.

The technique outlined above is exactly that used in this program, except that the initial value of the Lagrange multiplier, $\lambda_0^{(1)}$, is obtained from

$$\lambda_0^{(1)} = -\frac{c}{b} \quad . \tag{4}$$

The expression used for the conversion of orthogonal direction cosines, m_1, m_2, m_3, to non-orthogonal direction cosines, cos A, cos B, cos C, are

$$\begin{aligned} \cos A &= m_1 \sin\gamma + m_2 \cos\gamma \\ \cos B &= m_2 \\ \cos C &= \frac{m_1(\cos\beta - \cos\gamma\cos\alpha)}{\sin\gamma} + m_2 \cos\alpha \\ &\quad + \frac{m_3}{\sin\gamma}\left[1 - \cos^2\alpha - \cos^2\beta - \cos^2\gamma + 2\cos\alpha\cos\beta\cos\gamma\right]^{\frac{1}{2}} \end{aligned} \tag{5}$$

6. Input.

The data tape input to this program is shown in table 7. The number N must be equal to the cell location of the last x coordinate; therefore, there will be N+1 atoms included in the orthogonalization and interatomic distance calculations. In general, for a set of N+1 points, there are $\frac{N(N+1)}{2}$ different interatomic distances, many of which may be too long to be of interest. The

Table 7. Input data tape.

Cell	Contents	Remarks
	6 0000 04 0500	
0500	0 0000 00 0NNN.	N = last x cell ($0 \le N \le 499$)
1	0 0000 D.D DDDD	D_{max} in Å ($0 \le D < 100$)
2	0 000a a.a aaaa	a in Å ($0 \le a < 100$)
3	0 000b b.b bbbb	b in Å ($0 \le b < 100$)
4	0 000c c.c cccc	c in Å ($0 \le c < 100$)
5	± 0000.αα αααα	cos α ($-1 \le \cos\alpha \le 1$)
6	± 0000.ββ ββββ	cos β ($-1 \le \cos\beta \le 1$)
7	± 0000.γγ γγγγ	cos γ ($-1 \le \cos\gamma \le 1$)
	6 0000 04 0000	
0000	00xx.xx xxxx	Fractional x coordinates; note that the last x is entered in cell 0000 N ($-100 < x < 100$).
⋮	⋮	
0000+N	00xx.xx xxxx	
	6 0000 04 1000	
1000	00yy.yy yyyy	Fractional y coordinate ($-100 < y < 100$).
⋮	⋮	
1000+N	00yy.yy yyyy	
	6 0000 04 2000	
2000	00zz.zz zzzz	Fractional z coordinate ($-100 < z < 100$).
⋮	⋮	
2000+N	00zz.zz zzzz	
	6 0000 04 3000	
3000	0 0 iii jj jkkk	List of m bond angles with a 9 in the first variant position of the last word. ($0 \le i, j, k \le 499$)
⋮	⋮	
2999+m ($m \le 500$)	0 9 iii jj jkkk	

Table 7. (continued)

Cell	Contents	Remarks
	6 0000 04 4000	
4000	0 000w ww 0 iii	First set of best plane atoms with an 8 in the first variant position of the last word. $(0 \le i \le 499;\ 0 \le w \le 999)$
⋮	⋮	
⋮	0 800w ww 0 iii	
⋮	⋮	p sets of atoms, each with an 8 in the last word.
⋮	0 000w ww 0 iii	Last set of atoms with a 9 in the last word.
⋮	⋮	
3999+n $(n \le 500)$	0 900w ww 0 iii	
	6 0000 30 1500	Branch to start of program.

program running time may be significantly reduced by printing only those interatomic distances that are less than a selected value D_{max}.

The x, y, and z fractional atomic coordinate lists begin in cell 0000, 1000, and 2000, respectively. These lists must be in the same order and of the same length.

The atom numbers i, j, k, which must be entered for the bond angles program, are equal to the cell locations of the x coordinates of the atoms selected.

If an atom is entered with weight $w = 0$ in a best plane calculation, it will be omitted from the least-squares fitting, but its distance from the plane will be printed. This is useful, for example, for finding the deviation of hydrogen atoms from the best plane of a ring of heavy atoms to which the hydrogen atoms are bonded.

7. Program operation.

A flow chart of the operation sequence for this program is shown in figure 2. The desired combination of the four parts of the program may be selected by means of the program control switches, as outlined in table 8.

The operating instructions for this program are as follows:

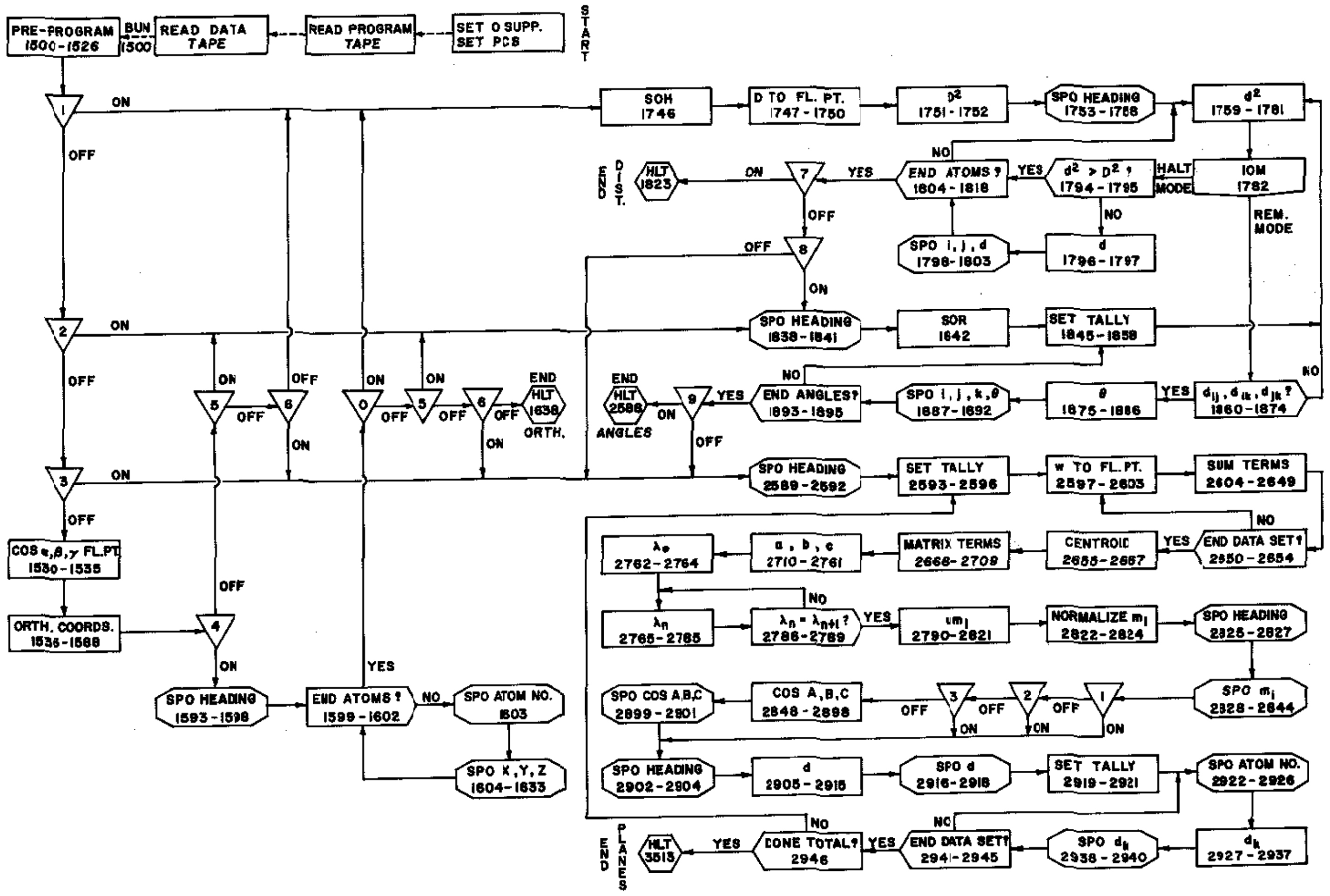

Figure 2. Program flow chart for the calculation of orthogonalized coordinates, interatomic distances, bond angles, and least-squares planes.

Table 8. Program control switch selections.

PCS ON	Response
None	Orthogonalization, distances, angles, planes
1	Distances, angles, planes
2	Angles, planes
3	Planes
4	Orthogonalization (SPO)
5	Orthogonalization, angles, planes
6	Orthogonalization, planes
7	Orthogonalization, distances
8	Orthogonalization, distances, planes
9	Orthogonalization, distances, planes
1,7	Distances
1,8	Distances, planes
1,9	Distances, angles
2,9	Angles
5,9	Orthogonalization, angles
4,0	Orthogonalization (SPO), distances, angles, planes
4,5	Orthogonalization (SPO), angles, planes
4,6	Orthogonalization (SPO), planes
4,0,7	Orthogonalization (SPO), distances
4,0,8	Orthogonalization (SPO), distances, planes
4,0,9	Orthogonalization (SPO), distances, angles
4,5,9	Orthogonalization (SPO), angles

1) Set the "Leading Zero Suppress" switch on the console in the on (up) position and the "Hold PZT to Zero" switch in the normal (down) position.
2) Read in the program tape.
3) Set the selected program control switches.
4) Set up the output for SPO commands.
5) Read in the data tape.
6) The program begins with a BUN to cell 1500. The computer will carry out the desired calculations and halt with rC = 0000 00 1638, 0000 00 1823, 0000 00 2588 or 0000 00 3513, depending upon whether the orthogonalization, interatomic distances, bond angles or least-squares plane program is the last performed.

8. Output.

If program control switch 4 is on, the orthogonalized coordinates in Angstrom units will be printed. The output for the interatomic distances program is a list of the pairs of atoms and the corresponding distances in Angstrom units. The bond angles output is a list of the sets of three atoms and the corresponding angles in degrees. The first part of the best planes output is the direction cosines of the normal to the plane based on the orthogonal axes. If the crystal has non-orthogonal axes, the direction cosines with respect to those axes will also be printed. The second part of the best planes output is the distance of the origin from the plane and a list of the deviations of each atom from the plane, a negative deviation indicating the atom lies to the origin side of the plane.

III. Preliminary X-Ray Diffraction Studies of Anemonin.

1. Introduction.

Anemonin is a white, crystalline compound with the empirical formula $C_{10}H_8O_4$. From a study of the reduction and hydrolysis products of anemonin, several investigators (13-15)

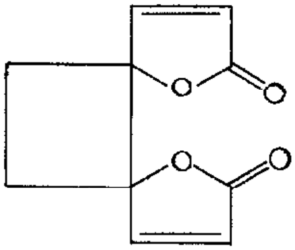

I

have concluded that the structure is that shown (I). There are, of course, three possible stereoisomers of I, *meso*-anemonin (Ia) and *d* and *l*-anemonin (Ib). Harris (16) has concluded from a

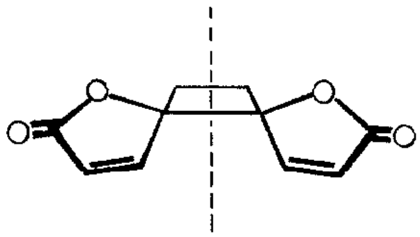

Ia

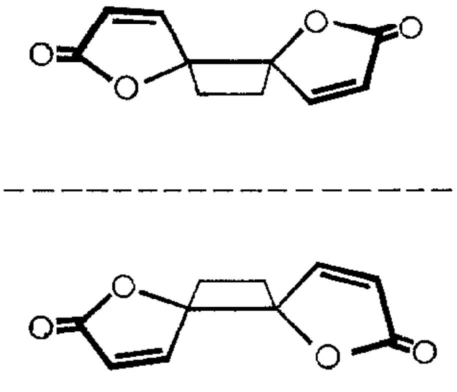

Ib

study of the substituted 1,2-cyclobutanediol formed in the reduction of anemonin, that the two vicinal lactone rings are cis, and therefore anemonin has the meso configuration. Since there is some room for doubt in the Harris structure proof, an X-ray diffraction study of this compound was initiated in order to ascertain, by an independent method, the stereochemistry of anemonin. In addition, anemonin is of interest because of its unusual spiro ring structure.

2. Preliminary crystallographic data.

A sample of impure anemonin was obtained from E. S. Olson. This material was recrystallized from chloroform to give a crystalline sample which, however, did not exhibit a distinct melting point (lit. (17) m. p. 157-158°). Examination of these crystals under a microscope showed that anemonin crystallizes in an acicular habit with many well developed faces. The macroscopic symmetry of the crystals, figure 3, indicated that the point group is D_{2h}, an observation which was later supported by the determination of the space group. A suitable crystal was mounted with its needle zone axis parallel to the goniometer axis and goniometric measurements were taken. Table 9 tabulates these measurements; figure 4 is a stereographic projection plotted from them.

A 20° oscillation photograph was taken with the needle zone axis, c, as the rotation axis. Measurements from this film gave a value of 11.62 Å for c. From the hk0 Weissenberg photograph, the

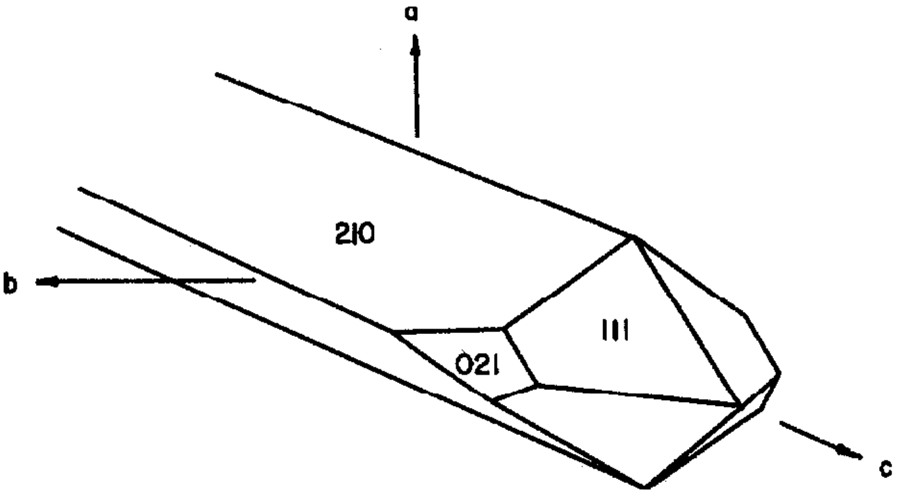

Figure 3. A typical crystal of anemonin with its faces indexed and the positions of the crystallographic axes indicated.

Table 9. Goniometric measurements taken on a crystal of anemonin.

Longitude	Latitude	Index
34° 06'	0° 00'	$\bar{2}\bar{1}0$
99° 17'	0° 04'	$\bar{2}10$
213° 47'	359° 45'	210
278° 14'	0° 06'	$2\bar{1}0$
15° 10'	37° 12'	$\bar{1}\bar{1}1$
119° 31'	36° 44'	$\bar{1}11$
194° 53'	36° 09'	111
297° 25'	37° 00'	$1\bar{1}1$
336° 11'	25° 42'	$0\bar{2}1$
156° 00'	25° 01'	021

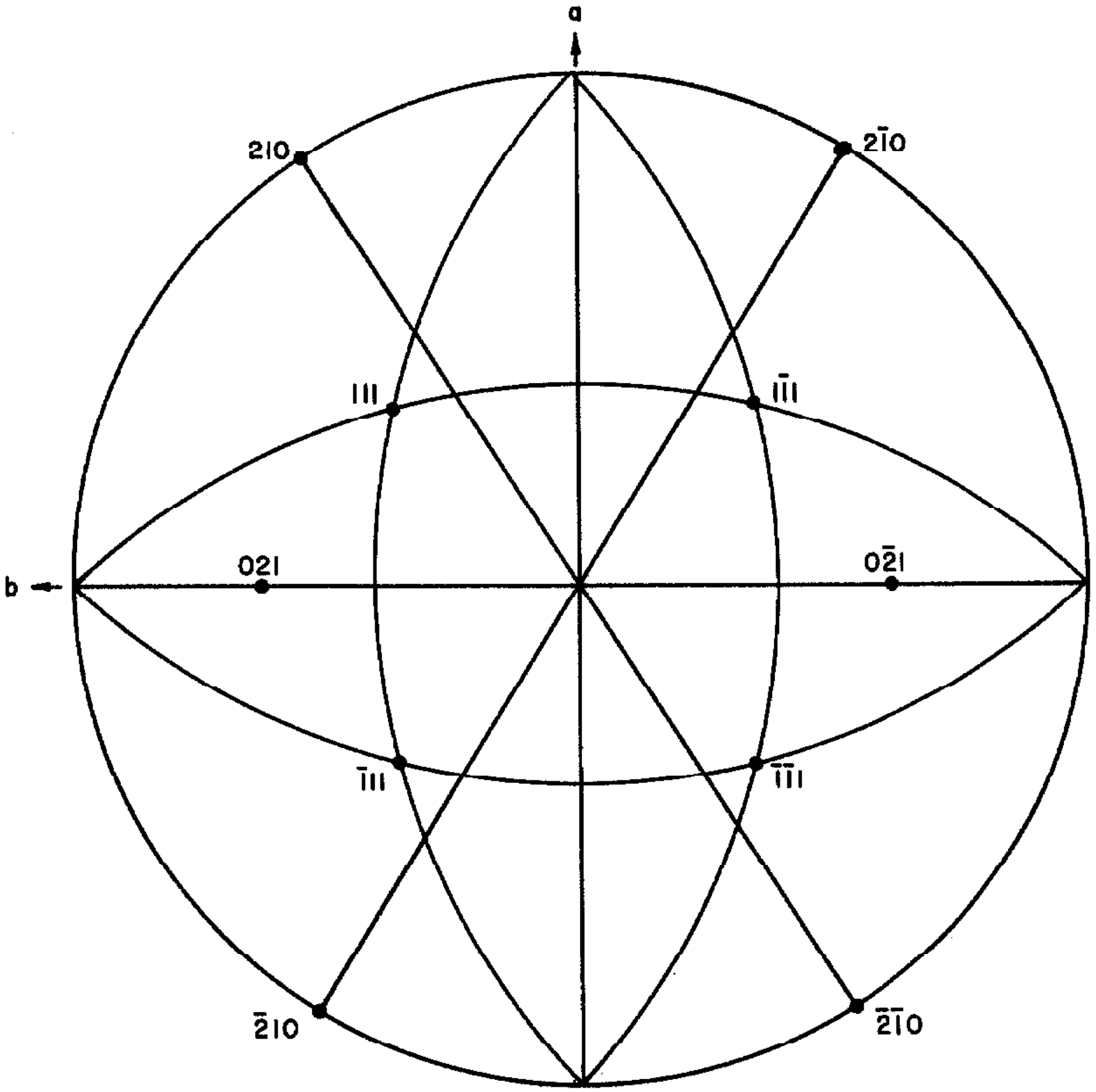

Figure 4. A stereographic projection of a crystal of anemonin plotted from the data in table 9. The c axis is normal to the plane of the projection.

values of a, 13.91 Å, and b, 11.12 Å, were calculated. Higher layer line photographs (hk1 to hk7 incl.) were obtained by the equi-inclination Weissenberg technique. Since this investigator intends to collect complete three-dimensional intensity data on this compound, two sets of three films each were used for each layer line. The first set was given a long exposure (10-12 hours) and the other a short exposure (2-4 hours). Observation of systematic extinctions gave the following conditions limiting possible reflections: $hk\ell$, no conditions; $0k\ell$, $k = 2n$; $h0\ell$, $\ell = 2n$; $hk0$, $h = 2n$. These conditions are compatible only with the centrosymmetric, orthorhombic space group D_{2h}^{15} - Pbca. The density of a crystal of anemonin was determined to be about 1.45 g. cc.$^{-1}$ by the flotation method, using a mixture of ether and carbon tetrachloride in which the crystal would neither rise nor sink. Assuming eight molecules in the unit cell, the calculated density is 1.42 g. cc.$^{-1}$

References to Appendix

1. M. J. Buerger, Crystal-structure Analysis, John Wiley and Sons, New York, 1960, pp. 609-611.

2. International Tables for X-Ray Crystallography, The Kynoch Press, Birmingham, England, 1959, vol. II.

3. H. Weyerer, Acta Cryst., 13, 821 (1960).

4. B. D. Cullity, Elements of X-Ray Diffraction, Addison-Wesley, Reading, Mass., 1956, pp. 324-333.

5. A. Taylor and H. Sinclair, Proc. Phys. Soc. (London), 57, 126 (1945).

6. A. J. Bradley and A. H. Jay, Proc. Phys. Soc. (London, 44, 563 (1932).

7. J. B. Nelson and D. P. Riley, Proc. Phys. Soc. (London), 57, 160 (1945).

8. J. B. Hess, Acta Cryst., 4, 209 (1951).

9. V. Schomaker, J. Waser, R. E. Marsh and G. Bergman, Acta Cryst., 12, 600 (1959).

10. D. M. Blow, Acta Cryst., 13, 168 (1960).

11. A. Hybl, Ph. D. Dissertation, California Institute of Technology, Pasadena, 1961, pp. 157-160.

12. J. B. Scarborough, Numerical Mathematical Analysis. The Johns Hopkins Press, Baltimore, 1950, pp. 192-198.

13. Y. Ashima and A. Fujita, Acta Phytochim., 1, 1 (1922).

14. C. Grundman and E. Kohler, J. Am. Chem. Soc., 77, 2332 (1955).

15. M. Nakazahi, Kogaku no Ryoiki, 3, 108-10 (1949).

16. J. E. Harris, Ph. D. Dissertation, Brown University (1958); *Dissertation Abst.*, 20, 887 (1959).

17. *The Merck Index*, Merck and Co., Inc., Rahway, N. J., 7th ed., 1960, p. 79.

PROPOSITIONS

I. A Dimeric Bifurcated Hydrogen Bond.

1. Proposal.

It is proposed that the crystal structure of 2-hydroxy-1-phenazinecarboxylic acid contains a most unusual feature, a dimeric bifurcated hydrogen bond. The author is of the opinion, from the evidence presented below, that the carboxyl hydrogen atom of this compound is both intra- and intermolecularly hydrogen bonded.

2. Introduction

In general, hydrogen bonds are formed between two, and only two, atoms of electronegative elements (1). Only a few cases have been reported in which it has been shown that a hydrogen atom is bonded to three such atoms. The first, and perhaps best documented of these, was reported in the crystal structure of glycine by Albrecht and Corey (2). Because of four close approaches between the nitrogen atom of one molecule and oxygen atoms of neighboring molecules, these investigators proposed that glycine exists as a zwitter ion, with two of the quaternary nitrogen hydrogens each bonded to a different oxygen atom and the third hydrogen atom bonded to two other oxygen atoms. They referred to the latter type of hydrogen bond as a "bifurcated" bond. Later, in a more precise determination, Marsh (3) essentially confirmed the results of Albrecht and Corey. The bond lengths and angles measured for the bifurcated bond, as given by

Marsh, are shown below. Burns and Levy (4) have reinvestigated this structure using neutron diffraction, and have determined the values 2.41 Å and 2.10 Å for the H···O and H···O' bond distances.

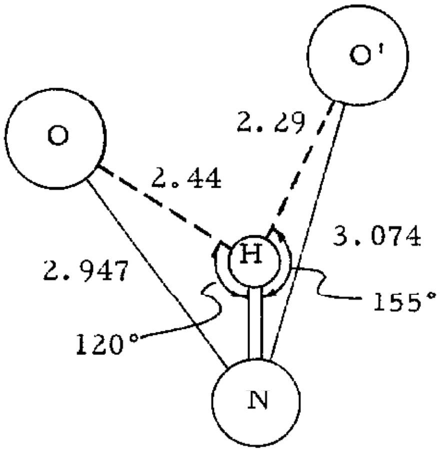

At least two other examples of bifurcated hydrogen bonds have been reported. Wright and Marsh (5) have reported a relatively long, and therefore probably weak, $\text{N-H}\genfrac{}{}{0pt}{}{\cdots\text{Cl}}{\cdots\text{O}}$ bifurcated bond in the crystal structure of *l*-lysine monohydrochloride dihydrate. Also, the crystal structure of nitramide, NH_2NO_2, as determined by Beevers and Trotman-Dickenson (6), indicates that both hydrogen atoms form bifurcated bonds of the type

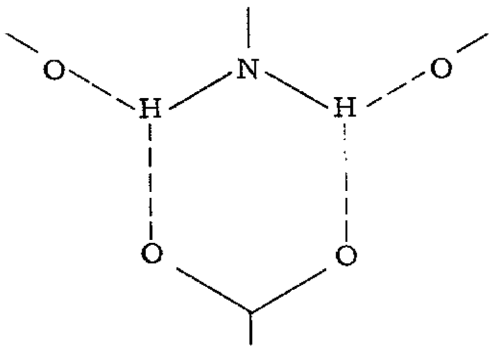

3. Discussion.

The partially refined crystal structure of 2-hydroxy-1-phenazinecarboxylic acid, as reported earlier by the author (see this thesis, Part III), contains a surprising feature; the distance between the O_{16} (see figure 13 and table 8, Part III) carboxyl oxygen atoms in two adjacent molecules related by a center of symmetry is only 2.80 Å. Since the average uncertainty in the interatomic distances in this determination is about ± 0.03 Å, the O_{16}-$O_{16'}$ distance is probably significantly short for the van der Waals contact between two oxygen atoms bearing hydrogens. It was expected that the molecule would be completely internally hydrogen bonded, as 1-phenazinecarboxylic acid has been shown to be (see this thesis, Part III). However, in light of the close intermolecular oxygen-oxygen approach, the author is led to propose that each carboxyl hydrogen atom is bonded both intramolecularly to N_{13} and intermolecularly to O_{16} in an adjacent molecule across the center of symmetry. If this is the case, it would be the first recognized example of a bifurcated hydrogen bond which is both intra- and intermolecularly bonded.

In the hope of substantiating the hypothesis presented above, a careful examination was made of the electron density in the vicinity of O_{16}. Generally one would not presume to look for hydrogen atom peaks on an electron density map from a structure which has been refined to an R factor of only 0.24; however, the surprisingly good resolution shown by the molecular plane Fourier map (figure 11, Part III) encouraged the author to try. A three-dimensional electron density map was calculated in intervals of 0.01x, 0.02y, and 0.02z in the vicinity of O_{16}, using the Burroughs 220 computer. Figure 1 shows the most interesting of several sections which were plotted. This section, which is taken parallel to (010) at y = 0.16, shows three unresolved peaks in addition to the O_{16} and C_{15} peaks. The two peaks below and to the right of O_{16} in figure 1, may be ruled out as possible hydrogen locations since neither is in a position to form a hydrogen bond; a carboxyl hydrogen atom which does not participate in a hydrogen bond is unlikely. This leaves one remaining peak which seems to be ideally located for the type of bond which the author proposes. If the coordinates of the assumed hydrogen atom, as derived from this peak with the condition that the O_{16}-H bond length be approximately 1.0 Å, are taken to be x = 0.010, y = 0.180, and z = 0.025, the calculated bond lengths and angles seem quite reasonable. The latter are shown in figure 2 on a diagram of the proposed hydrogen bonding scheme. In this model O_{16} and the carboxyl hydrogen atom deviate from the best plane of the molecule (see table 10, Part III), in a direction away from the center of symmetry, by 0.1 Å and 0.4 Å, respectively. The distance between the two symmetry related carboxyl hydrogen atoms is given as 1.97 Å,

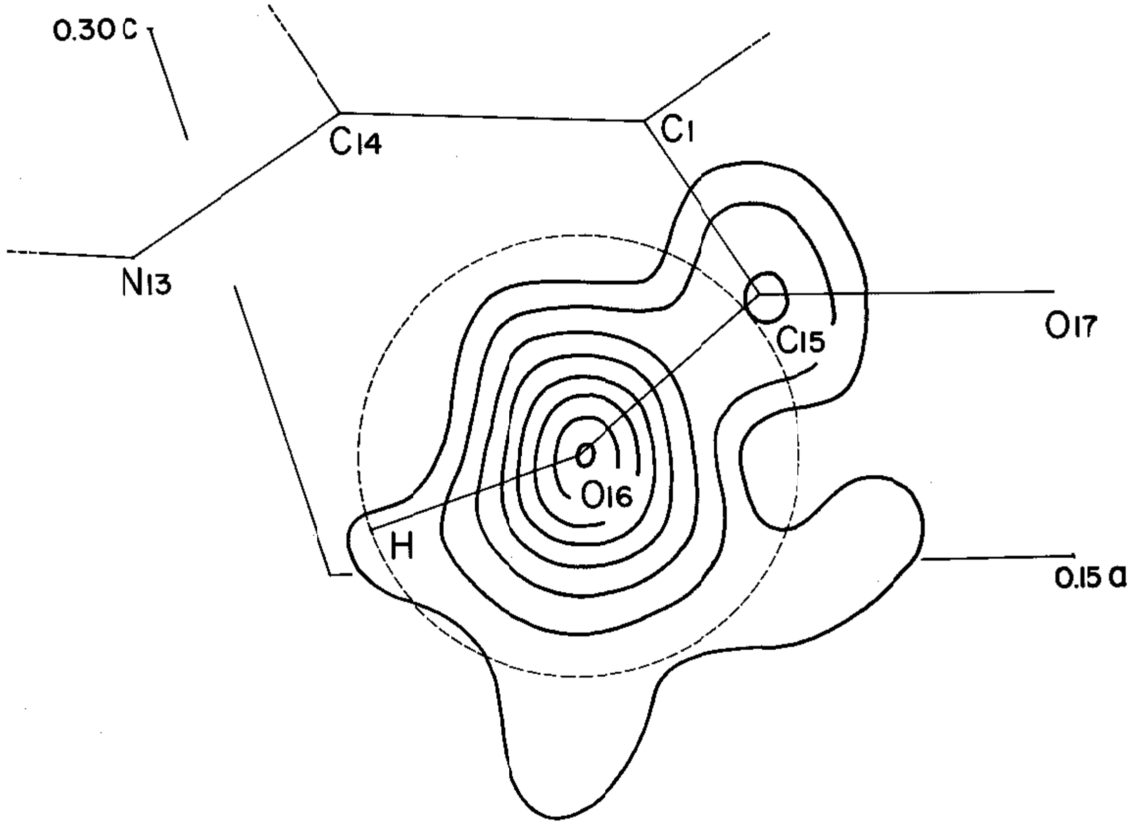

Figure 1. Electron density section in the vicinity of O_{16} in 2-hydroxy-1-phenazine-carboxylic acid. The section is taken parallel to (010) at y = 0.16. The first contour is drawn at 0.5 e. $Å^{-3}$ and the remaining contours at 1, 2, 3 ... e. $Å^{-3}$. The dotted line is the trace of a sphere 1.0 Å in radius which is centered at O_{16}.

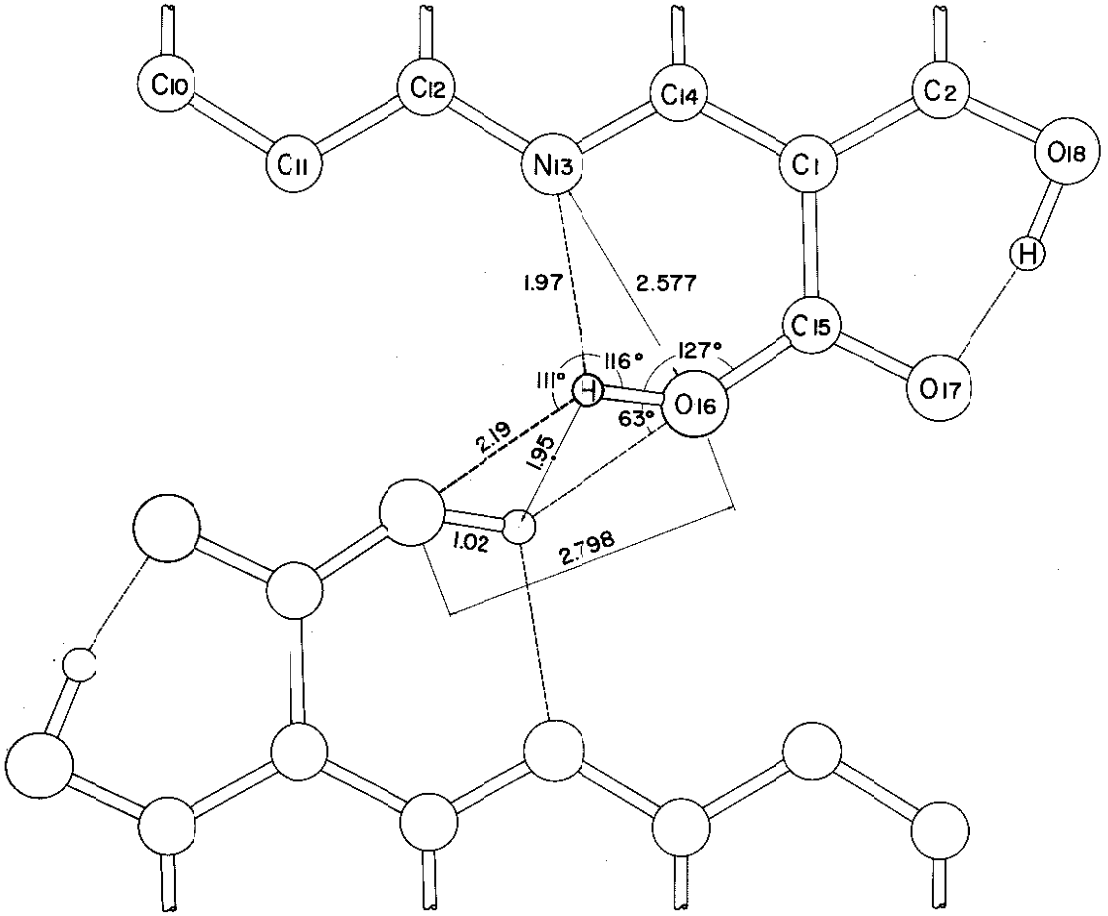

Figure 2. Proposed hydrogen bonding scheme for 2-hydroxy-1-phenazine-carboxylic acid, with the approximate interatomic distances and angles indicated. The dotted lines represent hydrogen bonds.

which is shorter than the usual van der Waals contact. However, this distance may be increased somewhat if the O_{16}-H bond is shortened or if the hydrogen atom is twisted further out of the plane of the molecule, away from the center of symmetry.

4. Conclusion.

Although at this stage of refinement one can do no more than speculate as to the location of the carboxyl hydrogen atom in the crystal structure of 2-hydroxy-1-phenazinecarboxylic acid, the author believes that the hydrogen bonding scheme proposed above is essentially correct. If this is so, the stronger of the two "branches" of the bifurcated hydrogen bond is probably the one to N_{13}. The fact that 1-phenazinecarboxylic acid does not form a similar intermolecular hydrogen bond is probably attributable to van der Waals packing forces which are too complicated to assess. In conclusion, one must consider the possibility that 2-hydroxy-1-phenazinecarboxylic acid exists as a zwitter ion, with the carboxyl hydrogen atom transferred to N_{13}. The author has rejected this idea since 1-phenazinecarboxylic acid does not appear to exist as a zwitter ion in the crystalline form and because it does not explain the close O_{16}-$O_{16'}$ approach in the hydroxy derivative. The distance from N_{13} to $O_{16'}$ is too long (3.42 Å) for hydrogen bond formation.

References to Proposition I

1. L. Pauling, "Nature of the Chemical Bond," Cornell University Press, Ithaca, N. Y., 1960, pp. 449-454.

2. G. Albrecht and R. B. Corey, J. Am. Chem. Soc., 61, 1087 (1939).

3. R. E. Marsh, Acta Cryst., 10, 814 (1957); ibid., 11, 654 (1958).

4. J. H. Burns and H. A. Levy, Am. Cryst. Ass'n. Meeting, June (1958).

5. D. A. Wright and R. E. Marsh, Acta Cryst., 15, 54 (1962).

6. C. A. Beevers and A. S. Trotman-Dickenson, ibid., 10, 34 (1957).

II. Calculation of Atomic Coordinates from Molecular Dimensions.

1. Proposal

It is proposed that a computer program be written to derive from the approximate dimensions of a molecule the best set of atomic coordinates relative to an arbitrary orthogonal axial system. The author has formulated the equations necessary to perform the calculations by the least-squares method. Such a program should be of particular interest to the organic chemist since it would allow one to describe more accurately the geometry of complex molecules and the spatial relationships of reacting species.

2. Introduction

The author has presented earlier (see Appendix to this thesis, part II) a computer program for the calculation of interatomic distances and angles from orthogonal atomic coordinates. The reverse process, the determination of orthogonal coordinates from interatomic distances and angles, is also frequently of interest. The two calculations are quite different however. If one has a set of n atoms, for which the coordinates have been determined experimentally, it is possible to calculate from these 3n parameters a unique set of $(n^2 - n)/2$ interatomic distances and $n!/2(n-3)!$ bond angles. If, however, one has a set of data consisting of interatomic distances and bond angles which have been estimated or experimentally determined, one cannot calculate a unique set of coordinates but can only hope to calculate the set which will best fit the data.* The author suggests that the best fit in this case may be found from the least-squares method by minimizing with respect to both the interatomic distances and bond angles, simultaneously.

3. Discussion

In the discussion which follows, no attempt will be made to explain the method of least-squares (see for example, ref. 3), but only to derive the expressions necessary for the proposed computer program.

The observational equations which relate the interatomic distances, D_{ij}, and the cosines of the bond angles θ_{ijk}, to the orthogonal coordinates are of the form

$$D_{ij} = [(x_i - x_j)^2 + (y_i - y_j)^2 + (z_i - z_j)^2]^{\frac{1}{2}} \tag{1}$$

and

$$\cos \theta_{ijk} = \frac{D^2_{ij} + D^2_{jk} - D^2_{ik}}{2D_{ij} D_{jk}} \tag{2}$$

Since i, j and k may be any atom numbers i→n, we may write

---

* A similar problem arises in surveying and astronomy and has been treated by the method of least-squares for the relatively simple problem of triangulation (1, 2), in which one wishes to obtain only the most probable values for the angles of a triangle, subject to the condition that the sum of the angles be equal to 180°.

$$D = f(x_1, y_1, z_1, \ldots\ldots x_n, y_n, z_n) \tag{3}$$

and

$$C = g(x_1, y_1, z_1, \ldots\ldots x_n, y_n, z_n) \tag{4}$$

where $C = \cos\theta$. D and C are not linear functions of x_i, y_i and z_i and therefore we cannot determine the best set of atomic coordinates directly, but rather must calculate successive shifts, Δx_i, Δy_i, Δz_i, to be applied to an initial set of approximate coordinates. The determination of this initial set of coordinates will be discussed in more detail later. Using Taylor's series expansion, we may obtain linear observational equations for ΔD ($= D_{obs} - D_{calc}$) and for ΔC ($= C_{obs} - C_{calc}$); the expressions are

$$\Delta D = \sum_i^n \left(\Delta x_i \frac{\partial D}{\partial x_i} + \Delta y_i \frac{\partial D}{\partial y_i} + \Delta z_i \frac{\partial D}{\partial z_i}\right) \tag{5}$$

and

$$\Delta C = \sum_i^n \left(\Delta x_i \frac{\partial C}{\partial x_i} + \Delta y_i \frac{\partial C}{\partial y_i} + \Delta z_i \frac{\partial C}{\partial z_i}\right) \tag{6}$$

Both D and C are functions of the same parameters and we may conveniently minimize the sum of the squares of the residuals for both quantities together; that is

$$\Sigma\, w_D (D_{obs} - D_{calc})^2 + \Sigma\, w_C (C_{obs} - C_{calc})^2 \tag{7}$$

must be a minimum. Since we are minimizing with respect to two different quantities with different dimensions, the weights, w_D and w_C, must be taken inversely proportional to the squares of the absolute uncertainties in D and C, respectively; hence

$$\sqrt{w_D} = \frac{1}{\sigma_D} \qquad \text{and} \qquad \sqrt{w_C} = \frac{1}{\sigma_C} \tag{8}$$

Table 1 shows the matrix of normal equations which may be derived from observational equations 5 and 6. The partial derivative terms in the matrix elements are defined below; for the interatomic distances D_{ij},

$$\frac{\partial D}{\partial x_i} = \frac{x_i - x_j}{D_{ij}} \tag{9}$$

where i and j may be interchanged, and, for $\cos\theta_{ijk}$,

$$\frac{\partial C}{\partial x_i} = \frac{(D^2_{ij} - D^2_{jk} + D^2_{ik})(x_i - x_j) - 2D^2_{ij}(x_i - x_k)}{2D_{jk}\,D_{ij}^3} \tag{10}$$

$$\frac{\partial C}{\partial x_j} = \frac{(D^2_{ij}D^2_{jk} - D^4_{jk} + D^2_{ik}D^2_{jk})(x_i - x_j) + (D^2_{jk}D^2_{ij} - D^4_{ij} - D^2_{ik}D^2_{ij})(x_j - x_k)}{2D_{ij}^3\,D_{jk}^3} \tag{11}$$

$$\frac{\partial C}{\partial x_k} = \frac{(D^2_{jk} - D^2_{ij} + D^2_{ik})(x_j - x_k) - 2D^2_{jk}(x_i - x_k)}{2D_{ij}\,D^3_{jk}} \tag{12}$$

$$\begin{bmatrix} \sum_m w_D\left(\frac{\partial D}{\partial x_1}\right)^2 + \sum_n w_C\left(\frac{\partial C}{\partial x_1}\right)^2 & \sum_m w_D\left(\frac{\partial D}{\partial x_1}\right)\left(\frac{\partial D}{\partial y_1}\right)+\sum_n w_C\left(\frac{\partial C}{\partial x_1}\right)\left(\frac{\partial C}{\partial y_1}\right)\cdots \\ \sum_m w_D\left(\frac{\partial D}{\partial y_1}\right)\left(\frac{\partial D}{\partial x_1}\right)+\sum_n w_C\left(\frac{\partial C}{\partial y_1}\right)\left(\frac{\partial C}{\partial x_1}\right) & \sum_m w_D\left(\frac{\partial D}{\partial y_1}\right)^2 +\sum_n w_C\left(\frac{\partial C}{\partial y_1}\right)^2 \quad \cdots \\ \sum_m w_D\left(\frac{\partial D}{\partial z_1}\right)\left(\frac{\partial D}{\partial x_1}\right)+\sum_n w_C\left(\frac{\partial C}{\partial z_1}\right)\left(\frac{\partial C}{\partial x_1}\right) & \sum_m w_D\left(\frac{\partial D}{\partial z_1}\right)\left(\frac{\partial D}{\partial y_1}\right)+\sum_n w_C\left(\frac{\partial C}{\partial z_1}\right)\left(\frac{\partial C}{\partial y_1}\right)\cdots \\ \sum_m w_D\left(\frac{\partial D}{\partial x_2}\right)\left(\frac{\partial D}{\partial x_1}\right)+\sum_n w_C\left(\frac{\partial C}{\partial x_2}\right)\left(\frac{\partial C}{\partial x_1}\right) & \sum_m w_D\left(\frac{\partial D}{\partial x_2}\right)\left(\frac{\partial D}{\partial y_1}\right)+\sum_n w_C\left(\frac{\partial C}{\partial x_2}\right)\left(\frac{\partial C}{\partial y_1}\right)\cdots \\ \vdots & \vdots \end{bmatrix} \begin{bmatrix} \Delta x_1 \\ \Delta y_1 \\ \Delta z_1 \\ \Delta x_2 \\ \vdots \end{bmatrix} = \begin{bmatrix} \sum_m w_D \Delta D\left(\frac{\partial D}{\partial x_1}\right)+\sum_n w_C \Delta C\left(\frac{\partial C}{\partial x_1}\right) \\ \sum_m w_D \Delta D\left(\frac{\partial D}{\partial y_1}\right)+\sum_n w_C \Delta C\left(\frac{\partial C}{\partial y_1}\right) \\ \sum_m w_D \Delta D\left(\frac{\partial D}{\partial z_1}\right)+\sum_n w_C \Delta C\left(\frac{\partial C}{\partial z_1}\right) \\ \sum_m w_D \Delta D\left(\frac{\partial D}{\partial x_2}\right)+\sum_n w_C \Delta C\left(\frac{\partial C}{\partial x_2}\right) \\ \vdots \end{bmatrix}$$

Table 1. Normal equations matrix for a program to calculate the best set of atomic coordinates from the molecular dimensions.

where j is the atom at the vertex of the angle. The partial derivatives with respect to y_i, y_j and y_k or z_i, z_j and z_k may be obtained from equations 9 through 12 simply by substituting y or z for x wherever it occurs in these expressions. The interatomic distance D_{ij} will contribute only to those matrix elements with the subscripts i and/or j; similarly, the cosine of the angle θ_{ijk} will contribute only to those terms with the subscripts i and/or j and/or k. After the matrix in table 1 has been inverted, the shifts, Δx_i, Δy_i, Δz_i, can be calculated directly. These may then be added to the initial atomic coordinates and the whole process repeated cyclicly until convergence is obtained.

The rate of convergence, and indeed whether or not the process will converge on the right structure at all, depends upon the accuracy of the initial atomic coordinates. Obviously one can calculate atomic coordinates only for molecules with a unique configuration; hence, the estimated or observed interatomic distances and bond angles, along with any restrictions on the coordinates, must be sufficient to define such a configuration. To illustrate this point, suppose one wishes to calculate atomic coordinates, relative to a set of molecular axes, for the heavy atoms in a molecule of camphor, shown in figure 1. The orientation of the molecule with respect to the chosen axes must first be defined. In this case we require that the origin lies halfway between atoms 1 and 4, along x, and that atom 7 lies on the z axis.

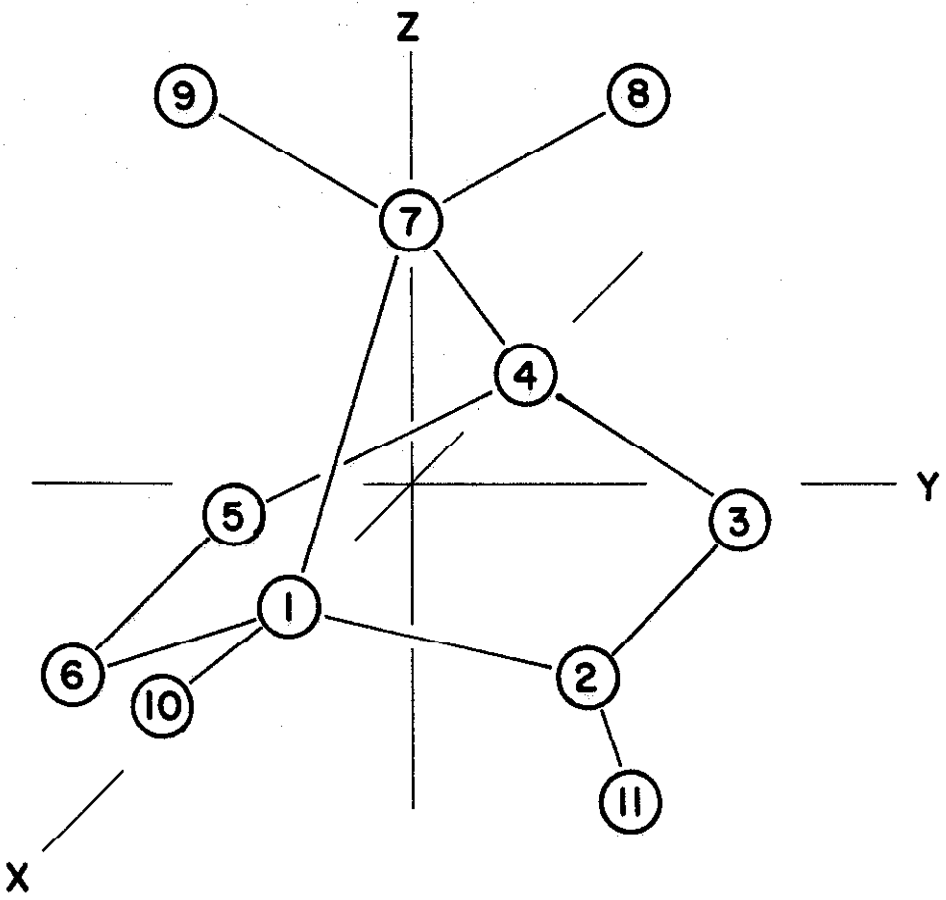

Figure 1. Camphor molecule showing the orientation of the molecular axes.

Table 3. A set of possible restrictions on the atomic coordinates of the camphor molecule shown in figure 1. The quantities a, b, c ... etc., are coordinates to be determined.

Atom	x	y	z
1	a	0	0
2	b	c	-d
3	-e	f	-d
4	-a	0	0
5	-g	-h	-d
6	g	-h	-d
7	0	0	i
8	0	j	k
9	0	-j	k
10	ℓ	m	n
11	p	q	-r

The directions of these atoms along the axes must also be indicated, since the mirror image of the molecule will have the same interatomic distances and angles. We may, if we wish, add other conditions to further restrict the system. For example, we may require that atoms 2, 3, 5 and 6 lie in a plane normal to the z axis and that atoms 7, 8 and 9 lie in a plane normal to the x axis. There are many possible restrictions on the atomic coordinates of the camphor molecule; one set of restrictions is listed in table 2. The quantities a, b, c, ... etc., are unknown coordinates and are the only ones which need be calculated. Thus, the order of the least-squares matrix for this case is reduced from 33 to 17. Although there are only 17 coordinates to be determined, there are as many as 12 bond distances and 21 bond angles from which to find the best fit.

The method used above to introduce restrictions on some of the atomic coordinates undoubtedly gives high weight to these coordinates. An alternative method would be to introduce these rigorous conditions by way of the Lagrange multiplier (see for example, p. 137, this thesis). However, this complicates the calculations considerably and is really not necessary since the observational weights, w_D and w_C, can be assigned only subjectively.

The calculation of the initial set of approximate atomic coordinates will probably be the most difficult part of the program to write. Although the author has thought about the problem at some length, all the difficulties have not yet been resolved. The program must be able to recognize, from the list of coordinate restrictions, the key atoms which define the orientation of the molecule (such as atoms 1, 4 and 7 in the example given above) and calculate coordinates for them. It should proceed to the other atoms, one by one, and calculate approximate coordinates for each. However, the program must not return to an atom for which it has already calculated coordinates since the new coordinates may be slightly different.* If there is insufficient information to derive a unique location for any atom, the program should be able to recognize this and omit the atom from the least-squares refinement. Writing such a program for a particular molecule would be relatively easy; however, writing one which will be applicable for any molecule will require considerably more thought, but undoubtedly can be done.

4. Conclusion.

The program outlined above should be of particular interest to those studying organic structures and reaction mechanisms. It will allow one to quickly obtain reasonably accurate atomic coordinates from estimated bond lengths and angles. From these coordinates one may conveniently describe the stereochemistry of a molecule, calculate the distance between neighboring groups, the angle between

---

* This is referred to in surveying texts as a "closing error."

two orbitals, the direction cosines of the line of attack of a reacting species, etc. The program might, of course, be of interest wherever it is desired to calculate relative coordinates for an array of points.

References to Proposition II

1. E. R. Cary, "Geodetic Surveying," John Wiley and Sons, Inc., New York, 1916, pp. 235-269.

2. D. Greene, "An Introduction to Spherical and Practical Astronomy," Ginn and Co., Boston, 1890, pp. 115-150.

3. E. Whittaker and G. Robinson, "The Calculus of Observations," Blackie and Sons, London, 1944, pp. 209-259.

III. The Structure of Anemonin.

1. Proposal.

The author proposes a reinvestigation of the structure of anemonin in order to finally settle the question of the relative orientation of the two lactone rings on the cyclobutane ring. It is suggested that this may be done by comparing the rate of 1, 2-diol cleavage of the sodium salt of tetrahydroanemonin with the rates of cleavage for the *cis*- and *trans*-1, 2-diol isomers of the sodium salt of tetrahydroanemonin-3, 4-dicarboxylic acid. A novel method is proposed for the synthesis of the latter *cis*- and *trans*-1, 2-diols.

2. Introduction.

It has been observed (1) that cattle which feed upon certain species of plants, such as *Anemone pulsattila* or *Ranunculus*, frequently contract lymphodenosis, an inflammation of the lymphatics. Steam distillation of fresh, ground plants of the above species, followed by extraction of the organic material into chloroform and removal of solvent, produces a small yield of a light yellow oil with rubefacient and vesicant properties (2). This oil has been shown by synthesis (3) to be γ-hydroxyvinylacrylolactone (or protoanemonin or aneminol (I)). Upon standing, I dimerizes to give a white, crystalline

I II

compound (II) with the empirical formula, $C_{10}H_8O_4$. From a study of the reduction and hydrolysis products of II, several investigators (3-5) have concluded that the structure of the dimer, called anemonin, is that shown. As was mentioned earlier in the presentation of the

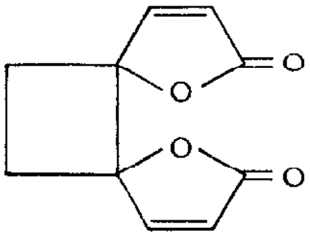

II

preliminary X-ray diffraction studies on this compound (see Appendix, this thesis, part III), there are three possible stereoisomers of II, *meso*-anemonin (lactone rings *cis*) and *d* and *ℓ*-anemonin (lactone rings *trans*). The author describes below a possible method to distinguish between the *cis* and *trans* structures.

3. Discussion.

Harris (6) has recently studied the structure of anemonin and has concluded from the rates of lead tetraacetate 1,2-diol cleavage of two reduction products, 1,2-di(3-hydroxypropyl)-1,2-cyclobutanediol (III) and the sodium salt of tetrahydroanemonin (IV)

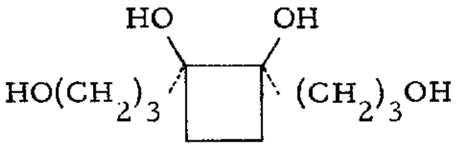

III

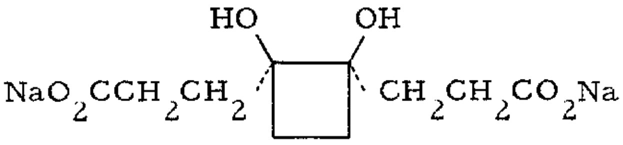

IV

that the lactone rings in the parent compound have the *cis* configuration. The sodium salt IV is obtained from anemonin by the hydrogenation of the double bonds to give tetrahydroanemonin, followed by hydrolysis of the lactone rings. Tetrol (the name applied by Harris to III) may be prepared from tetrahydroanemonin by further reduction with lithium aluminum hydride. Harris found that III and IV are cleaved rapidly by lead tetraacetate to give decane-1,10-diol-4,7-dione (V) and dilevulinic acid (VI), respectively. He had, however,

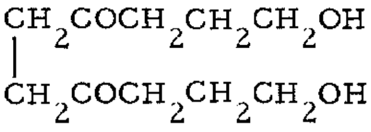

$$\begin{array}{l} CH_2COCH_2CH_2CH_2OH \\ | \\ CH_2COCH_2CH_2CH_2OH \end{array}$$

V

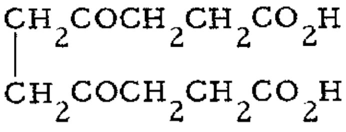

$$\begin{array}{l} CH_2COCH_2CH_2CO_2H \\ | \\ CH_2COCH_2CH_2CO_2H \end{array}$$

VI

no other ditertiary 1,2-cyclobutanediol with which to compare the rates of cleavage. The best models available were the *cis* and *trans* isomers of bicyclo-[4.2.0]-octane-7,8-diol (VII), a disecondary

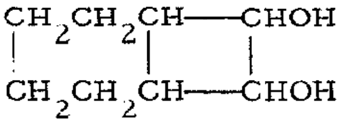

VII

1,2-butanediol. As Harris admits, there are significant differences in the reactivities of ditertiary and disecondary 1,2-diols. For example, the formation of a boric acid adduct has been used by Cope and Herricks (7) to distinguish the *cis* isomer of VII from the *trans* isomer; however, neither III nor IV, which are both purported to be *cis*-1,2-diols, forms a boric acid complex.

Although the *cis* structure proposed by Harris for anemonin is quite possibly correct, it would be reassuring to investigate the rates of lead tetraacetate cleavage for the *cis* and *trans* isomers of a ditertiary 1,2-butanediol which is closely related to IV. The compounds which the author proposes be studied are the *cis* and *trans*-1,2-diol isomers of the sodium salt of tetrahydroanemonin-3,4-dicarboxylic acid (VIII). These isomers probably can be prepared rather easily by the sequence of reactions in figure 1. Albanesi and Tovaglieri (8) and Sauer *et al.* (9) have reported the synthesis of the *cis* and *trans* isomers of $\Delta^{2,2'(5H,5'H)}$-bifuran-5,5'-dione (bifurandione, IX) by the high pressure reaction of acetylene and carbon monoxide in the presence of cobalt octacarbonyl and an inert solvent.

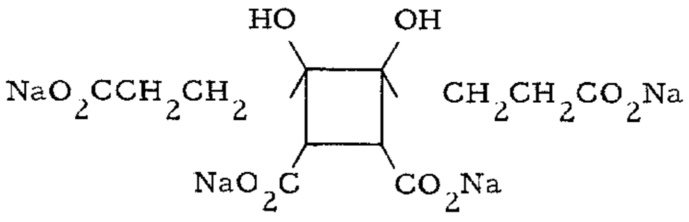

cis and *trans* VIII

Figure 1. Proposed synthesis of the two 1,2-diol isomers of the sodium salt of tetrahydroanemonin-3,4-dicarboxylic acid.

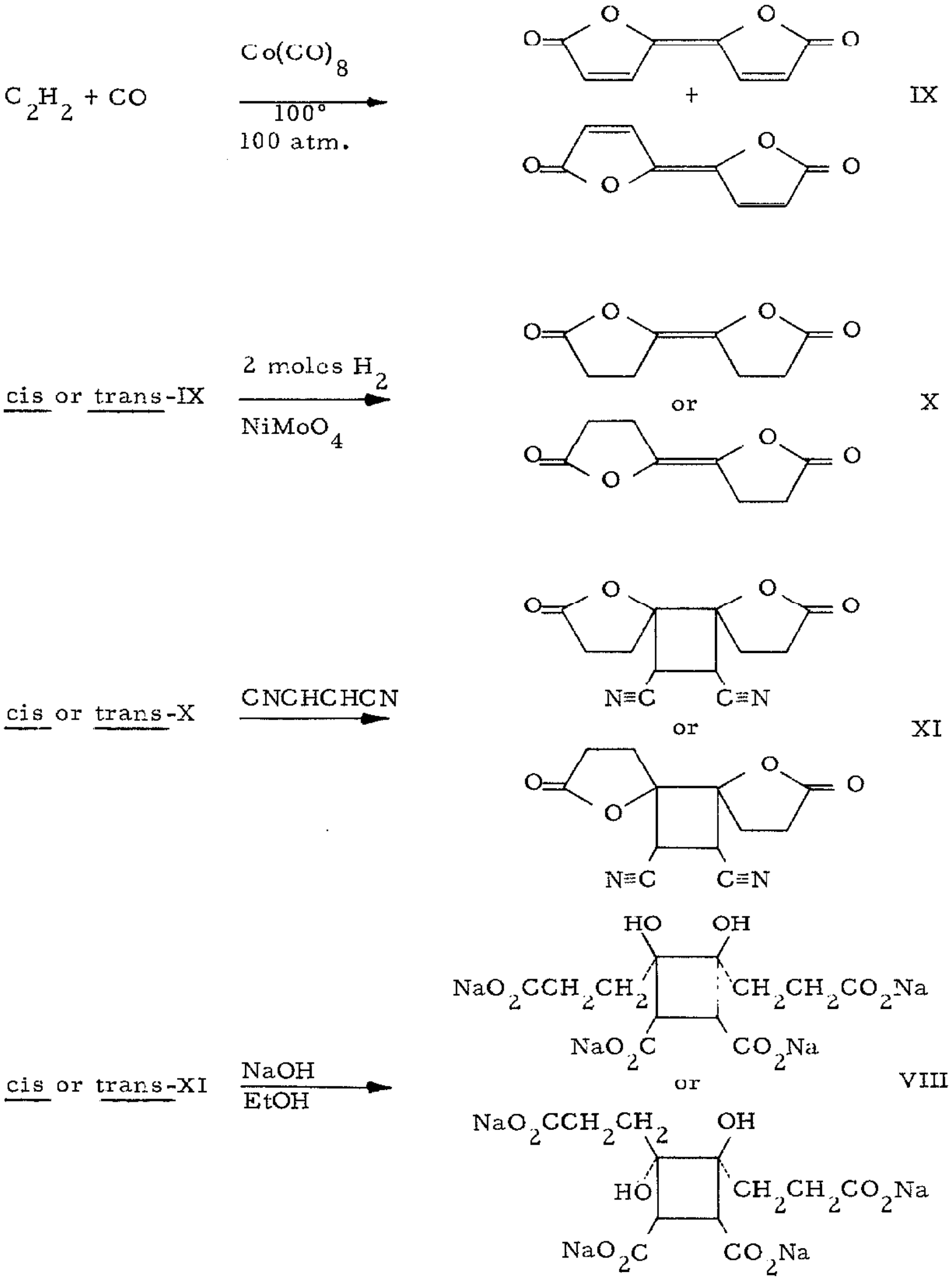

The *cis* and *trans* isomers of IX are readily separated by fractional crystallization and have been well characterized (8-12). Holmquist *et al.* (10) have found that all the C-C double bonds in IX may be hydrogenated with an excess of hydrogen and a nickel molybdate catalyst; however, if the amount of hydrogen is limited to one mole, only one of the lactone ring double bonds is hydrogenated. It seems probable, then, that a second mole of hydrogen would add to the other lactone ring double bond to give either of the two tetrahydrobifurandiones (X). Treatment of X with maleonitrile should give the cycloaddition product XI which can be saponified to give either of the two 1,2-diol isomers of the sodium salt of tetrahydroanemonin-3,4-dicarboxylic acid (VIII).*

4. Conclusion.

In conclusion, it may be mentioned that the two isomers of bifurandione (IX) are intriguing starting materials from which to attempt the total synthesis of both *meso* and *dl* anemonin. Unfortunately, it appears that the lactone ring double bonds of IX are more reactive to addition than the bridge double bond. This is evidenced by the fact that Diels-Alder adducts are formed first with the lactone double bonds (12). However, the possibility of a stereospecific synthesis of anemonin from IX should be studied further.

---

* There are two possible orientations of the cyano groups on *cis*-XI, but either is acceptable.

References to Proposition III

1. N. Hellström, Kgl. Lantbruke-Högskol. Ann., 22, 297 (1956); C. A., 51, 4558a.

2. M. Bergman, Ber. schweiz botan. Ges., 54, 399 (1944).

3. Y. Asahima and A. Fujita, Acta Phytochim., 1, 1 (1922).

4. C. Grundman and E. Kober, J. Am. Chem. Soc., 77, 2332 (1955).

5. M. Nakazahi, Kogaku no Ryoiki, 3, 108 (1949).

6. J. E. Harris, Ph. D. Dissertation, Brown University (1958).

7. A. C. Cope and E. C. Herrick, J. Am. Chem. Soc., 72, 983 (1950).

8. G. Albanesi and M. Tovaglieri, Chim. e ind., 41, 189 (1959); C. A., 19872d (1959).

9. J. C. Sauer, R. D. Cramer, V. A. Engelhardt, T. A. Ford, H. E. Holmquist and B. W. Howk, J. Am. Chem. Soc., 81, 3677 (1959).

10. H. E. Holmquist, F. D. Marsh, J. C. Sauer, and V. A. Engelhardt, ibid., 81, 3681 (1959).

11. E. A. Abrahamson, ibid., 81, 3692 (1959).

12. H. E. Holmquist, J. C. Sauer, V. A. Engelhardt and B. W. Howk, ibid., 81, 3686 (1959).

IV. The Molecular Structure of the BF_3-$(C_5H_5)_2WH_2$ Adduct.

1. Proposal.

It is proposed that the structure recently postulated for the boron trifluoride adduct of dicyclopentadienyltungsten dihydride is not consistent with chemical and structural evidence. An alternative structure which seems more reasonable is proposed.

2. Introduction.

In recent years a number of metallocene hydrides have been prepared with one or more hydrogen atoms covalently bonded to the metal atom. The first such compound, $(C_5H_5)_2ReH$ (I), was prepared by Green and coworkers (1) from the reaction of rhenium chloride and sodium cyclopentadienide in tetrahydrofuran. The existence of a covalent Re-H bond in I was postulated from nuclear

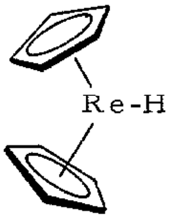

I

magnetic resonance spectra because of the appearance of a single proton peak at exceptionally high field (diamagnetically very well shielded). These investigators, in a later paper (2), reported the preparations of $(C_5H_5)_2TaH_3$, $(C_5H_5)_2MoH_2$ and $(C_5H_5)_2WH_2$. They also found that the latter two compounds, as well as $(C_5H_5)_2ReH$ could be protonated with HCl to give $(C_5H_5)_2MoH_3{}^+$, $(C_5H_5)_2WH_3{}^+$ and $(C_5H_5)_2ReH_2{}^+$. From their studies of these ions they concluded that the order of basicity for the parent metallocene hydrides is

$$(C_5H_5)_2ReH > (C_5H_5)_2WH_2 > (C_5H_5)_2MoH_2.$$

Curphey et al. (3) have studied the protonation of ferrocene, osmocene and ruthenocene in boron trifluoride hydrate (H_2O-BF_3) and find the order of basicity to be

$$(C_5H_5)_2Fe > (C_5H_5)_2Ru > (C_5H_5)_2Os.$$

These observations have been recently confirmed by Levenberg (4).

The results obtained by the workers mentioned above may be explained in part by the molecular orbital treatment of Ballhausen and Dahl (5). They make the logical assumption that the ring-metal-ring axis is bent in these compounds and, on this basis, construct a set of nine molecular orbitals by hybridizing the appropriate d, s and p metal orbitals. Three of these orbitals are directed toward each ring and the remaining three lie in the equatorial (xy) plane, as shown. In ferrocene, for example, there are 18 electrons involved in bonding (5 from each ring and 8 from the iron atom); 12 of which

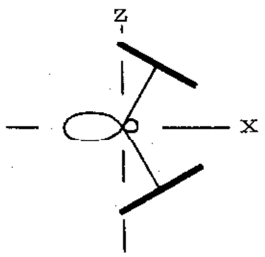

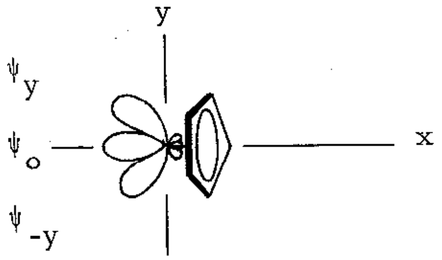

are used in the iron-ring bonds. The other six electrons, according to Ballhausen and Dahl, occupy the three equatorial orbitals and may be used for bonding. Thus, ferrocene would be expected to accept a proton to give $(C_5H_5)_2FeH^+$ but should not form a neutral hydride. By the same reasoning, the species listed in table 1 may be expected to exist, assuming only hydrides with no more than one positive charge are possible. As was mentioned earlier, most of the compounds in this list have been prepared.

The crystal structure of dicyclopentadienylmolybdenum dihydride has been determined from X-ray diffraction analysis by Bennett and coworkers (6). They found, in agreement with the Ballhausen-Dahl molecular orbital model, that the cyclopentadienyl rings are tilted, the dihedral angle being 25 ± 3°. These investigators also claim to have determined the approximate locations of the hydrogen atoms from a difference Fourier synthesis. They report a value of 90 ± 10° for the H-Mo-H angle, also in agreement with the molecular orbital model. One surprising feature of this crystal structure is the eclipsed conformation of the rings, causing the maximum steric interaction. This point will be discussed in more detail later.

Table 1. Some of the metallocene hydride species which may be predicted to exist from the molecular orbital treatment of Ballhausen and Dahl (5). The top heading indicates the total number of electrons in the three equatorial bonding orbitals. Those species containing 4 or 5 electrons in these orbitals are presumably paramagnetic.

4e	5e	6e
$(C_5H_5)_2TaH$	$(C_5H_5)_2TaH_2$	$(C_5H_5)_2TaH_3$
$(C_5H_5)_2W$	$(C_5H_5)_2WH$	$(C_5H_5)_2WH_2$
$(C_5H_5)_2WH^{\oplus}$	$(C_5H_5)_2WH_2^{\oplus}$	$(C_5H_5)_2WH_3^{\oplus}$
$(C_5H_5)_2Mo$	$(C_5H_5)_2MoH$	$(C_5H_5)_2MoH_2$
$(C_5H_5)_2MoH^{\oplus}$	$(C_5H_5)_2MoH_2^{\oplus}$	$(C_5H_5)_2MoH_3^{\oplus}$
	$(C_5H_5)_2Re$	$(C_5H_5)_2ReH$
	$(C_5H_5)_2ReH^{\oplus}$	$(C_5H_5)_2ReH_2^{\oplus}$
		$(C_5H_5)_2Os$
		$(C_5H_5)_2OsH^{\oplus}$
		$(C_5H_5)_2Ru$
		$(C_5H_5)_2RuH^{\oplus}$
		$(C_5H_5)_2Fe$
		$(C_5H_5)_2FeH^{\oplus}$

3. Discussion.

In a recent communication, Shriver (7) has reported that dicyclopentadienyltungsten dihydride and boron trifluoride form a 1:1 addition compound, for which he postulates the structure II. This investigator examined the infrared spectra of $(C_5H_5)_2WH_2$ and of its BF_3 adduct and concluded from the negligible shift in the W-H stretching frequency (from 1921 to 1917 cm.$^{-1}$) that the BF_3 group is not linked to the metal atom through hydrogen bonds. The unlikely possibility of BF_3 interaction with one of the cyclopentadienyl rings was ruled out by the failure of ferrocene to form a similar complex. He suggests, then, that the only remaining possibility is a metal-boron covalent bond which utilizes the ψ_o orbital proposed by Ballhausen and Dahl.

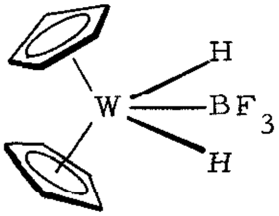

II

Although Shriver's structure for this adduct seems reasonable enough at first glance, a study of the steric requirements of the two rings and the two hydrogen atoms leads the author to propose that there cannot be a metal-boron interaction strong enough to be called a covalent bond. Assuming that the structure of dicyclopentadienyltungsten dihydride is similar to that of the molybdenum compound* described above, the distance between the two hydrogen atoms, which presumably bond with the ψ_y and ψ_{-y} orbitals, is approximately 2.4 Å, or roughly the normal van der Waals contact distance for hydrogen (9). According to Ballhausen and Dahl, the ψ_o orbital contains two electrons and bisects the 90° H-W-H angle. However, as is evidenced by the weakly basic nature of $(C_5H_5)_2WH_2$ compared to $(C_5H_5)_2ReH$, this orbital is sterically hindered from forming a strong covalent bond. Green and coworkers (2) have observed that the weakly bonded proton on $(C_5H_5)_2WH_3{}^+$ exchanges with solvent protons in a D_2O-DCl mixture, the exchange being complete in a few minutes. They have also observed that $(C_5H_5)_2TaH_3$ is more unstable and reactive than either $(C_5H_5)_2WH_2$ or $(C_5H_5)_2MoH_2$. Although Green and coworkers make no attempt to correlate these properties with a sterically "blocked" orbital, this does seem a logical explanation.

In order to form a tungsten-boron covalent bond (bond length ≅ 2.2 Å) in the tungsten dihydride it would be necessary to increase significantly the H-W-H angle, perhaps to as much as 150-180°. This must be accompanied by an increase in the dihedral angle of the

---

* This assumption is probably valid since tungsten and molybdenum form the same types of compounds with nearly identical bond distances and angles (8).

cyclopentadienyl rings or an appreciable lengthening of the metal-ring bonds. From a study of a model of $(C_5H_5)_2WH_2$ and from the crystal structure of $(C_5H_5)_2MoH_2$, it seems unlikely that the dihedral angle can be larger than about 30° without introducing serious steric interactions between the rings, especially since they are probably eclipsed in the tungsten derivative. Thus, structure II seems a poor choice for the BF_3-$(C_5H_5)_2WH_2$ adduct.

4. Conclusion.

Although there are several alternative structures which seem more reasonable than II, the best of these (III) is shown below.

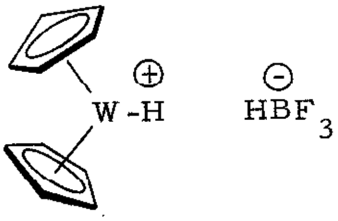

III

This ionic structure, in which a hydride ion has been transferred from tungsten to boron, would explain Shriver's observations that the adduct has no appreciable BF_3 vapor pressure and is insoluble in hydrocarbon solvents. It would also be more consistent with the general observation that metallocenes do not react in solution with BF_3, except to protonate the metal atom (2-4). Structures II and III could be easily distinguished since the latter should be paramagnetic. It would be most interesting and informative to determine, by neutron diffraction, the structure of this unusual compound.

References to Proposition IV

1. M. L. H. Green, L. Pratt and G. Wilkinson, J. Chem. Soc., 3916 (1958).

2. M. L. H. Green, J. A. McCleverty, L. Pratt and G. Wilkinson, J. Chem. Soc., 4854 (1961).

3. T. J. Curphey, J. O. Santer, M. Rosenblum and J. H. Richards, J. Am. Chem. Soc., 82, 5249 (1960).

4. M. Levenberg, private communication (1963).

5. C. J. Ballhausen and J. P. Dahl, Acta Chem. Scand., 15, 1333 (1961).

6. M. J. Bennett, M. Gerlock, J. A. McCleverty and R. Mason, Proc. Chem. Soc., 357 (1962).

7. D. F. Shriver, J. Am. Chem. Soc., 85, 3509 (1963).

8. "Tables of Interatomic Distances and Configuration in Molecules and Ions," The Chemical Society (London), 1958, pp. 80-82.

9. L. Pauling, "Nature of the Chemical Bond," Cornell University Press, Ithaca, N. Y., 1960, p. 260.

V. A Fungus Reputed to Possess Contraceptive Properties.

1. Proposal.

It is proposed that a thorough investigation be made of a mushroom reputed to have contraceptive effects when eaten by women. This fungus, which is indigenous to a remote valley on the island of New Guinea, was identified as a result of the author's interest in the subject; it is a species previously unrecorded on that island.

2. Introduction.

The rapidly burgeoning population of the world has stimulated the effort to find new methods of contraception which are harmless, effective, inexpensive and simple to use. Although none of the many methods presently used for contraception meet all these requirements, the oral ovulation inhibitors probably come the closest. The best known of these is the widely used drug "Enovid," manufactured by G. D. Searle and Co. (1). The principal constituents of this preparation are norethynodrel (17α-ethynyl-17β-hydroxy-5(10)-estren-3-one) (I) and a small amount (10-15%) of the 3-methyl ether

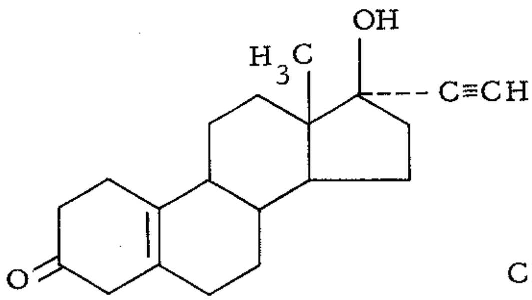

I

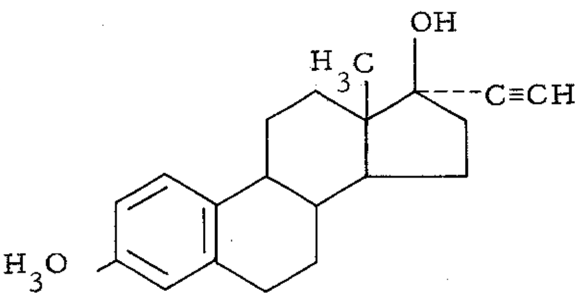

II

of ethynylestradiol (17α-ethynyl-1,3,5-estratriene-3,17β-diol) (II) which occurs as an impurity and enhances the estrogenic activity of I. Although it is essentially 100% effective, apparently harmless and easy to take, it is, at the present time, too expensive for general distribution in the poorer countries of the world. Hence, the search has continued for more easily obtainable drugs.

The problem of fertility control, in both the positive and negative sense, has been of concern to mankind for centuries. Primitive peoples in all parts of the world have used and still use various herbs and plants to affect fertility. DeLaszlo and Henshaw (2) have reported over sixty such materials which interfere with ovulation, implantation, gestation or spermatogenesis, permanently or only temporarily. Laboratory screening of extracts of these plants has produced discouraging results; all are either too dangerous for general use or have other undesirable features. However, because so many valuable drugs have been extracted from plants used by primitive peoples for generations, this is still an active field of investigation.

3. Discussion.

In the spring of 1962, J. W. Kessel brought to the author's attention a reference from a rather obscure multi-volume compendium entitled "Mushrooms, Russia and History," by Wasson and Wasson (3). The pertinent part of this reference is quoted below.

Thomas Gilliard, an ornithologist of the American Museum of Natural History specializing in the birds of New Guinea, first drew our attention to the Mount Hagen reference. He did more: he suggested that we address a letter to a Catholic missionary working downstream from the Mount Hagen range and inquire about a peculiar fungal practice among the natives there. The Wahgi is a river that runs east and then south into the Gulf of Papua. Below Mount Hagen but still far from the sea it drains a valley shut in on the north by the Bismark range and on the south by the Kubor mountains. The natives, known as the Chimbu people, are linguistically and culturally distinct from the Mount Hagen tribesmen, though ethnically similar. It seems that among them chastity is not prized as a virtue in young unmarried women, and that to avoid children they eat a certain fungus. Later, when they marry, they give up the fungus and proceed to bear children without let or hinderance. We sent off our letter to Father John Nilles, a member of the Society of the Divine Word, to his station at Mingende, in the Central Highlands of the Territory of New Guinea, and in due course his reply confirmed Mr. Gilliard's report:

"I know (he wrote) of one kind of mushroom that is used by women as a means of preventing conception or procuring abortion. A native has

> brought me two specimens of that kind, of which I send you two cross sections. It grows on old tree stumps in the bush from 6,000 feet up on the slopes of the Chimbu and Wahgi valleys. When fresh the color on the top is brown, and white underneath. Small slices are cut off, cooked by the woman between hot stones, and eaten with cooked sweet potatoes."
>
> On receiving this gracious communication from Father Nilles, we forwarded the mushroom samples at once to Professor Roger Heim in Paris. They were insufficient for definitive identification, but Professor Heim felt confident that the specimens belonged to a genus known in France as ungulina, and probably to the species called by French mycologists the ungulina auberiana (Mont.) Pat. This particular species is abundant throughout the tropics and belongs to the polypores with rigid trama. It staggers under the burden of twenty or thirty competing scientific names; in the collections of the New York Botanical Garden the specimens carry the designation rigidoporus microporus.

This reference sufficiently intrigued the author that an attempt was made to verify the story. In a letter to Dr. D. Shaw, chief plant pathologist for the Department of Agriculture, Stock and Fisheries at Port Moresby (the capital of the Australian mandate of New Guinea), the author cited the Wasson report and requested her help in tracking down the alleged anti-fertility mushroom. In reply, Dr. Shaw wrote that she was unaware of the use of this mushroom, but would attempt to contact Father John Nilles, who, she had learned, was still in New Guinea. Several months later Dr. Shaw wrote that she had received a letter from Father Nilles, the pertinent section of which is quoted below.

> The statement of Mr. Gilliard is not entirely correct. The Chimbu people are in the strict sense those natives who live in the Chimbu River valley, a river that has its origin from three or four contributories at the foot of the Bismark Range and flows southwest into the Waghi River. Also the Chimbu people are a one linguistic group which lives mainly in the Chimbu valley but stretches into the Wahgi valley on both sides of the river, I would say, with its dialects, about 20 miles east and west from the flow of the Chimbu into the Wahgi.
>
> That chastity among the Chimbus be not prized as a virtue I would not agree despite the fact that not all girls enter marriage as virgins. Besides it is a matter of conjecture if that fungus is used in order to prevent conception or cause abortion. The natives seem not to know the difference. Some years ago I had a talk with the late Miss Camilla Wedgwood, anthropologist, and although she had only worked among the natives of the coastal area, she was convinced that the natives of New Guinea as a whole do not know

> means of preventing conception. Though I could not prove this statement, I would agree to that today.
>
> That fungus, besides a number of other plants, roots and wild fruits, of which I have sent a whole collection about 10 years ago to Dr. Winterbotham in charge of the Anthropology Section of the Medical School in Brisbane (never heard anything after that) are used mainly orally and not so much by the young girls but by the young women who are supposed not to have children until 3-4 years after marriage, and are believed when eaten, given by a magician connected with magical spells, to prevent having children. Whether or not those means have the chemical qualities causing abortion I could not state, that would have to be investigated by a chemical laboratory. I wonder if that has been done at the Medical School in Brisbane with that collection of mine.
>
> So far I have not been able to make further observations regarding the mushrooms. I shall try to trace that woman who gave me the information some years ago and ask her to bring me a full-sized specimen of that fungus which I shall forward to you.

In her last letter, dated February, 1963, Dr. Shaw informed the author that she had received from Father Nilles two fruiting bodies of the fungus in question and that these had been identified by an overseas specialist. Interestingly enough, the specimens were found to belong to a different genus from that tentatively identified by Professor Heim, one which had not been previously recorded on the island of New Guinea. Unfortunately, Dr. Shaw neglected to mention the correct genus name in her letter.

4. Conclusion.

The author has no more information about the alleged anti-fertility mushroom than that presented above; however, this is certainly sufficient to propose that a thorough investigation of all aspects of this problem be initiated. The true nature of the contraceptive or abortive properties of this fungus can probably be determined from feeding tests with small laboratory animals. Such tests are usually carried out by examining vaginal smears of the treated animals in order to observe any change in the normal oestrous cycle or by histological examination of the reproductive organs and glands of the animals. Should it be shown that this mushroom contains one or more physiologically active principles, further chemical investigation, aimed at determining the molecular structures of these constituents, would be in order.

It is possible, perhaps even probable, that the purported contraceptive properties of this fungus will prove to be nothing more than the superstition of a primitive people. However, the problem of finding suitable agents for fertility control is urgent and no possibility should be overlooked.

References to Proposition V

1. "Enovid for Long-term Ovulation Control," G. D. Searle and Co., 1961.
2. H. deLaszlo and P. S. Henshaw, Science, 119, 626 (1954).
3. V. P. Wasson and R. S. Wasson, "Mushrooms, Russia and History," Pantheon Press, vol. II, 1957, pp. 215-6.